



UNIVERSIDADE FEDERAL DE OURO PRETO - ESCOLA DE MINAS
DEPARTAMENTO DE ENGENHARIA CIVIL
PROGRAMA DE PÓS-GRADUAÇÃO EM ENGENHARIA CIVIL



OBTENTION OF ECO-EFFICIENT CEMENT-BASED COMPOSITES USING INDUSTRIAL WASTE

José Maria Franco de Carvalho

**Ouro Preto
2019**

OBTENTION OF ECO-EFFICIENT CEMENT-BASED COMPOSITES USING INDUSTRIAL WASTE

José Maria Franco de Carvalho

Advisor: Prof. Dr. Ricardo André Fiorotti Peixoto

Thesis presented to the Postgraduate Program in Civil Engineering, Department of Civil Engineering, Federal University of Ouro Preto, in partial fulfillment of the requirements for the degree of Doctor of Science in Civil Engineering, area: structures and construction.

Ouro Preto
March 2019.

C331o Carvalho, José Maria Franco de .
Obtention of eco-efficient cement-based composites using industrial waste
[manuscrito] / José Maria Franco de Carvalho. - 2019.
230f.: il.: color; grafs; tabs.

Orientador: Prof. Dr. Ricardo André Fiorotti Peixoto.

Tese (Doutorado) - Universidade Federal de Ouro Preto. Escola de Minas.
Departamento de Engenharia Civil. Programa de Pós-Graduação em Engenharia
Civil.

Área de Concentração: Estruturas e Construção.

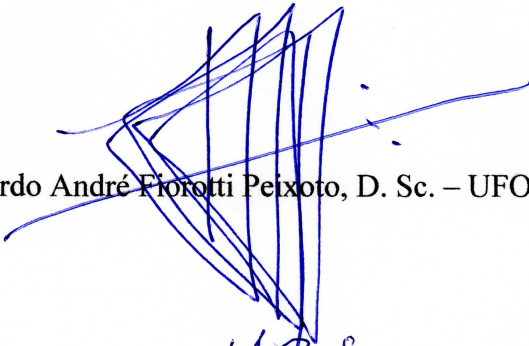
1. Concreto eco-eficiente. 2. Cimento belítico. 3. Adição mineral reciclada
engenhairada. 4. Rejeito industrial. 5. Reciclagem. I. Peixoto, Ricardo André
Fiorotti. II. Universidade Federal de Ouro Preto. III. Título.

CDU: 624.01


OBTENÇÃO DE MATRIZES CIMENTÍCIAS ECOEFICIENTES UTILIZANDO REJEITOS INDUSTRIAIS

AUTOR: JOSÉ MARIA FRANCO DE CARVALHO

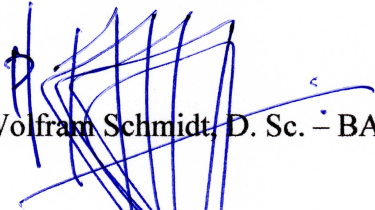
Esta tese foi apresentada em sessão pública e aprovada em 07 de março de 2019, pela Banca Examinadora composta pelos seguintes membros:



Prof. Ricardo André Fiorotti Peixoto, D. Sc. – UFOP (Presidente)



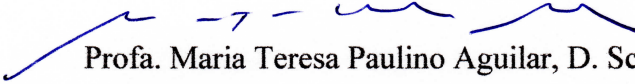
Prof. Guilherme Jorge Brigolini Silva, D. Sc. – UFOP



Prof. Wolfram Schmidt, D. Sc. – BAM



Prof. Bruno Luis Daminieli, D. Sc. – USP



Profa. Maria Teresa Paulino Aguilar, D. Sc. – UFMG

This doctoral thesis was developed in cooperation between the Graduate Program in Civil Engineering (PROPEC), Department of Civil Engineering (DECIV), Federal University of Ouro Preto (UFOP), Ouro Preto, Brazil, under the supervision of Prof. Dr. Ricardo André Fiorotti Peixoto; and the Department of Safety of Structures, Federal Institute for Materials Research and Testing (BAM), Berlin, Germany, under the supervision of Prof. Dr. Ing. Wolfram Schmidt; with funding from the Coordenação de Aperfeiçoamento de Pessoal de Nível Superior (CAPES), Brazil.

*To Prof. Dr. Rita de Cássia Silva Sant'Anna Alvarenga
(in memorian)*

Acknowledgments

Firstly, I would like to express my sincere gratitude to my advisor Prof. Dr. Ricardo André Fiorotti Peixoto, for the continuous support of my Doctoral study and related research, for his friendship, confidence, patience, motivation, and shared knowledge. His guidance was always precise, and he knew how to identify and extract the best of me. I could not have a better advisor and mentor for my Doctoral study.

I am very grateful to Prof. Dr. Wolfram Schmidt for advising me during my research stay in Berlin. Dr. Schmidt was always very kind, patient, confident in my work and generous, providing me the best conditions and support.

Besides my advisors, I would like to thank the members of my thesis committee: Prof. Dr. Bruno Luís Damineli, Prof^a. Dr^a. Maria Teresa Paulino Aguilar, and Prof. Dr. Guilherme Jorge Brigolini Silva, for their generosity in accepting the invitation and honoring me with their contributions to the improvement of this work.

My sincere thanks also to Dr. Pedro Portella, that made our research stay at Berlin possible, and also Dr. Hans-Carsten Kühne and Dr. Andreas Rogue, who together with Dr. Schmidt, provided me the opportunity to join their team as visiting researcher at BAM, giving me access to the laboratories and research facilities.

I would like to acknowledge the agency CAPES for financial support during my research stay in Berlin, granting me the PDSE scholarship.

Thanks are also due to the following laboratories and their teams for the equipment use and collaborations: Laboratory of Materials for Civil construction – UFOP, Laboratory of Construction Materials – UFV; Laboratory of Electronic Microscopy NANOLAB – UFOP.

Many thanks to the Research Group on Solid Waste – RECICLOS-CNPq and its supporters CAPES, CNPq, FAPEMIG, and Fundação Gorceix. Without its support and structure, the development of this research would not be possible.

I thank my “family RECICLOS” for the friendship, support with the experiments, stimulating discussions, partnership in academic projects, and for all learning together and fun we have had in the last four years. Without them, this work would not be

possible. Also, I thank my teammates at the BAM laboratories for the support in my research stay in Berlin, and all shared moments, talks and knowledge.

I would like to thank the Federal University of Ouro Preto (UFOP), Pro-Rector of Research (PROPP) and Post-Graduation and to the Graduate Program in Civil Engineering (PROPEC) for the opportunity to carry out this work and training.

Many thanks to the Federal University of Viçosa (UFV), and the Department of Civil Engineering (DEC), for the dismissal of my teaching activities during the doctorate and the support. I thank my colleagues, professors at the Structures Sector, for authorizing my training assuming my lectures, and also, for the friendship and support.

I would like to register, also, my acknowledgment to my former advisors Prof. Dr. João Batista Marque de Souza Jr. (Master), and Prof. Dr. Rita de Cassia Silva Sant'Anna Alvarenga (Bachelor). I also acknowledge all the professors that believed in me along my life, and who worked so that I could develop this work.

Many friends and relatives have participated in my life, who I am very grateful for all support, encouragement, learning, prayers, and demonstrations of friendship and affection. They all are very important to me.

I would like to express my gratitude to my parents: my father, Juarez (*in memorian*), and my mother, Beatriz. I owe them my life and my formation based on love and guided by justice. Also to my brother, Eder, an example of integrity and intelligence. I thank them all the support and prayers.

All my best words of gratitude to my brave wife, Marly, for all love, understanding, patience, and support.

Above all, I thank God for providing me such opportunities and people, and has guided me and supported me. To him praise, honor, and glory forever.

Abstract

Portland cement is the main responsible for the low environmental performance of cement-based composites since its production implies the emission of large amounts of carbon dioxide in the atmosphere. Achieving more eco-efficient concrete, therefore, means an effective contribution to mitigating human-made impacts. The search for less aggressive binders and the partial substitution of Portland cement for supplementary materials of low environmental impact are effective mitigation routes that are explored in this thesis. Concomitantly, the consumption of by-products from other productive sectors as inputs in the production of concrete, besides being an effective way of saving natural resources, provides an adequate destination to environmental liabilities. Thus, as part of the work related to this research, a low environmental impact cement produced entirely with industrial and mining wastes was successfully proposed and obtained. This material presented technological characteristics compatible with belitic cements obtained with conventional materials. In addition, supplementary fine materials so-called Engineered Recycled Mineral Admixtures were designed and produced to partially replace Portland cement and increase the packing density of the fine fraction in cementitious matrices. An extensive characterization program of these materials was conducted, as well as performance evaluation in pastes, mortars and concretes, including rheology, hydration kinetics, cementing properties and mechanical performance. Finally, these materials were used in the production of densely packed concretes, where the great potential of the proposed products in the obtention of cement-based composites with high mechanical strength and/or high eco-efficiency was observed.

Resumo

O cimento Portland é o principal responsável pelo baixo desempenho ambiental de matrizes cimentícias, uma vez que sua obtenção implica na emissão de grande quantidade de dióxido de carbono na atmosfera. Obter concretos mais ecoeficientes, portanto, significa uma contribuição efetiva na mitigação dos impactos causados pelo homem. A busca por ligantes menos agressivos e a substituição parcial de cimento Portland por materiais suplementares de baixo impacto ambiental são rotas de mitigação efetivas que são exploradas nesta tese. Concomitantemente, o consumo de subprodutos de outros setores produtivos como insumos na produção de concretos, além de ser uma forma eficaz de economizar recursos naturais, fornece destinação adequada a passivos ambientais. Assim, como parte dos trabalhos relacionados a esta pesquisa, um cimento de baixo impacto ambiental produzido inteiramente com rejeitos industriais e de mineração foi proposto e obtido com sucesso. Este material apresentou características tecnológicas compatíveis com cimentos belíticos obtidos com materiais convencionais. Adicionalmente, materiais finos suplementares denominados aqui Adições Minerai Recicladas Engenheiradas foram projetadas e produzidas, com o objetivo de substituir parcialmente o cimento Portland e aumentar a densidade de empacotamento da fração fina em matrizes cimentícias. Um extenso programa de caracterização desses materiais foi conduzido, bem como de avaliação de desempenho em pastas, argamassas e concretos, compreendendo reologia, cinética de hidratação, propriedades cimentantes e desempenho mecânico. Por fim, esses materiais foram utilizados na produção de concretos densamente empacotados, onde verificou-se o grande potencial dos produtos propostos na obtenção de matrizes cimentícias de elevada resistência mecânica e/ou elevada ecoeficiência.

Table of contents

ACKNOWLEDGMENTS.....	VI
ABSTRACT.....	VIII
RESUMO.....	IX
TABLE OF CONTENTS.....	X
CHAPTER 1 - GENERAL INTRODUCTION.....	1
1.1 Introduction.....	2
1.1.1 Portland cement and impacts related to its production	2
1.1.2 Binder efficiency in cement-based composites.....	3
1.1.3 Binder optimization.....	4
1.1.4 Supplementary cementing materials (SCM).....	4
1.1.5 Consumption of non-renewable natural resources in civil construction.....	5
1.1.6 Use of industrial wastes in cement-based composites.....	6
1.2 Objectives of the research.....	6
1.3 Presentation and structure of this thesis.....	7
1.4 References.....	10
CHAPTER 2 - LOW ENVIRONMENTAL IMPACT CEMENT PRODUCED ENTIRELY FROM INDUSTRIAL AND MINING WASTE.....	14
2.1 Introduction.....	15
2.2 Experiment.....	18
2.3 Results and discussion.....	22
2.3.1 Characterization of the raw materials.....	22
2.3.2 Raw meal proportioning.....	24
2.3.3 Mineralogical composition.....	27

2.3.4 Cement physical and mechanical properties.....	30
2.4 Conclusion.....	34
2.5 Acknowledgements.....	35
2.6 References.....	36

CHAPTER 3 - PRODUCTION AND EVALUATION OF ENGINEERED RECYCLED MINERAL ADMIXTURES OBTAINED FROM BASIC OXYGEN FURNACE SLAG, IRON ORE TAILINGS, QUARTZ TAILINGS AND QUARTZITE TAILINGS.....45

3.1 Introduction.....	46
3.2 Experimental.....	48
3.2.1 Physical, chemical and mineralogical characterization.....	48
3.2.2 Grinding evaluation.....	49
3.2.3 Production and characterization of the ERMA's.....	50
3.2.4 Performance tests in blended cement pastes and mortars.....	51
3.3 Results and discussion.....	54
3.3.1 Characterization of the raw material.....	54
3.3.2 Grinding evaluation and production of the ERMA's.....	57
3.3.3 Particle size distribution, specific surface area and morphology.....	59
3.3.4 Influence of the ERMA's in the rheology and interaction with superplasticizers...	62
3.3.5 Influence of the ERMA's in the hydration kinetics.....	66
3.3.6 Pozzolanic activity.....	71
3.3.7 Mechanical performance and durability.....	73
3.4 Conclusion.....	76
3.5 Acknowledgements.....	76
3.6 References.....	77

CHAPTER 4 - MORE ECO-EFFICIENT CONCRETE: AN APPROACH ON OPTIMIZATION IN THE PRODUCTION AND USE OF WASTE-BASED SUPPLEMENTARY CEMENTING MATERIALS.....86

4.1 Introduction.....87

4.2 Material and methods..... 89

4.2.1 Materials..... 89

4.2.2 Production and characterization of the powders.....92

4.2.3 Dosing of superplasticizer..... 94

4.2.4 Determination of the maximum experimental packing density..... 94

4.2.5 Characterization of the sand-concretes.....96

4.2.6 Eco-efficiency evaluation.....97

4.2.7 Durability.....98

4.3 Results and discussion.....98

4.3.1 Production and characterization of the powders..... 98

4.3.2 Performance of the powders as SCMs in densely packed sand-concretes..... 102

4.4 Conclusion..... 116

4.5 Acknowledgments..... 118

4.6 References.....118

CHAPTER 5 - REACTION SPEED AND RHEOLOGICAL BEHAVIOR OF CEMENT-BLENDED PASTES CONTAINING ENGINEERED RECYCLED MINERAL ADMIXTURES OBTAINED FROM STEEL SLAG, IRON ORE TAILINGS, QUARTZ TAILINGS AND QUARTZITE TAILINGS.....126

5.1 Introduction.....127

5.2 Material and methods.....131

5.2.1 Materials..... 131

5.2.2 Processing of the raw wastes and production of the mineral admixtures (powders). 133

5.2.3 Evaluation of the ζ -potential.....134

5.2.4 Rheology.....135

5.2.5 Reaction speed.....	137
5.3 Results and discussion.....	138
5.3.1 Characterization.....	138
5.3.2 Evaluation of ζ -potential of the studied powders.....	141
5.3.3 Influence of the powders in the rheological behavior of blended pastes.....	144
5.3.4 Influence of PCE-based superplasticizers on the rheological behavior.....	147
5.3.5 Reaction speed.....	152
5.4 Conclusion.....	156
5.5 Acknowledgment.....	157
5.6 References.....	158
CHAPTER 6 - PUSHING THE LIMITS OF CONCRETE ECO-EFFICIENCY USING ENGINEERED RECYCLED MINERAL ADMIXTURES AND RECYCLED AGGREGATES.....	169
6.1 Introduction.....	170
6.2 Experimental.....	172
6.2.1 Materials.....	172
6.2.2 Mix design.....	178
6.2.3 Mixing procedure and determination of the water content.....	179
6.2.4 Mechanical performance.....	180
6.2.5 Physical properties in the hardened state.....	180
6.2.6 Expansibility in autoclave.....	181
6.2.7 Isothermal calorimetry.....	181
6.3 Results and discussion.....	181
6.3.1 Proportioning.....	181
6.3.2 Grain packing, water consumption, and rheological behavior.....	183
6.3.3 Mechanical performance and eco-efficiency evaluation.....	188
6.3.4 Physical characterization in the hardened state.....	192

6.3.5 Considerations on applicability and feasibility	192
6.5 Conclusions.....	199
6.6 Acknowledgments.....	200
6.7 References.....	200
CHAPTER 7 - FINAL CONSIDERATIONS	209
7.1 Low-impact binders.....	210
7.2 The role of grinding in producing highly effective engineered recycled mineral admixtures.....	210
7.3 Highly eco-efficient concretes.....	211
7.4 By-products used in this research.....	212
7.5 Proposals for future works.....	213
7.6 General conclusion.....	214

Chapter 1

General introduction

Abstract

Improvement in performance in association with a reduction in emissions and consumption of natural resources are the keys to obtaining more eco-efficient products. Concrete is the most consumed human-made material worldwide, and a massive amount of natural resources in the form of aggregates is consumed to attend the demand for this material. However, Portland cement is the principal responsible for the low environmental performance of concrete due to the high emission of CO₂ related to the production of clinker. Energetic optimization in the clinker production and reduction in emissions are some routes to obtain low-impact clinkers while partial replacement of Portland cement for low-impact supplementary cementing materials, use of recycled aggregates and improvement in binder efficiency are other even more effective measures to obtain more eco-efficient concretes.

1.1 Introduction

Increasing the sustainability of the construction industry is mandatory considering the unacceptable level of the impacts related. It is important to say that significant changes have been observed along the last decades, with substantial gains in efficiency and rational use of resources, but there are already lots to do in this subject. Additionally, given the numbers of the sector, effective actions in this sense have very significant impacts on a global perspective.

Remarkably, the obtention of concrete and other cement-based composites represents a large percentage of the impacts attributed to the construction industry, highlighting the consumption of natural resources and emission of greenhouse gases due to the Portland clinker production.

In this sense, the following discussions about the strategies to improve the ecoefficiency of the cement-based composites point routes in this direction and served as the basis for the development of the present research.

1.1.1 Portland cement and impacts related to its production

Responsible for 5-9% of the total CO₂ emissions, the Portland cement clinker is agreed by the scientific community as the main responsible for the low environmental performance of concrete (Iacobescu, et al., 2011; Ali & Hossain, 2011; Kajaste & Hurme, 2016; Torgal & Jalali, 2010). Despite the impacts, Portland cement is the most consumed binder in the construction industry, with the world production around 4,000 – 4,500 Mt nowadays (DNPM, 2015; Kajaste & Hurme, 2016; Wang, et al., 2016). The Portland cement and its increased consumption are closely related to the implementation and

modernization of the countries' infrastructure, and there are no short-term substitutes for this binder (Miller, et al., 2016). In this sense, by 2050, consumption of about 6,000 Mt of Portland cement is expected, mainly driven by India, China and other developing countries. (Torgal & Jalali, 2010).

1.1.2 Binder efficiency in cement-based composites

Increasing the amount of hydration products with the same amount of cement is one way in the search for more sustainable concretes, since increasing the efficiency of the binder may imply lower consumption or better performance. Powers and Brownnyard (1946) studied the hydration of cement pastes and the concept of degree of hydration, proposing an equation to quantify it, as well as the related volumes.

Cement particles are never 100% hydrated in a cement composite. Bentz e Conway (2001) stated that for water:binder ratios below 0.38, one portion of the cement always remain non-hydrated. Even for water:binder ratios higher than this limit, the water is unable to penetrate on the interior of the grains, and the hydration products themselves are the responsible for this stagnation once the hydration occurs from the exterior to the interior of the particles (Thomas, et al., 2009). In fact, the literature reports reduction in water:binder ratio as key to obtaining less porous high and ultra-high strength concretes, which means that a considerable part of the grains will inevitably remain unhydrated (Bentz & Conway, 2001).

Techniques for increasing the degree of hydration of the concrete comprise increasing the fineness of the cement particles, autogenous curing by providing water for longer within the matrix, use of nucleation seeds and increasing the number of nucleation sites through nanoparticles.

1.1.3 Binder optimization

This route involves the most effective strategies to mitigate the impacts, some of them with the potential to reduce the clinker consumption considerably in concretes (García-Gusano, et al., 2014; Kajaste & Hurme, 2016).

The development of superplasticizers was decisive in opening the way for the development of high and ultra-high strength cementitious composites with low water consumption and consequent low porosity (Hartmann, et al., 2011).

It is clear that techniques to improve the grain packing density are valuable tools for designing (eco-)efficient concretes (Castro & Pandolfelli, 2009). In this sense, the use of supplementary powdered materials (with or without cementing properties) with adequate particle-size distributions has pushed the limits of ultra-high strength concretes.

The high packing density, however, is obtained when the smaller particles fill the voids between larger particles in a complex rheological phenomenon involving the geometry of those particles and their ability in moving in such complex fluid medium. For smaller particles, also the great influence of attraction and repulsion forces take place. Additionally, the comprehension of the interactions of such particles with ions and admixture molecules in a dynamically changing environment is mandatory to propose mix designs on a rational basis.

1.1.4 Supplementary cementing materials (SCM)

SCMs are finely ground materials used in partial replacement of clinker in the concrete production (Juenger & Siddique, 2015). Depending on the physical-chemical action, they

are classified as cementing materials, pozzolans or fillers (Dal Molin, 2011). These materials are already used in the cement industry, and some of them are industrial by-products, such as ground granulated blast furnace slag and fly ash. Besides environmental benefits, they lead to improvements in the technological properties of concretes (BERNDT, 2009).

A variety of materials have been studied, and one of the main focus has been the use of waste in obtaining new SCMs (Juenger & Siddique, 2015). Some of the interest characteristics are physical, such specific surface area, particle size distribution, and grains' shape; chemical composition (particular interest for Si, Al and Ca), and mineralogical phases (cementing compounds and amorphous content) (Dal Molin, 2011; Juenger & Siddique, 2015).

1.1.5 Consumption of non-renewable natural resources in civil construction

In 2008, the world material consumption was ca. 10 tons/inhabitant/year, where 1/3 was used in the production of cement-based products (John, 2011). Oikonomou (2005) points the construction industry as responsible for 50% of the world material consumption, 40% of the energy and is responsible for 50% of the waste production.

The market of raw material for concrete production, especially aggregates, is primarily regional, once the transportation cost affects the final cost of the products sensitively (Kulaif, 2015). However, the highest demands are observed in big metropolitan regions, leading to scarcity in neighbor regions. As a consequence, increasing cost and impacts in obtaining such materials are observed.

1.1.6 Use of industrial wastes in cement-based composites

The management of solid waste is one of the most significant challenges worldwide (Zhang, et al., 2016). With the economic development, the production of waste increases fast, together with the increase in social, environmental, economic and in human health impacts (Meyers, et al., 2006; Zhang, et al., 2016; Aprianti, 2017).

The society has been pressured to find solutions for the problem of industrial waste management given the urgency of this subject imposed by environmental issues and public health, but also given the opportunity that the reuse of such materials can provide (Marshall & Farahbakhsh, 2013; Zhang, et al., 2016; Golçalves, et al., 2016).

In this sense, the construction industry has great potential to absorb considerable amounts of industrial wastes, saving natural resources at the same time that provides an adequate destination to environmental liabilities. For this reason, it is considered one of the most effective routes to increase the environmental performance of the sector.

1.2 Objectives of the research

The objective of this work was to obtain cement-based composites with improved eco-efficiency, enhancing the consumption of industrial and mining wastes as recycled raw materials, and reducing the impacts related to the consumption of Portland cement clinker. Therefore, the following specific objectives have been proposed:

- Producing and evaluating one cement with reduced CO₂ emission, obtained using industrial waste as raw materials.

- Proposing the obtention and optimization of powders for use in cement-based composites as supplementary materials based on industrial wastes.
- Proposing optimized mix designs for concretes and mortars based on concepts of grain packing improvement aiming improvements in eco-efficiency performance.
- Evaluating the technological performance of the proposed supplementary materials and cement-based composites containing them.
- Exploring the maximum performances possible to be reached using the proposed materials and techniques, regarding minimum cement consumption and maximum waste consumption.

1.3 Presentation and structure of this thesis

This thesis addresses the theme eco-efficient concretes exploring three main concepts, (i) reduction on CO₂ emissions embedded by reducing the Portland cement consumption or using low-emission binders; (ii) reduction in natural resources consumption by using alternative low-impact materials; and (iii) recycling of industrial residues as raw material, providing value and adequate destination to environmental liabilities.

Some industrial and mining residues were used in this study; they are basic oxygen furnace slag, iron ore tailings, quartzite mining tailings, quartz mining tailings and grits from pulp and paper industry. These residues have already been studied by some authors, including researchers of the Federal University of Viçosa and Federal University of Ouro Preto (RECICLOS research Group), and promising results have been found. In this collection, however, new routes and approaches are explored and presented in five articles (Chapters 2 to 6), comprising obtention and optimization of binders and supplementary materials, as well as, their application in highly (eco-)efficient cement-based products.

The use of residues as aggregates has been successfully studied and, by far, is the cheapest and direct way to incorporate high amounts of by-products in the production of concretes and mortars. There is no doubt that it represents a substantial positive impact in eco-efficiency by saving resources and consuming large amounts of waste (which is also shown in chapter 6 of this thesis). This strategy, however, has, *a priori*, no impact in the mitigation of another great eco-efficiency drawback of cement-based composites: the consumption of Portland cement.

Decarbonation of limestone, the main component of clinker, is an intrinsic chemical transformation and the primary source of CO₂ emissions in clinker production. The only way to reduce emissions in this regard is reducing the limestone content in the proportioning, which implies in cement poor in calcium silicates (remarkably C₃S). The second major source of CO₂ emission is the burn of fuels to maintain the high temperatures of the kiln. Other minor fonts could also be listed, but in a general way, for each ton of clinker produced, one ton of CO₂ is released into the atmosphere.

Obtaining eco-friendly belitic clinkers by reducing the embedded energy and CO₂ emissions is controversial considering its distinctive slow mechanical strength gain and consequent low market acceptance. In chapter 2 of this thesis, however, these concepts are discussed in a reported well-succeeded experience in obtaining a low-impact belitic cement produced entirely with industrial and mining wastes. There, alternative routes to mitigate the drawbacks are also explored. Additionally, few reports of rational proportioning and clinker production using only residues as raw material are reported, and despite the higher energy consumption and emissions, it is also applicable in obtaining alitic clinkers.

Use of supplementary cementing materials in partial replacement of clinker is the most effective way to mitigate the impacts of the Portland cement. In fact, the cement industry is intensively using ground granulated blast furnace slags, pozzolans, fly ash and even limestone fillers in the production of composed cements. Besides technological advantages, it is also very effective in reducing cost and the total emissions in cement production.

Many other residues from different productive chains could also be used in partial replacement of Portland cement as supplementary materials. Cementitious properties or filler effect, however, are properties that can be developed or potentiated using mechanical or thermal treatments. Of course, these processes represent costs, energy, and emissions; but also represent opportunities in a world concerned with environmental issues and sustainability. In this sense, four chapters of this thesis are devoted to production, characterization, performance, optimization, and application of supplementary materials obtained from basic oxygen furnace slags, iron ore tailings, quartz tailings, and quartzite tailings.

Grinding was the only route chosen to produce the fines and potentiate their performances, and the concept of particle packing guided the choice of the particle sizes. The particles' shapes and flow performances are also closely observed in chapters 3 and 5, where the concept of engineered recycled mineral admixture (ERMA) is proposed to designate materials produced to present specific properties and improved performance, in this case, related to particle packing.

In the very beginning, it became clear that obtaining fines with a particle size similar to Portland cement would represent no gains in improving the particle packing.

Additionally, the high fineness observed in modern Portland cement could represent an opportunity to design a less expensive supplementary material with an intermediate particle-size to be used in the gap between cement and fine sand. So, the third powder with particles smaller than that of cement would even refine the micropores.

In fact, chapter 4 shows that the strategy was very successful in improving the mechanical and eco-efficiency performances in densely packed sand-concretes. In this study, it became clear that the fine powders were very effective in improving mechanical performance as a result of filler effect and cementitious properties. The coarse powders, on the other hand, consistently improved the flow behavior of the paste and proved to be able to replace larger amounts of cement for a not so great loss on mechanical performance. So, better results regarding cement intensity were found despite the reduced compressive strength.

Finally, chapter 6 explores the limits of eco-efficiency in concretes based on the concepts discussed in this work. In addition to cement replacement by the proposed ERMA, total replacement of conventional aggregates by recycled aggregates also took place in this specific study. As a result, concretes with conventional compressive strength were obtained with impressive low amounts of Portland cement and more than 95% of recycled material by volume of solids were possible.

1.4 References

Ali, M. B. & Hossain, M. S., 2011. A review on emission analysis in cement industries. *Renewable and Sustainable Energy Reviews*, Issue 15, pp. 2252-2261.

Aprianti, E., 2017. A huge number of artificial waste material can be supplementary cementitious material (SCM) for concrete production – a review part II. *Journal of cleaner production*, Volume 142, pp. 4178-4194.

Bentz, D. P. & Conway, J. T., 2001. Computer modeling of the replacement of “coarse” cement particles by inert fillers in low w/c ratio concretes: Hydration and strength. *Cement and Concrete Research*, 31(3), pp. 503-506.

Castro, A. L. & Pandolfelli, V. C., 2009. Review: Concepts of particle dispersion and packing for special concrete production. *Cerâmica*, Volume 55, pp. 18-32.

Dal Molin, D. C. C., 2011. Adições minerais. In: G. C. Isaia, ed. *Concreto Ciência e Tecnologia*. São Paulo: IBRACON, pp. 261-310.

DNPM, 2015. *Sumário mineral 2015*, Brasília: s.n.

García-Gusano, D. et al., 2014. Life cycle assessment of the Spanish cement industry: implementation of environmental-friendly solutions. *Clean Technologies and Environmental Policy*, 17(1), pp. 59-73.

Golçalves, D. R. R. et al., 2016. Evaluation of the economic feasibility of a processing plant for steelmaking slag. *Waste Management & Research*, 34(2), pp. 107-112.

Hartmann, C., Jeknavorian, A., Silva, D. & Benini, H., 2011. Aditivos Químicos para Concretos e Cimentos. In: G. C. Isaia, ed. *Concreto Ciência e Tecnologia*. São Paulo: IBRACON, pp. 347-380.

Iacobescu, R. I. et al., 2011. Valorisation of electric arc furnace steel slag as raw material for low energy belite cements. *Journal of Hazardous Materials*, pp. 287-294.

John, V. M., 2011. Concreto sustentável. In: G. C. Isaia, ed. *Concreto Ciência e Tecnologia*. São Paulo: IBRACON, pp. 1843-1870.

Juenger, M. C. G. & Siddique, R., 2015. Recent advances in understanding the role of supplementary cementitious materials in concrete. *Cement and Concrete Research*, Volume 78, pp. 71-80.

Kajaste, R. & Hurme, M., 2016. Cement industry greenhouse gas emissions e management options and abatement cost. *Journal of Cleaner Production*, Issue 112, pp. 4041-4052.

Kulaif, Y., 2015. Sand for construction. In: M. a. E. Ministry, ed. *Mineral Summary 2015*. Brasília: Brazilian National Department of Mineral Production - DNPM, pp. 26-27.

Marshall, R. E. & Farahbakhsh, K., 2013. Systems approaches to integrated solid waste management in developing countries. *Waste Management*, Volume 33, pp. 988-1003.

Meyers, G. D., McLeod, G. & Anbarci, M. A., 2006. An international waste convention: measures for achieving sustainable development. *Waste Management*, Volume 24, pp. 505-513.

Miller, S. A., Monteiro, P. J. M., Ostertag, C. P. & Horvath, A., 2016. Comparison indices for design and proportioning of concrete mixtures taking environmental impacts account. *Cement and Concrete Composites*, Issue 68, pp. 131-143.

Oikonomou, N. D., 2005. Recycled concrete aggregates. *Cement and concrete composites*, 27(2), pp. 315-318.

Powers, T. C. & Brownyard, T. T., 1946. Studies of the physical properties of hardened Portland cement paste. *Journal Proceedings*, 43(9), pp. 101-132.

Thomas, J. J., Jennings, H. M. & Chen, J. J., 2009. Influence of nucleation seeding on the hydration Mechanisms of Tricalcium Silicate and Cement. *The Journal of Physical Chemistry C 113*, pp. 4327-4334.

Torgal, F. P. & Jalali, S., 2010. *A Sustentabilidade dos Materiais de Construção*. 2nd. ed. Guimarães: s.n.

Wang, W. et al., 2016. A Material Flow Analysis (MFA)-based potential analysis of eco-efficiency indicators of China's cement and cement-based materials industry. *Journal of Cleaner Production*, Volume 112, pp. 787-796.

Zhang, M. et al., 2016. Manifest system for management of non-hazardous industrial solid wastes: results from a Tianjin industrial park. *Journal of Cleaner Production*, Volume 133, pp. 252-561.

Chapter 2

Low environmental impact cement produced entirely from industrial and mining waste

José Maria Franco de Carvalho; Paula Anunciação Matias Campos; Keoma Defáveri; Guilherme Jorge Brigolini; Leonardo Gonçalves Pedroti; and Ricardo André Fiorotti Peixoto

Abstract

Proper disposal of industrial waste, the need to conserve non-renewable resources and high CO₂ emissions are the major environmental issues at the present time. A significant portion of emissions from Portland cement production is related to the energy required to maintain the clinker kiln at a temperature of approximately 1450°C, which is necessary for alite formation. The alternative belite phase, however, requires lower temperatures for its formation (below 1250°C). Although belite is less reactive than alite, it is equally efficient in higher hydration times. Thus, a belitic cement produced entirely with industrial waste (grits from the pulp and paper industry, steel slag, and quartzite mining tailings) is presented in this research. The raw meal was proportioned based on Bogue calculation and the firing was performed in a muffle furnace at a temperature of 1250°C. Also, a reference belitic cement was produced with limestone and clay under the same conditions. The results showed that both cements presented high belite contents and expected technological performances. The reference belitic cement revealed a higher reactivity, while the waste cement proved to be a technically feasible low impact alternative

Keyword: Belitic cement, low environmental impact cement, recycling of industrial waste, sustainable cement.

Journal of Materials in Civil Engineering, 2019, 31(2): 04018391

This manuscript was submitted on March 6, 2018; approved on August 27, 2018; published online on December 7, 2018. This paper is part of the Journal of Materials in Civil Engineering, © ASCE, ISSN 0899-1561. DOI: 10.1061/(ASCE)MT.1943-5533.0002617

2.1 Introduction

Cement production accounts for 5-7% of total global CO₂ emissions and about 3% of total anthropogenic emissions of greenhouse gases, mainly as a result of energy consumption in clinker kiln and limestone decarbonation (Iacobescu et al., 2011; Ali & Hossain, 2011; Kajaste & Hurme, 2016). In 2014, the world cement production was 4,180 Mt (DNPM, 2015) with a tendency to grow, considering its closely relationship with the development of nations (Miller et al., 2016). The availability of the raw materials, the relative simplicity of the production processes and simplicity of use make ordinary portland cement (OPC) the main economic alternative for production of durable concretes. The alternative belitic cement, however, is characterized for reduced energy demand and the CaCO₃ content in its constitution, which makes it more economical and eco-efficient than OPC for similar technological performance at later ages. The combination of the CO₂ emission-reduction strategy and waste consumption from other industrial chains in obtaining binder materials for durable concretes has an improved eco-efficiency and economic potential. In addition, strategies to improve compressive strength at early ages are critical to the commercial acceptance of this product and must also be considered.

The major raw materials used in the manufacture of portland cement include high purity calcitic limestone (CaCO₃), and clay (SiO₂, Al₂O₃ and Fe₂O₃). Corrective materials are also commonly used to adjust the SiO₂, Al₂O₃ and Fe₂O₃ contents (Battagin, 2011; Ishak & Hashim, 2015). Practical experience and research investigations led to the definition of modules and ranges of values used in the design of cement raw materials proportioning based on the main constituent oxide contents. These parameters, which facilitate production and ensure a reasonable degree of performance of the clinker, are the lime

saturation factor (LSF), the silica ratio (SR) and the alumina ratio (AR) (UN-HABITAT, 1993). In addition, the Bogue calculation (1929) consists of a simple and useful method to estimate the amounts of the four main phases of portland cement clinker from its chemical composition [alite (C_3S), belite (C_2S), aluminate phase (C_3A), and ferrite phase (C_4AF)]. Widely used in industry, this method is applicable to cements with $Al_2O_3 : Fe_2O_3$ ratios greater than or equal to 0.64, and it assumes that the four main mineral phases of the clinker have an exact composition and are totally crystalline (Mehta & Monteiro, 2006; WHD, 2017). Although the results of the Bogue calculation show considerable deviations from the quantitative ones actually observed (Crumbie et al., 2006; Stutzman et al., 2014), its application as a reference in research is frequently reported (Aloui et al., 2008; Vilaplana et al., 2015; Iacobescu et al., 2016; Koumpouri & Angelopoulos, 2016).

Belitic cement production requires a reduced energy consumption compared with OPC due to the reduction in temperature required for belite formation ($750-1250^\circ C$), which makes it environmentally interesting (Hewlett, 2004). In addition, for the production of belitic clinker, the lime saturation factor is the most important proportion. A reduction in this factor leads to an increase in the belite content and a reduction in the alite content, which is also associated to a reduction in the total CO_2 emission (Hewlett, 2004). A clinker that is practically alite-free is obtained with the lime saturation factor around 75% (Hewlett, 2004). Given its environmental advantages, several studies with belitic cements have been reported in the literature (Popescu et al., 2003; Kacimi et al., 2009; Bouzidi et al., 2014).

Belitic cements, however, have a considerably slower compressive strength gain, because the belite hydration reactions are much slower than those of alite (Londono-Zuluaga et

al., 2017). On the other hand, these cements present less hydration heat and a compressive strength equivalent to OPC in older ages (Taylor, 1990).

Another important environmental issue that demands attention is the large generation and inadequate disposal of industrial waste, the production of which is increasing and the impacts of which are diverse and potentially dangerous for the human community (Meyers et al., 2006; Zhang et al., 2016; Aprianti, 2017). In addition, scarcity of natural resources and the need to conserve them pressures the productive sector to improve the efficiency of their processes, such as reducing waste and encouraging the reuse of by-products as raw materials. In this sense, the construction industry presents itself as an important actor, because it has a great capacity to incorporate by-products of other industrial processes into its products.

In this context, the scientific community has played an important role in promoting research on incorporation of industrial by-products into construction materials. As a result, several by-products once considered waste have been proved to be quality raw materials, and their use has become more and more popular. Examples include blast furnace slag, fly ash, and rice husk ash, which are widely used in the production of blended cements (Battagin, 2011). Several other by-products with promising results have been studied in construction applications, such as steel slag (Diniz et al., 2017; Marinho et al., 2017; Da Silva et al., 2016), mining tailings (Bastos et al., 2016; Sant'ana Filho et al., 2017; Fontes et al., 2016), waste from ornamental stone production (Altoé et al., 2012; Pedroti et al., 2014; Dias et al., 2016) and waste from the pulp and paper industry (Pineiro et al., 2013; Fassoni et al., 2016; Santos et al., 2017).

Other sustainable cements can be found in the literature, for example, successful studies of belitic cements, cements incorporating industrial waste, and the association of these two. (Iacobescu et al., 2011; Vilaplana et al., 2015; Iacobescu et al., 2016; Fassoni et al., 2016).

This work proposes a belitic cement produced entirely with industrial waste as raw material. The basic waste characterization, the proportioning, and the cement production are reported as well as the chemical, mineralogical and technological characterization of the final product. In order to compare the results, a reference belitic cement produced with limestone and clay was also tested. Finally, strategies to improve the compressive strength gain at earlier ages were also evaluated.

2.2 Experiment

The raw materials used in this study were the pulp and paper industry by-product grits (GRT), basic oxygen furnace slag (BOFS) from the steel industry, and quartzite mining tailings (QMT). The BOFS came from an industrial plant located in João Monlevade, Minas Gerais, Brazil. The material was received at the Federal University of Ouro Preto in granular form (particle size 9.5-25 mm) and it was kept in a storage yard, subjected to weathering, for approximately three years. The QMT was obtained from a facility in Itabirito, Minas Gerais, Brazil, and was a weathered friable material with particle size 0.001-6.3 mm. A grits sample, obtained from the calcium hydroxide recovery in the *kraft* process for pulp and paper production, was obtained from an industrial plant located in the eastern region of Minas Gerais state, Brazil. The material had a grayish color and a granular form, with particle size 0.1-6.3 mm. For the production of the reference belitic cement, samples of limestone and clay obtained from a cement manufacturer in the

metropolitan area of Belo Horizonte were used. Finally, gypsum was used to regulate the setting time.

Chemical analyses of the raw materials were carried out by X-ray fluorescence (XRF) spectrometry (PANalitical, Epsilon3^x, Malvern Panalytical, Malvern, Worcestershire, UK), and X-ray diffraction (XRD) were used for the identification of the mineralogical phases (Bruker, Billerica, Massachusetts, D2 PHASER 2nd generation, Cu K α radiation, 40 kV, 30 mA, 2θ range 5°-70°, step 0.01°, and speed 1 °/minute). These analyses were performed in oven dried samples ($105 \pm 5^\circ\text{C}$ for 24h) with particle sizes less than $45\mu\text{m}$, ground in a high efficiency planetary ball mill (Retsch PM 100, Haan, North Rhine-Westphalia, Germany) with a 250 mL ZrO₂ jar and ZrO₂ spheres, at 400 rpm for 5 min.

The raw meal mixtures were estimated from Bogue's equations (Bogue, 1929) (Equations 1 to 4) with adjustments in the quality indexes lime saturation factor (LSF), alumina ratio (AR) and silica ratio (SR) (Equations 5-7). The values of the quality indexes were compared to those adopted in the cement industry (UN-HABITAT, 1993). Spreadsheets in Microsoft Excel were programmed to aid in calculation. Two blends were designed, one for each belitic clinker cement: the waste clinker and the reference clinker.

Equation 1

$$\%C_3S = 4,071CaO - 7,6SiO_2 - 6,718Al_2O_3 - 1,43Fe_2O_3 - 2,85SO_3$$

Equation 2

$$\%C_2S = 2,867SiO_2 - 0,754C_3S$$

Equation 3

$$\%C_3A = 2,650Al_2O_3 - 1,692Fe_2O_3$$

Equation 4

$$\%C_4AF = 3,043Fe_2O_3$$

Equation 5
$$LSF = \frac{100 CaO}{2,8 SiO_2 + 1,2 Al_2O_3 + 0,65 Fe_2O_3}$$

Equation 6
$$SR = \frac{SiO_2}{Al_2O_3 + Fe_2O_3}$$

Equation 7
$$AR = \frac{Al_2O_3}{Fe_2O_3}$$

To prepare the raw meal, the raw materials were ground separately in a Marconi (Piracicaba, São Paulo, Brazil) MA500 horizontal ball mill. The grinding times were adjusted to achieve 80% by weight of the material passing through a #200 sieve (75 µm). The characteristics of the ball mill are listed in Table 1.

Table 1. Characteristics of the ball mill used in this research.

Parameter	Values
Jar volume (cm ³)	10 367
Useful volume (cm ³)	3 422
Material volume per cycle (cm ³)	1 740
Rotational speed (rpm)	200
Stainless steel balls [quantity / diameter (mm)]	7/22, 17/28, 34/31, 11/38, 16/41

The blends were prepared and homogenized. Pellets with diameter 15-20 mm were produced using minimum water consumption and oven dried at 105 ± 5 °C for 24 h. The decarbonation of the pellets was carried out in a Jung (Blumenau, Santa Catarina, Brazil) TB03013 electric muffle furnace at 1,000 °C for 4 h. After that, the furnace temperature was raised to 1,250 °C, and the clinker was burned for 40 min. The oven heating rate was 10°C/min. A rapid cooling protocol was applied to stabilize the α' and β-C₂S polymorphic forms. It consisted of immediate removal of the red-hot material from the furnace after the burning period (temperature between 1,000 °C and 1,250 °C) and forced air cooling

application to bring it down to handling temperature. To potentiate the process, the pellets were fragmented during the cooling.

The clinkers were ground in a ball mill (Marconi MA500) to produce a material with specific surface area exceeding 3000 cm²/g, which corresponds to the minimum requirement applicable to high early strength cements according to more severe Brazilian specification NBR 5733 (ABNT, 1991a). In order to ensure the required fineness, the maximum grinding time observed for the more exigent raw material was applied (180 min). Gypsum was added to cement clinkers (5% by weight) in order to adjust the setting time.

The chemical composition of the produced clinkers was obtained by x-ray fluorescence (PANalytical Epsilon3^x) and the results were compared to the predicted values. The crystalline phases were identified using x-ray diffraction (Bruker D2 PHASER 2nd generation). The Rietveld refinement method was applied in the mineralogical quantification using PANalytical HighScore Plus V3.0 software and the ICDD PDF4 + database v. 2016. Fluorite was used as an internal standard (10% by mass).

The obtained cements were characterized according to the test methods prescribed by current Brazilian standards. Table 2 presents the technological tests applied to the cements produced (references and brief descriptions). The compressive strength tests were performed in cylindrical test specimens Ø50 × 100 mm produced with standard 1:3 mortars (cement: Brazilian standard sand) in accordance with method NBR7215 (ABNT, 1996b). The specimens were tested at ages of 7, 28, 56, 90, and 180 days.

Three strategies to improve the early strength of the waste cement were evaluated: (1) reduction in the water:cement ratio by using a chemical superplasticizer; (2) improvement

of the cement fineness by high-efficiency grinding; and (3) ordinary portland cement blending (10% by weight). A polycarboxylate-based superplasticizer (McBauchemie, Powerflow, Bottrop, North Rhine-Westphalia, Germany) and a high early strength portland cement (ASTM type III) were used. The additional high-efficiency grinding was performed in a Retsch PM100 planetary ball mill for 15 minutes at 400rpm, using 100mL material volume and 191 Ø5mm + 99 Ø10mm ZrO₂ balls. In this evaluation, reduced cylindrical specimens were produced (Ø35 × 40 mm). A sample composed of two specimens were taken for each determination and the highest of the two values obtained from the compressive test was taken as the compressive strength of the sample.

Table 2. Technological tests performed on produced cements.

Test	Reference	Description
Specific surface area	NBR NM 76 (ABNT, 1996a)	Blaine air permeability
Density	NBR NM 23 (ABNT, 2001)	Le Chatelier flask test
Setting time	NBR NM 65 (ABNT, 2003)	Vicat needle test
Soundness (expansion)	NBR 11582 (ABNT, 2016)	Le Chatelier mold test
Compressive strength	NBR 7215 (ABNT, 1996b)	Compressive strength in Ø50X100 mm cylindrical specimens

2.3 Results and discussion

2.3.1 Characterization of the raw materials

The results of the chemical analysis of the raw materials are listed in Table 3 and the main mineralogical phases observed in the XRD diffractograms are presented in Table 4. Table 5 lists the grinding times of the raw meal for the required fineness and mill characteristics presented in Table 1.

Table 3. Chemical composition (oxides) of raw materials.

Oxides	Grits (%)	QMT (%)	BOFS (%)	Limestone (%)	Clay (%)
SiO ₂	1.8	80.0	14.4	3.1	63.2
Al ₂ O ₃	0.9	15.9	3.7	2.1	20.1
Fe ₂ O ₃	0.4	0.4	32.1	1.1	8.7
CaO	94.3	-	37.1	91.7	0.9
MgO	0.5	0.1	5.6	0.7	1.2
K ₂ O	0.2	2.8	-	0.3	4.2
Na ₂ O	-	-	-	-	-
SO ₃	0.9	0.0	0.3	0.2	-
MnO	-	-	3.7	-	-
Cr ₂ O ₃	-	-	0.7	-	-
Others	1.0	0.8	2.4	0.8	1.7
LOI	41.4	1.2	1.1	40.0	5.2

Table 4. Main mineralogical phases observed in the XRD diffractograms of samples of raw materials.

Raw material	Mineralogical phases
Grits	Calcite and alunite
QMT	Quartz and muscovite
BOFS	Larnite, brownmillerite, helvine, wustite, magnesite, periclase, calcite, and lime
Limestone	Calcite and quartz
Clay	Quartz, muscovite, and kaolinite

Table 5. Grinding times of raw materials.

Component	Grinding time (min)
Grits	45
QMT	55
BOFS	180
Limestone	60
Clay	30

Grits had a CaO content of 94.3% and loss on ignition of 41.4%, evidencing its carbonate nature, which was confirmed in XRD analysis and was in good agreement with what has been reported in the literature (Souza & Cardoso, 2008). The reduced potassium and

sodium contents are interesting for cement production, permitting good durability with respect to alkali-aggregate reactions in cement-based composites. Compared with limestone, grits had a very similar composition. The QMT presented the highest Al_2O_3 (15.9%) and silica (80.0%) contents among all the studied wastes, replacing clay in the waste cement. It also had the lowest grinding time of all tested wastes (friable material, high weathering grade). BOFS had a significant percentage of CaO (37.1%) and SiO_2 (14.4%). However, it was the main source of Fe_2O_3 (32.1%). Once small Fe_2O_3 quantities are demanded, the result limits its use. On the other hand, the presence of mineralogical phases with high hardness, such as larnite (hardness 6 in Mohs scale), helvine (6 – 6.5) and wustite (5.5) contributed to the high grinding time observed (180 min), which makes the process more expensive. In this respect, its use in small quantities contributed positively to energy demand. The limestone had high CaO content (91.7%), and the main impurities observed were SiO_2 (3.1%) and Al_2O_3 (2.1%). The clay had very suitable SiO_2 , Al_2O_3 and Fe_2O_3 contents for cement production (63.2%, 20.1%, and 8.7%, respectively), indicating no need for the use of corrective materials (Battagin, 2011). The limestone grinding time was 60 minutes, slightly higher than for the grits, because it was non-weathered rock. The clay was subjected to milling for 30 minutes in order to promote disintegration of the clods.

2.3.2 Raw meal proportioning

The blends were proportioned from the chemical composition of the raw materials, and the results are listed in Table 6.

After burning, new chemical analyses were conducted on the obtained clinkers, and the results were compared with those calculated. The results of the estimated chemical

compositions (calculated) of the clinkers and effective chemical compositions observed by XRF are listed in Table 7. Table 8 presents the results of the Bogue calculation for the main phases of portland cement and the chemical parameters silica ratio, alumina ratio, and lime saturation factor.

Table 6. Proportioning of raw meal blends for production of waste cement clinker and reference cement clinker.

Raw material	Proportion (% by weight)
Waste cement	
Grits	70.0
QMT	20.7
BOFS	9.3
Reference cement	
Limestone	75.5
Clay	24.5

Table 7. Chemical composition (oxides) of clinkers: calculated and effective observed in the XRF results.

Oxides	Waste cement		Reference cement	
	Calculated	XRF	Calculated	XRF
SiO ₂	26.1%	25.6%	24.1%	23.1%
Al ₂ O ₃	5.6%	3.9%	8.4%	6.6%
Fe ₂ O ₃	4.5%	5.6%	3.8%	4.1%
CaO	59.5%	58.3%	60.1%	63.2%
MgO	1.0%	0.8%	0.9%	0.8%
K ₂ O	0.9%	0.3%	1.7%	1.0%
Na ₂ O	-	1.5%	-	-
SO ₃	0.6%	2.8%	0.1%	0.3%
MnO	0.5%	0.6%	-	-
Cr ₂ O ₃	0.1%	0.1%	-	-
Others	1.1%	0.5%	0.9%	0.8%

The proposed methodology presented satisfactory results. The estimated and effective SiO₂ and CaO contents presented considerably small deviation in both the waste cement and the reference cement. The estimated and effective Fe₂O₃ contents showed deviations

of 19.6% and 7.7% for the waste and reference cements, respectively. The largest deviation was observed for Al₂O₃ contents (-43.5% and -27.7%).

Table 8. Results of Bogue calculations and chemical parameters of the produced cements estimated from calculated chemical composition and obtained from XRF effective results.

Parameter	Waste cement		Reference cement	
	Estimated	Effective	Estimated	Effective
SR	2.57	2.69	1.98	2.18
AR	1.24	0.70	2.23	1.62
LSF	0.72	0.73	0.75	0.84
C ₃ S	0.0%	8.5%	0.0%	31.7%
C ₂ S	74.9%	67.0%	69.0%	42.4%
C ₃ A	7.2%	0.9%	15.9%	10.5%
C ₄ AF	13.8%	17.0%	11.4%	12.4%

The most important deviation of chemical parameters was observed for the alumina ratio of the waste cement and the alumina ratio and lime saturation factor of the reference cement. As a consequence, the C₃A content predicted by Bogue calculation for the waste cement was very low (0.9%), and a high C₃S content was calculated for the reference cement (31.7%). Because clinkers were produced at insufficient temperature for C₃S formation, free lime (CaO) was expected to be found in clinker cement composition, which may imply expansion problems.

The differences between the estimated and the effective results are justified by the simplicity of the calculation method, but also by the limitations of the chemical analysis technique used (i.e., XRF). The semi-quantitative results using a general database (Omnia) did not allow a more accurate determination of the chemical composition of the raw materials and the cements.

2.3.3 Mineralogical composition

The mineralogical analyses were carried out on samples of the belitic waste cement and the reference belitic cement. Fluorite was used as an internal standard. The diffractograms are shown in Figure 1. Table 9 shows the result of the quantitative analysis of the mineralogical phases.

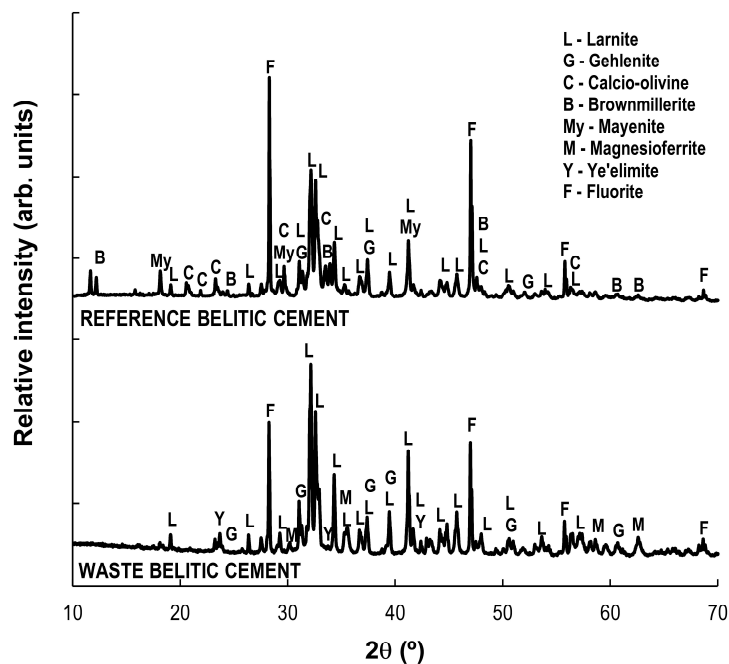


Figure 1. Diffractograms of the produced cements.

The waste cement revealed the presence of a very high belite content (78.6%), exceeding the amount predicted by Bogue calculation, and much higher than that observed in the reference cement (42.0%). This result shows that the waste performed well and the proportioning was successful. This phase (larnite β -C₂S) crystallizes at high temperatures, and, like the α -polymorph, had high reactivity and frequently occurs in cements (Pöllmann, 2002; Kacimi et al., 2009; Mindat, 2017a). However, a calcium-olivine content of 5.1% was observed in the reference belitic cement. This phase corresponds to

the γ -C₂S polymorph of larnite, and is known as dusting because of its large volume change and because it is weakly hydraulic at ambient temperature (Pöllmann, 2002; Yamnova et al., 2011). The nonoccurrence of this polymorph in the waste cement indicates that, in this sense, the cooling process was more effective for this one. It is also considered a good indicator, because this phase does not contribute to the strength gain.

Table 9. Results of quantitative analysis of mineral phases observed in produced cements.

Phase	Cement notation	Formula	Waste cement	Reference cement
Larnite (Belite)	β -C ₂ S	Ca _{8.00} Si _{4.00} O _{16.00}	78.6%	42.0%
Gehlenite	C ₂ AS	Ca _{4.00} Al _{4.00} Si _{2.00} O _{14.00}	4.3%	2.4%
Calcio-olivine	γ -C ₂ S	Ca _{8.00} Si _{4.00} O _{16.00}	-	5.1%
Brownmillerite	C ₄ AF	Ca _{8.00} Fe _{4.36} Al _{3.64} O _{20.00}	-	4.0%
Mayenite	C ₁₂ A ₇	Ca _{24.00} Al _{28.00} O _{65.99}	-	2.3%
Magnesioferrite	-	Mg _{8.00} Fe _{16.00} O _{32.00}	2.4%	-
Magnetite	-	Fe _{24.00} O _{32.00}	1.6%	-
Ye'elimite	C ₄ A ₃ \bar{S}	Ca _{8.00} Al _{12.00} S _{2.00} O _{32.00}	0.9%	-
Amorphous/Unknown	-	-	12.2%	44.3%

The gehlenite phase (C₂AS) occurred in both cements, but its content was higher in the waste belitic cement (4.3% versus 2.4%). By definition, C₂AS is a calcium silicate-aluminate of the melilite family with low hydraulic properties, and its formation is therefore undesirable (Hewlett, 2004; Pimraksa et al., 2009). The formation of the gehlenite phase is related to the higher contents of silica in the mixtures, especially in the waste cement (25.6%) (Hewlett, 2004). Mayenite (C₁₂A₇) was the only calcium aluminate phase observed, and it occurred only in the reference cement, because the waste cement had reduced alumina content. This phase is commonly found in calcium-alumina cements (Bensted, 2002), but may occur as an additional constituent in cements with high alumina content (Pöllmann, 2002). It is considered the most reactive phase among all types of

calcium aluminates and has an important role in high early strength cements. For this reason, its quantity has to be carefully regulated by cement manufacturers (AZO, 2002; Pöllmann, 2002). In any case, it has been observed that the increase in the amount of the aluminate phase is feasible in belitic cements and represents an effective strategy for increasing compressive strength at early ages. Therefore, it should be evaluated in future work involving waste belitic cements.

Only the reference cement had the tetra-calcium aluminoferrite phase, also known as ferrite phase (brownmillerite, C_4AF). The hydraulicity of the ferrite phase depends on the formation conditions and more reactivity is obtained at low temperature ($\sim 1,200^\circ\text{C}$), which was the case of the studied cements (Hewlett, 2004). The occurrence of this phase in belitic cements is recurrent in the literature. Contrary to what was reported by Iacobescu et al. (2011), despite the elevation in the iron content by the addition of BOFS, the formation of tetra-calcium aluminoferrite phase was not observed in the waste cement. However, that can be explained by the reduced Al_2O_3 content available, because it was consumed in the formation of gehlenite (and ye'elimite). In this way, iron appears in the magnetite phase or combined with magnesium in the magnesioferrite phase. The presence of ye'elimite (calcium sulfoaluminate - $C_4A_3\bar{S}$), is common in sulfo-aluminous cements (Hewlett, 2004; Londono-Zuluaga et al., 2017), and its presence in the synthesis of sulfo-aluminous belitic cements has also been reported (Shen et al., 2015). This phase is formed from alumina, calcium carbonate, and calcium sulfate at temperatures between 1,100 and 1,300 °C. Ettringite is formed by the hydration of ye'elimite, which contributes to the mechanical strength at early ages. Due to its expansive behavior, ye'elimite is used as component of shrinkage-compensating agents (Han et al., 2016) and the presence of sulfur in the chemical composition of grits (0.9%) and BOFS (0.3%) explains the formation of this phase in the waste cement.

Magnesioferrite was found in the waste cement. This phase is characterized by its high density (4.6-4.7 g / cm³), and relatively high hardness (6-6.5 on the Mohs scale), among other properties (Mindat, 2017b). Magnesioferrite synthesis can occur from magnesium magnetite or MgO and Fe₂O₃ oxides at temperatures from 800°C to 900°C (Antao et al., 2002; Amani & Costa, 2013). The occurrence of magnesioferrite in steel slag and modified steel slag has been reported in the literature (Li et al., 2011; Masurero et al., 2004). The magnetite phase was also observed.

2.3.4 Cement physical and mechanical properties

The results of the physical and mechanical characterization of the waste and reference belitic cements studied are given in Table 10 and in Figure 2. For comparison purposes, Table 10 also lists the normative values for commercial OPCs according to current Brazilian specifications.

Table 10. Physical and mechanical characteristics of produced cements and current Brazilian standard requirements for ordinary portland cement.

Parameter	Brazilian standard requirements for OPC	Waste belitic cement	Reference belitic cement
Density (g/cm ³)	-	3.33	3.19
Residue in the #200 sieve (75 μm) (%)	≤ 6 ^(a)	1.24	0.26
Blaine specific surface area (cm ² /g)	≥ 3000 ^(a)	4515	5759
Initial setting time (h:min)	≥ 01:00	01:40	00:07
Final setting time (h:min)	≤ 12:00 ^(b)	04:40	00:14
Expansion (Le Chatelier mold test) (mm)	≤ 5	10	2
Compressive strength at 28 days (MPa)	(≥ 25 / ≥ 32 / ≥ 40) ^(c)	2.14	12.56

(a) Refers to type III cement, which is the most rigorous requirement in accordance to Brazilian standard NBR 5733 (ABNT, 1991a).

(b) Refers to type IS cement, which corresponds to the maximum value allowed in accordance to Brazilian standard NBR 5735 (ABNT, 1991b).

(c) Refers to compressive strength classes 25MPa, 32MPa and 40 MPa applicable to type IS cements in accordance to Brazilian standard NBR 5735 (ABNT, 1991b). The compressive strength of the Portland cement is determined by the method NBR7215 (ABNT, 1996b).

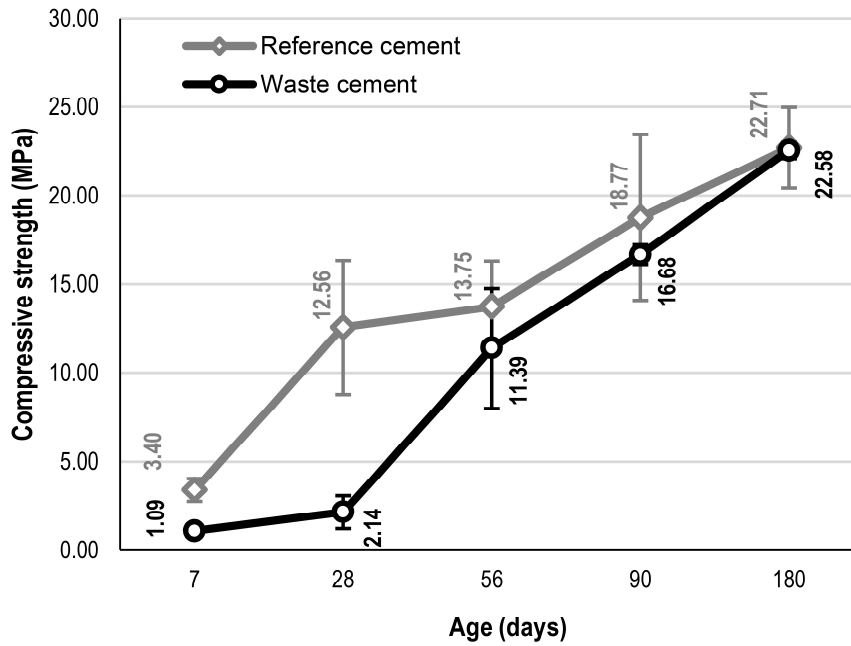


Figure 2. Compressive strength of the tested cements at ages of 7, 28, 56, 90, and 180 days [standard mortar, Brazilian method NBR 7215 (ABNT, 1996b)].

The belitic waste cement had a density of 3.33 g/cm^3 , which was 4.4% higher than that of the belitic reference cement. The high larnite content of the waste cement, the specific mass of which is $3.28\text{-}3.33 \text{ g/cm}^3$, contributed to this value. Magnesioferrite ($\text{Mg}_{8.00}\text{Fe}_{16.00}\text{O}_{32.00}$) and magnetite ($\text{Fe}_{24.00}\text{O}_{32.00}$) phases also contributed effectively to the higher density of this cement.

The reference cement had the best grindability and consequently higher fineness compared with the waste cement, which is evidenced by its specific surface area and its fineness index. Except for the calcium-olivine (hardness Mohs 6.5-7), the minerals that present the greatest hardness were observed exclusively or in greater quantity in the waste cement: larnite (Mohs hardness 6), gehlenite (5-6), and magnesioferrite (6-7). Brownmillerite, with hardness 3-3.5, was observed only in the reference cement.

The reference belitic cement had a very rapid setting time compared with OPC requirements and a superior compressive strength at the early ages compared with the

studied waste belitic cement. This is a very promising result because it can compensate the slow compressive strength gain, which is the major drawback of belitic cements. In this sense, the mayenite and ferrite phases may have contributed to the development of this property (Pöllmann, 2002). In addition, the ferrite phase had its reactivity potentiated by the formation temperature ($\sim 1200^{\circ}\text{C}$) (Hewlett, 2004). Another factor that contributed to the higher compressive strength of the reference belitic cement at early ages and fast setting time was its high fineness, evidenced by the results of specific surface area and residue in the # 200 sieve (0.075mm), 5759 cm^2/g and 0.26%, respectively. Finally, rapid cooling was reported in the literature as a condition for the production of highly reactive belitic cements (Popescu et al., 2003; Kacimi et al., 2009; Bouzidi et al., 2014). In this sense, the effectiveness of the cooling process was evidenced by the high content of the amorphous phase observed in both cements but mainly in the reference cement.

The high expansion observed in waste belitic cement may be related to the high sulfur content in the mixture and expansion of the ye'elinite phase (Han et al., 2016).

The mechanical strength of both cements at 90 days can be considered low compared with OPC; however, this was an expected behavior given the total absence of alite in these cements. In this sense, the results were in agreement with the literature. Belite reacts slowly with water, presenting little resistance until 28-day age, but its mechanical strength is equivalent to that of alite at 1 year of hydration (Taylor, 1990). The results show that the compressive strength of both cements tended to increase up to the age of 180 days, suggesting that it will probably reach considerably higher values at higher ages. The compressive strength curve of the waste cement was better-behaved, with considerably lower values until 28 days (2.14 MPa) and substantial gain thereafter (11.39 MPa at 56-day age, 16.68 MPa at 90 days, and 22.58 MPa at 180 days). This was expected behavior,

given the predominance of the belite phase (78.6%) and the absence of the $C_{12}A_7$ and C_4AF phases in its composition. The reference belitic cement, however, had a compressive strength considerably higher at 7 and 28 days (3.4 MPa and 12.56 MPa, respectively), given its $C_{12}A_7$ and C_4AF contents (4% and 2.3%, respectively), which contribute to compressive strength gain at early ages (Ramachandran et al., 2002; Pöllmann, 2002). The compressive strength of both cements tended to converge after the age of 28 days, as evidenced in the results of 56-, 90-, and 180-day aging.

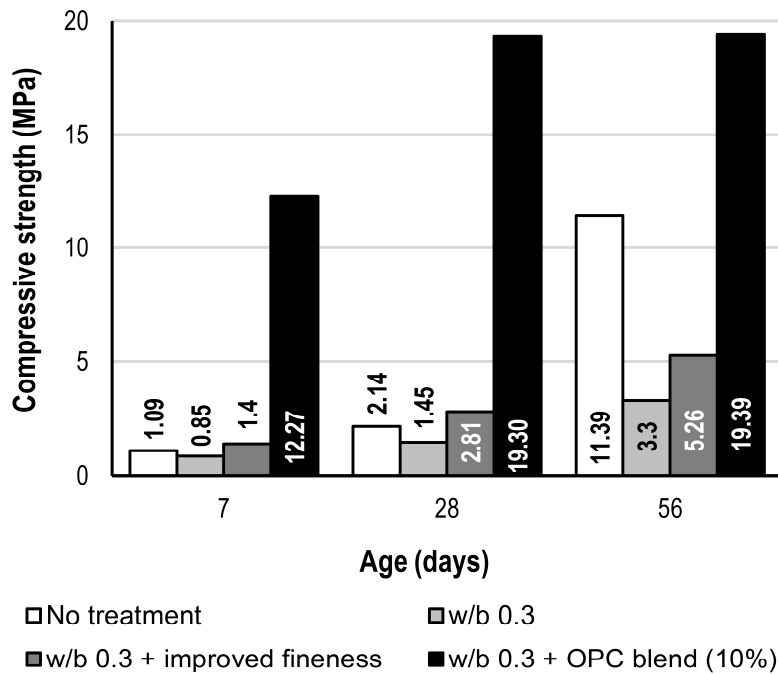


Figure 3. Results of the three proposed strategies to improve the compressive strength gain at early ages and the standard results of compressive strength of the waste belitic cement (7, 28, and 56 days).

The results of the three proposed strategies to improve the compressive strength at the early ages are shown in Figure 3. The reduction in the water:binder (w/b) was not effective in the present study and further investigations on the influence of the superplasticizer on the hydration kinetics are required to verify its retarding effect on this specific cement. The improvement of the fineness was also not efficient in producing significant gains in compressive strength at 7 and 28 days, and a reduction was observed

at 56 days compared with the untreated sample. The OPC blend was the only effective strategy. At 28 days, the OPC-blended sample reached 19.3 MPa, only 14% lower than the final strength reached at 180 days for the untreated sample. This simple procedure proved to be effective in mitigating the drawback of low compressive strength at early ages, with a reduced loss of eco-efficiency (considering the proposed low substitution rate of 10% by weight).

2.4 Conclusion

This paper evaluated a low environmental impact belitic cement produced entirely from industrial and mining waste were performed. Grits from the pulp and paper industry, basic oxygen furnace slag, and quartzite mining tailings were characterized and used as raw meal. A reference belitic cement was also produced using limestone and clay for comparison. The findings of this study are summarized as follows:

- The chemical and mineralogical characterization confirmed the similarities of grits and limestone as providers of CaO for clinker production. Quartzite was the main source of silica and alumina, and the Fe₂O₃ was supplied by the steel slag.
- The raw meal proportioning using the Bogue calculation proved to be efficient for obtaining optimized blends and belite-rich cement clinkers calcined at 1,250°C.
- Calcio-olivine, marvenite and brownmillerite were the minor mineralogical phases observed in the reference cement. Gehlenite, ye'elimite, magnetite, and magnesioferrite were observed in waste cement.
- The highest fineness and presence of marvenite and brownmillerite contributed for the rapid setting time of the reference belitic cement, and the waste cement

presented expansion values above that allowed for ordinary portland cements.

The other normative requirements were met.

- The mechanical strength gain of both cements was compatible with that expected for belitic cements. The reference cement had faster compressive strength gain at early ages than the waste cement; however, the compressive strength of the two cements converged at later ages.
- The reduction in water:binder ratio using a polycarboxylate-based superplasticizer and the increase in fineness proved to be ineffective as strategies to improve the compressive strength of the waste belitic cement at early ages. However, promising results were observed by mixing the waste belitic cement with 10% by weight ordinary portland cement, which corresponds to a simple and economic way to mitigate the drawback of the belitic cement with a reduced loss in its eco-efficiency.

2.5 Acknowledgements

The authors acknowledge the financial support provided by the Coordenação de Aperfeiçoamento de Pessoal de Nível Superior – Brasil (CAPES), Fundação de Amparo à Pesquisa do Estado de Minas Gerais – Brasil (FAPEMIG), Conselho Nacional de Desenvolvimento Científico e Tecnológico – Brasil (CNPq), Universidade Federal de Ouro Preto (UFOP), Universidade Federal de Viçosa (UFV), and Fundação Gorceix. Equipment and technical support provided by the Laboratory of Electronic Microscopy NANOLAB, Redemat, UFOP; the Laboratory of Construction Materials, Dept. of Civil Engineering, UFOP; and the Laboratory of Construction Materials, Dept. of Civil Engineering, UFV are gratefully appreciated. Thanks are also due to Brennand Cimentos

for support and supply of materials, and to the Research Group on Solid Waste RECICLOS-CNPq for infrastructure use and collaboration.

2.6 References

ABNT, 1991a. *NBR 5733: High early strength Portland cement - Specification*. Rio de Janeiro: Associação brasileira de Normas Técnicas - ABNT. (in Portuguese).

ABNT, 1991b. *NBR 5735: Blast furnace slag Portland cement - Specification*. Rio de Janeiro: Associação Brasileira de Normas Técnicas - ABNT. (in Portuguese).

ABNT, 1996a. *NBR NM 76: Portland cement - Determination of fineness by the air permeability method (Blaine method)*. Rio de Janeiro: Associação Brasileira de Normas Técnicas - ABNT. (in Portuguese).

ABNT, 1996b. *NBR 7215: Portland cement - Determination of compressive strength*. Rio de Janeiro: Associação Brasileira de Normas Técnicas - ABNT. (in Portuguese).

ABNT, 2001. *NBR NM 23: Portland cement and other powdered material - Determination of density*. Rio de Janeiro: Associação brasileira de Normas Técnicas - ABNT. (in Portuguese).

ABNT, 2003. *NBR NM 65: Portland cement - Determination of setting times*. Rio de Janeiro: Associação Brasileira de Normas Técnicas - ABNT. (in Portuguese).

ABNT, 2016. *NBR 11582: Portland cement - Determination of soundness by Le Chatelier test*. Rio de Janeiro: Associação Brasileira de Normas Técnicas - ABNT. (in Portuguese).

Ali, M.B. & Hossain, M.S., 2011. A review on emission analysis in cement industries. *Renew Sust Energ Rev*, (15), pp.2252-61. DOI: 10.1016/j.rser.2011.02.014.

Aloui, T., Ounis, A. & Chaabani, F., 2008. Maastrichtian Limestones of Feriana Mountain used in White Cement Production (Central West Tunisia). *J Am Ceram Soc*, 91(11), pp.3704-14. DOI: 10.1111/j.1551-2916.2008.02725.x.

Altoé, L.M. et al., 2012. Estudy of Natural and Degradation by Salt Spray of Red Ceramics Incorporated with Ornamental Rock Waste. *Mater Sci Forum*, 727-728, pp.1519-24. DOI: 10.4028/www.scientific.net/MSF.727-728.1519.

Amani, M.H. & Costa, A.C.S., 2013. Magnesioferrite synthesized from magnesian-magnetites. *Semina: Ciências Exatas e Tecnológicas*, 34(2), pp.135-44. DOI: 10.5433/1679-0375.2013v34n2p135.

Antao, S.M. et al., 2002. Thermal Analyses of Magnesioferrite. In Union, A.G. *American Geophysical Union, Fall Meeting 2002*. pp.#MR61A-1023.

Aprianti, E., 2017. A huge number of artificial waste material can be supplementary cementitious material (SCM) for concrete production – a review part II. *J Clean Prod*, 142, pp.4178-94. DOI: 10.1016/j.jclepro.2015.12.115.

AZO, 2002. *Calcium Aluminate Cements (CAC) - Phases and Structure of Calcium Aluminate Cements*. [Online] Available at: <https://www.azom.com/article.aspx?ArticleID=1635> [Accessed 07 november 2017].

Bastos, L.A.C., Silva, G.C., Mendes, J.C. & Peixoto, R.A.F., 2016. Using of iron ore tailings from tailing dams as road material. *J Mater Civil Eng*, 28(10), p.04016102. DOI: 10.1061/(ASCE)MT.1943-5533.0001613.

Battagin, A.F., 2011. Cimento Portland. In G.C. Isaia, ed. *Concreto Ciência e Tecnologia*. 1st ed. São Paulo: Arte Interativa. Ch. 6. pp.185-232. (in Portuguese).

Bensted, J., 2002. Calcium aluminate cements. In P. Barnes & J. Bensted, eds. *Structure and Performance of Cements*. 2nd ed. London: Spon Press. pp.114-39.

Bogue, R.H., 1929. Calculation of the compounds in Portland cement. *Ind Eng Chem Anal*, 1(4), pp.192-97. DOI: 10.1021/ac50068a006.

Bouzidi, M., Tahakourt, A., Bouzidi, N. & Merabet, D., 2014. Synthesis and Characterization of Belite Cement with High Hydraulic Reactivity and Low Environmental Impact. *Arab J Sci Eng*, 39(12), pp.8659-68. DOI: 10.1007/s13369-014-1471-2.

Crumbie, A., Walenta, G. & Füllmann, T., 2006. Where is the iron? Clinker microanalysis with XRD Rietveld, optical microscopy/point counting, Bogue and SEM-EDS techniques. *Cement Concrete Res*, 36(8), pp.1542-47. DOI: 10.1016/j.cemconres.2006.05.031.

Da Silva, M.J. et al., 2016. Feasibility Study of Steel Slag Aggregates in Precast Concrete Pavers. *ACI Mater J*, 113(4), pp.439-46. DOI: 10.14359/51688986.

Dias, L.S. et al., 2016. Rejeitos de mineração de quartzito para produção de argamassa colante. In *Anais do 22º Congresso brasileiro de Engenharia e Ciência dos Materiais - Natal - 06 a 10 de novembro de 2016*. Natal. pp.1-12. (in Portuguese).

Diniz, D.H., Carvalho, J.M.F., Mendes, J.C. & Peixoto, R.A.F., 2017. Blast Oxygen Furnace Slag as Chemical Soil Stabilizer for Use in Roads. *J Mater Civil Eng*, 29(9), p.04017118. DOI: 10.1061/(ASCE)MT.1943-5533.0001969.

DNPM, 2015. *Sumário mineral 2015*. Brasília: Departamento Nacional de Produção Mineral - DNPM. (in Portuguese).

Fassoni, D.P., Alvarenga, R.C.S.S., Pedroti, L.G. & Mendes, B., 2016. Clinker Production from Wastes of Cellulose and Granite Industries. *Characterization of Minerals, Metals, and Materials*, 2016, pp.691-96. DOI: 10.1007/978-3-319-48210-1_87.

Fontes, W.C., Mendes, J.C., Silva, S.N. & Peixoto, R.A.F., 2016. Mortars for laying and coating produced with iron ore tailings from tailing dams. *Constr Build Mater*, 112, pp.988-95. DOI: 10.1016/j.conbuildmat.2016.03.027.

Han, J., Jia, D. & Yan, P., 2016. Understanding the shrinkage compensating ability of type K expansive agent in concrete. *Constr Build Mater*, 116, pp.36-34. DOI: 10.1016/j.conbuildmat.2016.04.092.

Hewlett, P.O., 2004. *Lea's chemistry of cement and concrete*. 4th ed. Elsevier.

Iacobescu, R.I. et al., 2016. Ladle metallurgy stainless steel slag as a raw material in Ordinary Portland Cement production: a possibility for industrial symbiosis. *J Clean Prod*, 112(1), pp.872-81. DOI: 10.1016/j.jclepro.2015.06.006.

Iacobescu, R.I. et al., 2011. Valorisation of electric arc furnace steel slag as raw material for low energy belite cements. *J Hazard Mater*, pp.287-94. DOI: 10.1016/j.jhazmat.2011.09.024.

Ishak, S.A. & Hashim, H., 2015. Low carbon measures for cement plant - a review. *J Clean Prod*, 103, pp.260-74. DOI: 10.1016/j.jclepro.2014.11.003.

Kacimi, L. et al., 2009. Synthesis of belite cement clinker of high hydraulic reactivity. *Cement Concrete Res*, 39(7), pp.559-65. DOI: 10.1016/j.cemconres.2009.02.004.

Kajaste, R. & Hurme, M., 2016. Cement industry greenhouse gas emissions e management options and abatement cost. *J Clean Prod*, (112), pp.4041-52. DOI: 10.1016/j.jclepro.2015.07.055.

Koumpouri, D. & Angelopoulos, G.N., 2016. Effect of boron waste and boric acid addition on the production of low energy belite cement. *Cement Concrete Comp*, 68, pp.1-8. DOI: 10.1016/j.cemconcomp.2015.12.009.

Li, J., Yu, Q., Wei, J. & Zhang, T., 2011. Structural characteristics and hydration kinetics of modified steel slag. *Cement Concrete Res*, 41(3), pp.324-29. DOI: 10.1016/j.cemconres.2010.11.018.

Londono-Zuluaga, D. et al., 2017. Clinkering and hydration of belite-alite-ye'elimit cement. *Cement Concrete Comp*, 80, pp.333-41. DOI: 10.1016/j.cemconcomp.2017.04.002.

Marinho, A.L.B. et al., 2017. Ladle Furnace Slag as Binder for Cement-Based Composites. *J Mater Civil Eng*, 29(11), p.04017207. DOI: 10.1061/(ASCE)MT.1943-5533.0002061.

Masurero, A.B., DalMolin, D.C.C. & Vilela, A.C.F., 2004. Stabilization and technical feasibility of electric steel slag. *Ambient Constr*, 4(2), pp.57-81. (in Portuguese).

Mehta, P.K. & Monteiro, P.J.M., 2006. *Concrete - microstructure, properties, and materials*. New York: McGraw-Hill.

Meyers, G.D., McLeod, G. & Anbarci, M.A., 2006. An international waste convention: measures for achieving sustainable development. *Waste Manage*, 24, pp.505-13. DOI: 10.1177/0734242X06069474.

Miller, S.A., Monteiro, P.J.M., Ostertag, C.P. & Horvath, A., 2016. Comparison indices for design and proportioning of concrete mixtures taking environmental impacts account. *Cement Concrete Comp*, (68), pp.131-43. DOI: 10.1016/j.cemconcomp.2016.02.002.

Mindat, 2017a. *Larnite*. [Online] Available at: <https://www.mindat.org/min-2333.html> [Accessed 07 november 2017].

Mindat, 2017b. *Magnesioferrite*. [Online] Available at: <https://www.mindat.org/min-2501.html> [Accessed 08 november 2017].

Pedroti, L.G. et al., 2014. Incorporation of Granite Waste from Diamond Wire Sawing Process into Cement Matrix Concrete. *Mater Sci Forum*, 775-776, pp.571-76. DOI: 10.4028/www.scientific.net/MSF.775-776.571.

Pimraksa, K., Hanjitsuwan, S. & Chindaprasirt, P., 2009. Synthesis of belite cement from lignite fly ash. *Ceram Int*, 35(6), pp.2415-25. DOI: 10.1016/j.ceramint.2009.02.006.

Pinheiro, M.L. et al., 2013. Experimental evaluation of pressed blocks of soil-cement with grits addition. *Ambient Constr*, 13(2), pp.29-46. DOI: 10.1590/S1678-86212013000200004.

Pöllmann, H., 2002. Composition of cement phases. In P. Barnes & J. Bensted, eds. *Structure and Performance of Cements*. 2nd ed. London: Spon Press. Ch. 2. pp.25-56.

Popescu, C.D., Muntean, M. & Sharp, J.H., 2003. Industrial trial production of low energy belite cement. *Cement Concrete Comp*, 25(7), pp.689-93. DOI: 10.1016/S0958-9465(02)00097-5.

Ramachandran, V.S., Paroli, R.M., Beaudoin, J.J. & Delgado, A.H., 2002. *Handbook of thermal analysis of construction materials*. Norwich: Noyes Publications.

Sant'ana Filho, J.N. et al., 2017. Technical and environmental feasibility of interlocking concrete pavers with iron ore tailings from tailings dams. *J Mater Civil Eng*, 29(9), p.04017104. DOI: 10.1061/(ASCE)MT.1943-5533.0001937.

Santos, R.F. et al., 2017. Evaluation of Incorporation of Dregs in Mortar Production in Replacement of Hydrated Lime. *Mater Sci Forum*, 881, pp.351-56. DOI: 10.4028/www.scientific.net/MSF.881.351.

Shen, Y., Qian, J., Huang, Y. & Yang, D., 2015. Synthesis of belite sulfoaluminate-ternesite cements with phosphogypsum. *Cement Concrete Comp*, 63, pp.67-75. DOI: 10.1016/j.cemconcomp.2015.09.003.

Souza, T.I. & Cardoso, A.V., 2008. Utilização de resíduos sólidos da indústria de celulose kraft na fabricação de cimento; caracterização físico-química. In *Annals of the XVIII Brazilian Congress on Engineering and Material Science*. Porto de Galinhas. (in Portuguese).

Stutzman, P., Heckert, A., Tebbe, A. & Leigh, S., 2014. Uncertainty in Bogue-calculated phase composition of hydraulic cements. *Cement Concrete Res*, 61-62, pp.40-48. DOI: 10.1016/j.cemconres.2014.03.007.

Taylor, H.F.W., 1990. *Cement Chemistry*. London: Academic Press.

UN-HABITAT, 1993. *Small-scale production of Portland cement*. Nairobi: United Nations Centre for Human Settlements (Habitat).

Vilaplana, A.S. et al., 2015. Utilization of Ladle Furnace slag from a steelwork for laboratory scale production of Portland cement. *Constr Build Mater*, 94, pp.837-43. DOI: 10.1016/j.conbuildmat.2015.07.075.

WHD, 2017. *Portland cement clinker: The Bogue calculation*. [Online] Available at: <http://www.understanding-cement.com/bogue.html#> [Accessed 18th January 2017].

Yamnova, N.A., Zubcova, N.V., Eremin, N.N..Z.A.E. & Gazeev, V.M., 2011. Crystal Structure of Larnite β -Ca₂SiO₄ and Specific Features of Polymorphic Transitions in Dicalcium Orthosilicate. *Crystallography Reports*, 56(2), pp.210-20.

Zhang, M. et al., 2016. Manifest system for management of non-hazardous industrial solid wastes: results from a Tianjin industrial park. *J Clean Prod*, 133, pp.252-561. DOI: 10.1016/j.jclepro.2016.05.102.

Chapter 3

Production and evaluation of engineered recycled mineral admixtures obtained from basic oxygen furnace slag, iron ore tailings, quartz tailings and quartzite tailings

José Maria Franco de Carvalho, Keoma Defáveri, Júlia Castro Mendes, Wolfram Schmidt, Hans Carsten-Kühne, Ricardo André Fiorotti Peixoto

Abstract

One effective way to reduce the impact of concrete production is to replace the cement partially with supplementary materials originated from residues. To ensure technical feasibility and to enhance the performance of cement-based composites, the concept of engineered recycled mineral admixture (ERMA) is applied. ERMA's design and production aim at improving the properties of interest such as grain packing performance or cementing activity. In this work, ERMA's are obtained from four different industrial residues: basic oxygen furnace slag, iron ore tailings, quartz mining tailings, and quartzite mining tailings. The grinding performance was evaluated in three different programs, and the characterization included chemical and mineralogical composition, particle morphology and physical properties. Performance evaluations were carried out in blended pastes and mortars, including flow properties, hydration kinetics, durability, pozzolanic activity, and mechanical tests. The coarse ERMA's showed better flow performance, durability, and more economical production, while the fine ERMA's significantly improved mechanical performance by both filler effect and cementing action.

Keywords: Engineered recycled mineral admixtures, rheology, hydration kinetics, steel slag, mining tailings.

Cement and Concrete Composites

This manuscript was submitted on February 10th, 2019.

Current status: in review.

3.1 Introduction

In recent years, high- and ultra-high-performance concretes have been increasingly studied. Their development results from the availability of high technology materials, such as superplasticizers and mineral admixtures with binder properties, aided by the fineness and favorable morphological characteristics of engineered aggregates (Shi et al., 2015; Malier, 2018). The flowability properties of a powdered material intended to be used as filler and/or supplementary cementing material (SCM) are critical. The SCMs are traditionally defined as mineral admixtures that act in the cement-based composite by hydraulic or pozzolanic activity (Papadakis & Tsimas, 2002; Massazza, 1993; Snellings et al., 2012). The dispersion of their particles and their ability in moving through the mixture and occupy the spaces play critical roles for obtaining highly packed matrices with low water/binder ratios (Damineli, 2013; Maciel et al., 2018).

In addition, the concepts behind the achievement of high-performance concretes are also applied in obtaining products with lower environmental impact; both by employing residues from other production chains, and by reducing CO₂ emissions related to the cement production (Torgal & Jalali, 2010; García-Gusano et al., 2014; Kajaste & Hurme, 2016; Meyers et al., 2006; Zhang et al., 2016; Aprianti, 2017). In this sense, it is imperative to densify the microstructure – and the use of combined admixtures is a way to provide better results (Wu & Xin, 2018).

Recently, the characterization of pozzolan admixtures has been discussed, since some so-called pozzolans might play a role more related to physical action rather than a chemical one (Silva et al., 2018). In some cases, they may even present a mixed effect, involving dispersion, seed nucleation and consequent improvement in the degree of cement

hydration (Land & Stephan, 2012). The critical features of mineral admixtures acting as fillers are the specific surface area, particle size distribution, particle shape and density (Arvaniti et al., 2015a).

In this scenario, the present work studies the production and characterization of fines (powders) from industrial and mining residues for use in cement-based composites. The selected residues have been previously studied as aggregates or even as SCMs in concretes and mortars with promising results. They are: steelmaking slags (Diniz et al., 2017; Marinho et al., 2017; Da Silva et al., 2016), iron ore tailings from tailings dams (Bastos et al., 2016; Fontes et al., 2016; Sant'ana Filho et al., 2017; Fontes et al., 2018), quartz mining tailings (Dutra et al., 2014), and quartzite mining tailings (Dias et al., 2016; Mendes et al., 2019). This time, a novel investigation focused on the production of powders and their performance implications was carried out.

The materials were processed by high- and low-efficiency grinding in order to produce ERMAs with different particle size ranges, aiming at improving the packing density in cement-based composites. The materials were characterized for fineness and morphology, chemical and mineralogical composition, as well as the basic physical properties. Finally, tests in cement pastes and mortars with partial replacement of Portland cement for the proposed ERMAs were carried out. The evaluations included flow properties, interaction with polycarboxylate-based superplasticizers, influence on hydration kinetics, pozzolanic activity and mechanical performance.

The results obtained in this study contribute to the widening of the range of residues suitable for use as mineral admixtures. In this sense, the valuation of these by-products increases the sustainability aspect of society in a broader way, reaching various regions

with different economic vocations (Snellings et al., 2012; Aprianti, 2017). In addition, the limited supply of high-quality SCMs demands alternative regional substitutes, since it is generally accepted that higher cement replacement rates should be allowed and be assessed on the product performance (Scrivener & Kirkpatrick, 2008; Snellings et al., 2012).

3.2 Experimental

3.2.1 Physical, chemical and mineralogical characterization

The particle-size distributions of the raw residues were obtained by sieving, according to Brazilian Standard NBR NM 248 (ABNT, 2003), and the specific gravities were obtained by the le Chatelier flask method, NBR 16605 (ABNT, 2017). The particle size distribution of the powders was determined by the laser diffraction technique using a Bettersize 2000 device, and the chemical compositions of the samples were determined by X-ray fluorescence (XRF) using a PANalytical Epsilon3^x analyzer. These tests were performed in the Laboratory of Materials for Civil Construction / UFOP.

X-ray diffraction (XRD) technique was used to obtain the mineralogical characterization. The diffractograms were obtained in the Laboratory of Electron Microscopy – NANOLAB / UFOP, Brazil, using a Brucker D2 Phaser2nd generation device (Cu K α radiation, 40 kV, 30 mA, 10 - 70° 2 θ range, 0.02° step size, 1 s/step). The Rietveld refinement method was used for the quantitative mineralogical evaluation. To this purpose, the software X'Pert HighScore Plus v.3 and the databases ICDD pdf+ v.2016 were used. Fluorite was used as the internal pattern (10 % by mass). For the chemical and mineralogical characterization, samples with particle size ≤ 0.045 mm were obtained using agate mortar.

3.2.2 Grinding evaluation

Three grinding programs were tested to produce the ERMA: one low-efficiency grinding program (L), using a Marconi MA500 horizontal ball mill; and two high-efficiency grinding programs (H2 and H4), using a Retsch PM100 planetary ball mill. The grindings were performed by dry route. The devices' setups, as well as the grinding times, are shown in Table 1. The grinding evaluation and production of the ERMA were performed in the Laboratory of Materials for Civil Construction / UFOP, Brazil.

Table 1. Grinding programs: characteristics of the mills, setup parameters and grinding times.

Grinding program	Parameter	Information
Low-efficiency grinding (L)	Material (jar and balls)	Stainless steel
	Jar volume, cm ³	10,367
	Material volume, cm ³ (% jar volume)	1,740 (17%)
	Rotational speed, rpm	200
	Balls volume, cm ³ (% jar volume)	1,658 (16%)
	Balls (quantity / diameter, mm)	(7/22)(17/28)(34/31)(11/38)(16/41)
	Limit grinding time, min	180
High-efficiency grinding (H2)	Material (jar and balls)	ZrO ₂
	Jar volume, cm ³	500
	Material volume, cm ³ (% jar volume)	80 (16%)
	Rotational speed, rpm	200
	Balls volume, cm ³ (% jar volume)	64.3 (13%)
	Balls (quantity / diameter, mm)	(99/10)(191/5)
	Limit grinding time, min	120
High-efficiency grinding (H4)	Material (jar and balls)	ZrO ₂
	Jar volume, cm ³	250
	Material volume, cm ³ (% jar volume)	80 (32%)
	Rotational speed, rpm	400
	Balls volume, cm ³ (% jar volume)	64.3 (26%)
	Balls (quantity / diameter, mm)	(99/10)(191/5)
	Limit grinding time, min	45

For each program and material processed, grinding curves were obtained. They included the grinding times and the characteristic dimensions D10, D50 and D90 (where DN

corresponds to the opening of a theoretical sieve mesh, in mm, through which N % of the material passes). To this purpose, samples of the ground material weighing approximately 2 g were taken at the specified time intervals and analyzed according to particle size distribution, using the laser diffraction technique (Bettersize2000).

3.2.3 Production and characterization of the ERMAs

For each residue tested, two ERMAs with different particle sizes were evaluated in the performance tests: the henceforth called coarse ERMA (coarser-than-cement powder) and the henceforth called fine ERMA (finer-than-cement powder). The initial reference was selected considering the finest among the tested materials obtained in the L program for 30 minutes grinding time. Subsequently, the grinding times selected for the others were those to achieve similar fineness. The fine ERMAs intended to be the thinnest possible for each residue in the most efficient program.

The morphological evaluation was carried out using scanning electron microscope (SEM) images, obtained in the Laboratory of Electron Microscopy – NANOLAB / UFOP, using a Tescan Vega 3 microscope (high vacuum, SE images, 20 kV). The images were obtained from gold-coated powder samples (Quorum Q150).

The BET specific surface areas of the examined ERMAs were performed in a Micromeritics TriStar II device, using results of specific density determined by helium pycnometry (Porotec Pycnomatic ATC). These tests were performed in the Division of Technology of Construction Materials / BAM, Germany. The Blaine specific surface areas were determined according to ASTM C204 (ASTM, 2017) and NBR 16372 (ABNT, 2015). The Blaine measurements were performed in the Laboratory of Construction Materials / Federal University of Viçosa (UFV), Brazil.

We also propose a comparison between the measured results and theoretical specific surface areas of perfectly spherical particles with the same particle size distribution. The approximate specific surface areas (S) were calculated using Equations 1 and 2, where γ is the density of the considered material, and A and V are, respectively, the area (cm^2) and the volume (cm^3) of a sphere with a diameter corresponding to i % of the cumulative volume in the particle-size distribution obtained by laser diffraction.

Equation 1
$$S = \sum_{n=1}^{100} n_i A_i$$

Equation 2
$$n_i = 0.01 \cdot \frac{V_i}{\gamma}$$

3.2.4 Performance tests in blended cement pastes and mortars

3.2.4.1 Rheological evaluation and interaction with polycarboxylate-based superplasticizers

Rheological evaluations were conducted in the Division of Technology of Construction Materials / BAM (Germany) using a Viskomat NT rheometer (wing stirrer probe V0013, internal cup volume of 375 mL). The tests were carried out in blended cement pastes with a replacement rate of 10 % of the cement volume by the studied ERMAs. The solid volume fraction ϕ was fixed in 0.5 and deionized water at 20 ± 2 °C was used. A Portland cement CEM I 42.5 R was used in these tests.

The mixing procedure was performed in a mixer Kenwood Chef Classic Platin KM 416. The dry mixing process was carried out at low velocity for 60 s, after that, the water was added in the space of 30 s. Subsequently, two mixing periods of 1 min were performed in

high speed with a 30 s interval between them for scraping the bowl's wall and mixing paddle.

Two powder-type polycarboxylate-based superplasticizers (PCE) were used: the henceforth called PCE-LC (low backbone charge density, long graft chains), and the henceforth called PCE-HC (high backbone charge density, short graft chains). For the evaluations, the maximum PCE content was set in 0.25 % by equivalent cement mass (mass of cement correspondent to total volume of solids). This amount was divided into seven equal portions of 0.0357% added to the mixture along with the test.

The rotational speed was set at 240 rpm, and the torques were measured for each mixture and admixture contents. The time interval was set to 4 minutes for each determination to ensure the homogenization of the mixture and the stabilization of the measured torque values. The measurements were performed along the test, and the last values were taken.

3.2.4.2 Thermal analyses

The setting times were determined in the Laboratory of Construction Materials / UFV, Brazil, in blended pastes with a replacement rate of 25 % by volume. For this purpose, the Vicat needle test was performed (ASTM, 2013). For these tests, a high early strength cement CPV-ARI (ABNT, 1991) was used. The standard consistency paste was determined for the reference cement paste (100 % cement), and the same solid volume ratio was used in all tested blends ($\phi = 0.47$).

Isothermal calorimetry was used to obtain information on the exothermic reactions during hydration of blended cement pastes prepared at a cement replacement rate of 25 % by volume by the studied ERMA. The tests were performed in the Division of Technology

of Construction Materials / BAM using an 8-channel isothermal heat flow calorimeter (TAM Air). For this test, a Portland cement CEM I 42.5 R was used, and the solid volume of the pastes ϕ was set in 0.5.

TG/DTA evaluations were performed in REF cement-only pastes (Brazilian CPV-ARI) and blended pastes (cement replacement of 25 % by volume) at 28, 56 and 91 days. The pastes were prepared with a solid volume ratio $\phi = 0.47$ and stored in sealed containers. Moments before the tests, the samples were demolded, broken into small pieces and ground in an agate mortar in order to reach particle size ≤ 0.045 mm. The TG/DTA curves were obtained in the Laboratory of Materials for Civil Construction / UFOP, Brazil, using a Shimadzu DTG-60H device. It was used a platinum crucible, and the materials were heated from 25° to 1,000°C at 10°C·min⁻¹ in a N₂ atmosphere ($\mu\text{L}\cdot\text{min}^{-1}$). The evaluation consisted of calculations of the calcium hydroxide (CH) contents in the studied pastes. For this test, the peaks corresponding to the dehydroxylation of CH and decarbonation of calcium carbonate (CC) were identified, and their temperature ranges were defined using DTA curves. Thereafter, the corresponding weight losses were obtained from the TG curves; and the CH contents were calculated using Equation 3 (El-Jazairi & Illston, 1980), where CH% is the content of CH (in % by weight); W_{CH} and W_{CC} are weight losses correspondent to peaks of CH dehydroxylation and CC decarbonation, respectively; and W_i is the initial weight of the samples.

Equation 3
$$CH\% = \frac{4.11 \cdot W_{CH} + 1.68 \cdot W_{CC}}{W_i} \times 100\%$$

3.2.4.3 *Expansion in autoclave*

Soundness tests were performed in blended cement pastes with 25 % cement replacements by volume by the tested ERMA. The tests were conducted as prescribed

by the American standard ASTM C151 (ASTM, 2018) in the Laboratory of Materials for Civil Construction / UFOP, Brazil, using a Matest E070 autoclave. The pastes were prepared with a solid volume ratio $\phi = 0.47$ and prismatic specimens measuring 25 mm × 25 mm × 285 mm were molded. The tests were performed on specimens aged one day.

3.2.4.4 Compressive strength

Finally, the mechanical strength was analyzed in standard mortars, based on Brazilian standard NBR 5753 (ABNT, 2016). The mortars were produced with blended-cements and standard sand in the volume ratio 1:3. The water to fine ratio (w/f) was set in 1.46 by volume. The study was carried out in a reference cement mortar, and modified mortars with 25 % cement replacement by volume by the tested ERMAs. Cylindrical specimens measuring $\varnothing 50 \times 100$ mm were molded, demolded after 24 h, and maintained immerse in saturated lime water for the following 27 days. The tests were performed in the Laboratory of Materials for Civil Construction / UFOP, using a universal hydraulic press EMIC20000 equipped with a 200 kN load cell.

3.3 Results and discussion

3.3.1 Characterization of the raw material

BOFS showed the highest specific gravity (3.770 g/cm³), followed by IOT (3.537 g/cm³). These values indicate that the high addition of these powders can increase the density of the resulting composites. In some cases, it can be considered a disadvantage (e.g., structural concrete, transport logistic), but in other cases, it does not pose any technological problems (e.g., pavers). QT and QIT had specific densities of 2.956 g/cm³ and 2.744 g/cm³, respectively, which is consistent with siliceous materials such as quartz

sand, or rocky materials such as granite or gneiss. Therefore, no significant changes in the density of cementitious products are expected using these materials.

IOT was originally the thinnest material, with approximately 100 % of its particles having diameters of less than 1 mm. This represents an economic advantage to produce the powders since a reduced grinding time is expected. QIT covers a large particle-size-range (6 – 0.001 mm) with a high amount of powdery material in the raw state (~50 %). Additionally, its high rock weathering degree indicates a low grinding energy requirement. The original particle size distribution of the raw BOFS and QT was similar and compatible with the 4.75 to 12.5 mm particle size range applicable to coarse aggregates (ABNT, 2005). To produce powders, however, additional energy is consumed, compared to the IOT and QIT samples.

The results of the chemical characterization by XRF are shown in Table 2. Table 3 shows the mineralogical composition of the tested residues.

Much of the Ca content in the BOFS sample is in the form of silicates. In fact, BOFS diffractograms show the presence of larnite (Ca_2SiO_4), brownmillerite [$\text{Ca}_2(\text{Al,Fe})_2\text{O}_5$], and calcite (CaCO_3); however, reduced amounts of lime (CaO) were still found. Periclase (MgO) was also identified in relatively large amounts (7.1 %). Wuestite (FeO) and helvine [$\text{Mn}_4\text{Be}_3(\text{SiO}_4)_3\text{S}$] were also observed. The presence of larnite and brownmillerite indicates binding properties. Pozzolanic activity is also expected due to the presence of Si, Al, and high amorphous content. In fact, previous studies have also demonstrated the binding properties of BOFS (Diniz et al., 2017), mainly in old age.

Table 2. Chemical composition of the tested residues (given by the XRF analysis in oxides).

Parameter	Grits (%)	BOFS ^(a) (%)	IOT (%)	QT (%)	QIT (%)
SiO ₂ %	1.8	15.6	35.5	95.5	80.0
Al ₂ O ₃ %	0.9	4.4	5.8	1.5	15.9
Fe ₂ O ₃ %	0.4	31.2	56.9	1.9	0.4
CaO %	94.3	36.8	0.2	0.2	-
MgO %	0.5	5.0	0.2	-	0.1
K ₂ O %	0.2	-	-	-	2.8
Na ₂ O %	-	-	-	-	-
SO ₃ %	0.9	0.4	-	-	-
MnO %	-	3.5	-	-	-
Cr ₂ O ₃ %	-	0.8	-	-	-
V ₂ O ₅ %	-	0.1	-	-	-
P ₂ O ₅ %	-	1.5	-	-	-
TiO ₂ %	-	0.5	-	-	-
Other oxides, %	1.0	-	1.4	0.8	0.8
LOI, %	41.4	1.1	3.1	0.3	1.2

(a) After magnetic separation

Table 3. Mineralogical composition of the tested residues.

Residue	Phase	Reference chemical formula	Reference	Content (%)
BOFS	Larnite	Ca ₂ SiO ₄	ICSD 00-042-178	9.1%
	Brownmillerite	Ca ₂ (Al,Fe) ₂ O ₅	ICSD 98832	8.8%
	Periclase	MgO	ICSD 52023	7.1%
	Wuestite	FeO	ICSD 27237	6.3%
	Calcite	CaCO ₃	ICSD 20179	1.3%
	Helvine	Mn ₄ Be ₃ (SiO ₄) ₃ S	ICSD 201638	0.8%
	Lime	CaO	ICSD 163628	0.7%
	Amorphous		-	65.9%
IOT	Quartz	SiO ₂	ICSD 00-046-1045	56.2%
	Hematite	Fe ₂ O ₃	ICSD 88417	25.6%
	Goethite	Fe ⁺⁺⁺ O(OH)	ICSD 239324	18.2%
QT	Quartz	SiO ₂	ICSD 00-046-1045	100%
QIT	Quartz	SiO ₂	ICSD 00-046-1045	91.8%
	Muscovite	KAl ₂ (Si ₃ Al)O ₁₀ (OH) ₂	ICSD 74609	8.2%

Chemical and mineralogical compositions indicate that IOT is a crystalline and inert material, and thus no chemical binder action is expected. However, the filler effect,

promoting densely packed matrices, explains its good performance in cement-based composites (Sant'ana Filho et al., 2017; Fontes et al., 2018).

Predominance of SiO_2 and Al_2O_3 were observed in QIT sample as quartz and muscovite. Finally, the QT was predominantly quartz, with small amounts of Al_2O_3 and Fe_2O_3 . Studies on quartz fines as SCMs have been reported in the literature, some of which involving chemical activation by grinding culminating in pozzolanic properties (Benezet & Benhassaine, 1999; Vizcayno et al., 2010; Souri et al., 2015).

***3.3.2 Grinding evaluation and production of the ERMA*s**

The grinding curves are shown in Figure 1. The program H4, besides having presented the best results, also showed a very significant gain in the first 15 minutes, with a subsequent strong tendency to stabilization for all residues and characteristic dimensions. For BOFS and IOT, this trend was more evident, indicating that grinding times greater than 15 minutes for these two residues in the program H4 are not effective and represent a waste of energy.

The L-curves presented no stabilization, but reductions in the grinding rates along the time for all residues and characteristic dimensions. The same was observed in the H2-curves.

Considering the minimum grinding time in the L program (30 minutes), QIT and IOT reached the greatest (and very similar) fineness. For this reason, they were selected as the reference for the coarse ERMA

s used in this research. For BOFS, the required grinding time to reach the same fineness level was 180 minutes; for QT sample, 120 minutes.

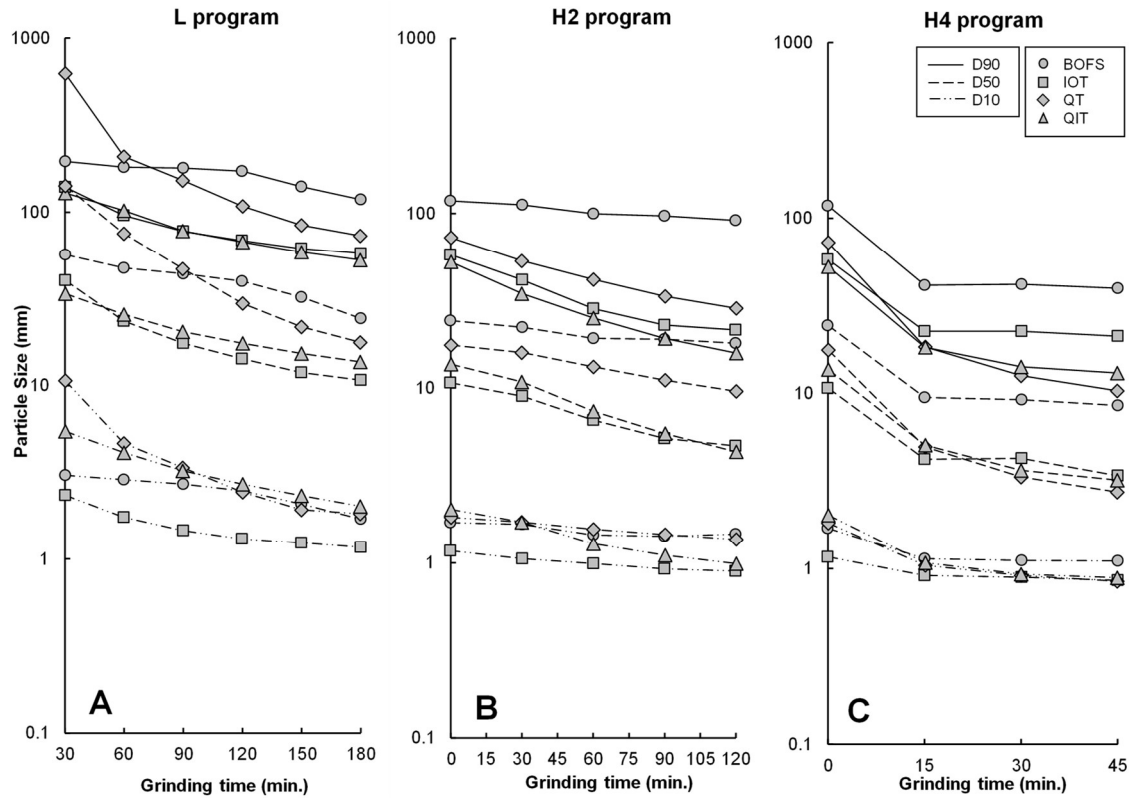


Figure 1. Grinding curves of the studied residues for the grinding programs adopted in this research: (A) low-efficiency program L; (B) high-efficiency program H2; and (C) high-efficiency program H4.

Four selected coarse ERMA and four selected fine ERMA were subjected to the characterization program and performance evaluations. The selected ERMA, the notations used on this point forward, the grinding programs and grinding times are listed in Table 4.

Table 4. RMA selected for the characterization program and performance evaluations: classification, notation, grinding programs used in the production and grinding times.

Classification	Notation	Grinding program	Grinding time (min)
Coarse ERMA	BOFS-L	L	180
	IOT-L	L	30
	QT-L	L	120
	QIT-L	L	30
Fine ERMA	BOFS-H	(L + H4)	(180 + 15)
	IOT-H	(L + H4)	(180 + 45)
	QT-H	(L + H4)	(180 + 45)
	QIT-H	(L + H4)	(180 + 45)

3.3.3 Particle size distribution, specific surface area and morphology

The particle size distribution curves are shown in Figure 2. The results of BET specific surface area and Blaine specific surface area are shown in Table 5. The results of the calculations of approximated theoretical specific surface areas of perfectly spherical particles with the same particle size distributions are also shown in the same table.

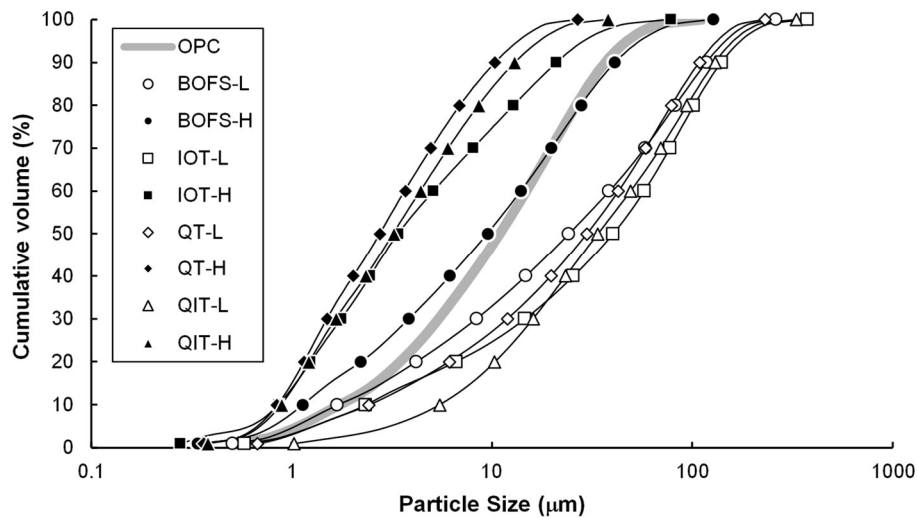


Figure 2. Particle size distribution curves of the selected ERMAs and the Brazilian CPV ordinary Portland cement (OPC).

Table 5. Results of Blaine specific surface area with test parameters and comparison with theoretical values

Material	Specific surface area (cm ² /g)		Theoretical (spherical particles) (cm ² /g)
	BET	Blaine	
BOFS-L	24252	3028	2635
BOFS-H	20678	4620	4660
IOT-L	29547	2202	2264
IOT-H	66522	6442	8369
QT-L	11039	3100	2736
QT-H	44123	11818	10605
QIT-L	3983	2386	1656
QIT-H	59054	11519	10428

The results of the specific surface area obtained using the BET technique and Blaine method differ significantly. As expected, the numerical results of the BET measurements are significantly larger (2 to 13 times), since the technique allows a detailed coverage of the surfaces with their protrusions and recesses. On the other hand, the viscous flow permeability is able to measure the external or surrounding area of the particles of a powdered sample (Shirai et al., 2011), which is not possible by adsorption methods (Lowell et al., 2012). In addition, the performance of a powdery material subject to an airflow provides an overview of its ability to move in a fluid medium.

For this reason, the results of the Blaine measurements are closer to the theoretical values calculated for spherical particles. However, the accuracy of Blaine results was significantly affected by the agglomeration of the clayey particles presented in IOT samples, leading to lower specific surface area values compared to the theoretical spherical particles.

SEM images of the selected ERMAs are shown in Figure 3. The general volumetric and equant shape of the BOFS-L particles explains the values of Blaine measurements close to theoretical spherical values, but their rugged surfaces lead to a relatively high BET specific surface area. High-efficiency grinding significantly reduced the roughness of the particles, reflecting in an unexpected reduction in BET results for BOFS-H. This strange behavior is also due to the fact BOFS-H has not achieved great fineness compared to other fine ERMAs. Moreover, the reduction in the BET specific area and the proximity of the Blaine measurement to the theoretical value confirm that high efficiency grinding resulted in a shape improvement in the BOFS-H particles, making them less rugged and more rounded.

Large angular particles (quartz) mixed with small and tabular ones (probably clay minerals) are the main features of the IOT powders. The high efficiency grinding improved the shape of the quartz particles, making them more equant and less rugged; but large amounts of thin clayey particles adhered onto larger ones were observed in both fine and coarse materials. It explains the reduced values of the Blaine specific surface area compared to the theoretically calculated value (agglomeration).

The QT-L powder comprises irregular angular particles with sharp edges. The low roughness and low presence of adhered material partially offset the less favorable geometry. On the other hand, the QT-H powder contains particles of regular geometry, predominantly volumetric (angular and subangular), with the edges being less sharp (tending to be rounded in some cases).

Finally, the QIT-L presented the worst morphological characteristics, which explains the large deviation between Blaine and theoretical specific surface areas. The particles are predominantly irregular, including tabular and acicular ones. Sharp edges were observed, but the surfaces are predominantly smoothed. Reduced amounts of small particles were observed, corresponding to the higher D10 value among the coarse ERMA's. As a result, this material presented the lowest BET value. The high-efficiency grinding promoted a significant improvement in the particle shape (of the larger ones), but the process produced many thin and tabular particles that increased the BET specific surface area. However, the Blaine specific surface area approached the theoretical value; this being probably due to the agglomeration of the thin particles (the same phenomenon observed for IOT).

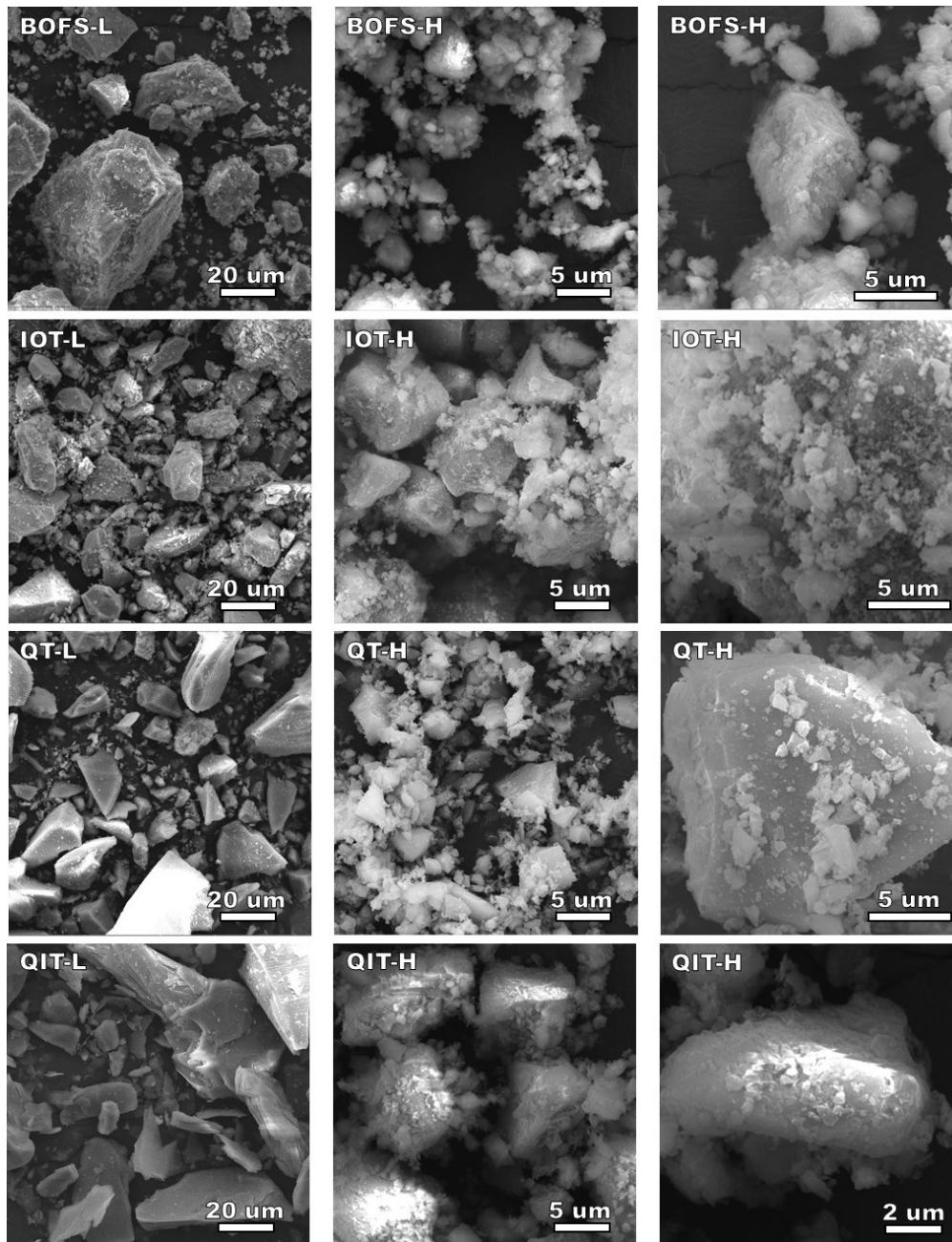


Figure 3. SEM micrographs of the studied powders: BOFS-L; BOFS-H; IOT-L; IOT-H; QT-L; QT-H; QIT-L; and QIT-H.

3.3.4 Influence of the ERMA's in the rheology and interaction with superplasticizers

Figure 4 shows the results of torque measurements in the rheological tests performed in cement pastes in the absence of chemical admixtures. The cement-only REF paste showed the highest torque of all tested pastes.

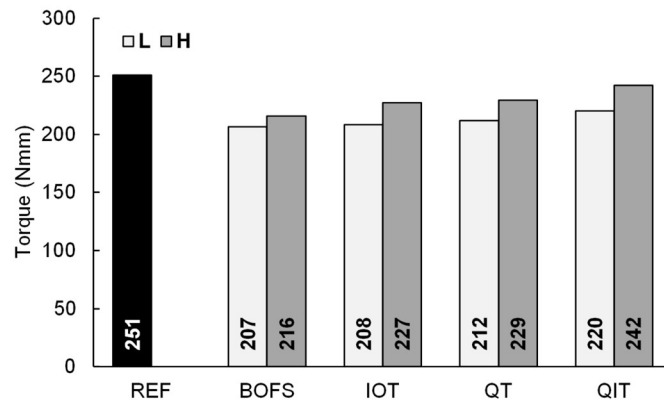


Figure 4. Results of torque measurement in the rheological tests performed in REF cement paste and blended pastes in the absence of chemical admixtures.

The behavior was governed by the particle size, but it was strongly affected by the particles' morphologies. The coarser ERMA showed the most effective plasticizer effect. The best overall result was observed for BOFS-L, followed by IOT-L and QT-L. Finally, QT-H, IOT-H and QIT-H pastes showed the highest torques. BOFS-L paste exhibited good flow despite the relatively high BET specific surface area of BOFS-L. This suggests that the flow performance was more affected by the envelope shape than by the surface roughness.

Finally, the increase in the specific surface area of the dry mixtures is usually related to an increase in shear stress (Shanahan et al., 2016). Nevertheless, the incorporation of the fine ERMA promoted a plasticizer effect, probably due to their favorable particle shapes. In addition, the grain packing enhancement reduced the volume of voids previously occupied by water, which increases the volume of water available to lubricate the system.

All tested ERMA showed good interaction with both polycarboxylate-based superplasticizers, PCE-LC and PCE-HC (Figure 5 and Figure 6, respectively). They demonstrated to be very effective in reducing shear stress, as expected (Park et al., 2005;

Puertas et al., 2005; Schober & Flatt, 2006). As a result, the blended pastes exhibited a pattern of torque reduction similar to REF paste.

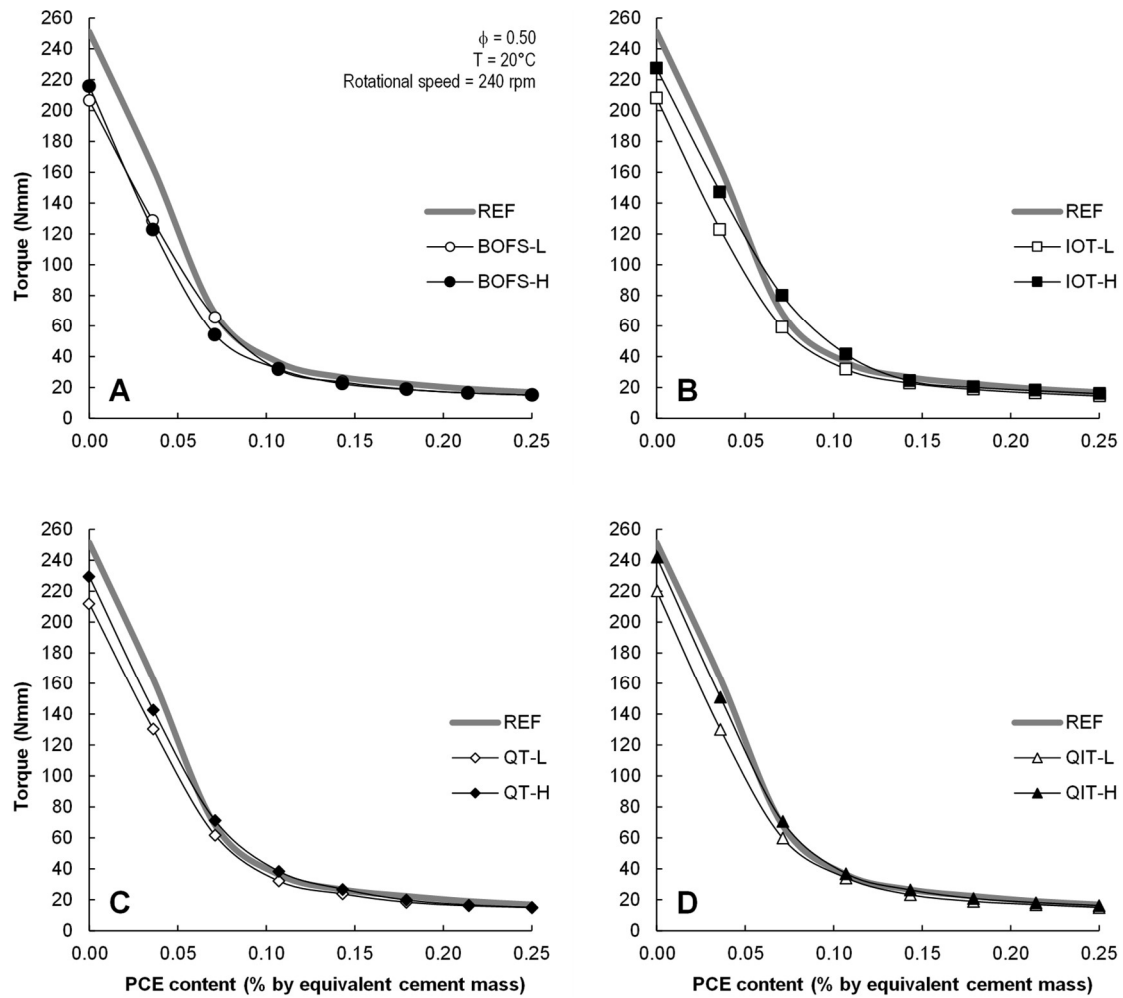


Figure 5. Curves Torque vs. PCE-LC content for the REF cement-only paste and blended pastes with (A) BOFS powders; (B) IOT powders; (C) QT powders; and (D) QIT powders.

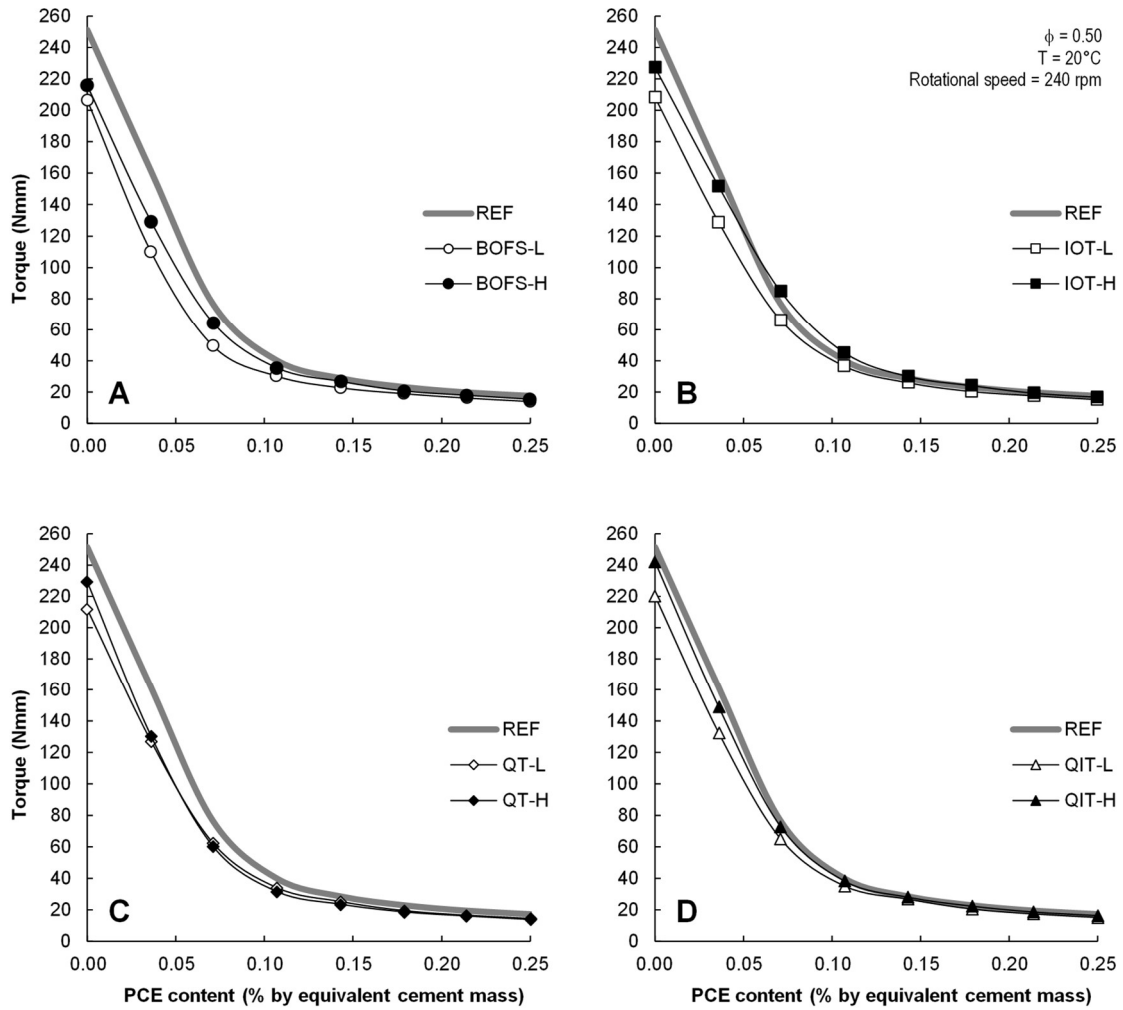


Figure 6. Curves Torque vs. PCE-HC content for the cement-only paste (REF) and blended pastes with (A) BOFS powders; (B) IOT powders; (C) QT powders; and (D) QIT powders.

No substantial differences in the torque values were observed for the two different PCEs. However, the pastes containing PCE-LC presented slightly lower values in both REF and blended pastes in most of the cases. Thus, PCE-LC was more effective in reducing the torque, mainly for the intermediary dosages. It suggests that, for the tested conditions, the long side chains of the PCE's molecules were more effective in reducing the shear stresses than the adsorption rate. Regarding the ERMA's, the particles' size and shape exerted greater influence on the pastes containing PCE-LC, while PCE-HC was more sensitive to ERMA's chemical and mineralogical compositions.

3.3.5 Influence of the ERMAs in the hydration kinetics

Figure 7 shows the results of setting times by the Vicat needle penetration test. The blended pastes with 25 % cement replacement by volume for the coarse ERMAs tended to have the most extended delays compared to REF paste. The pastes QIT-H (4 %), QT-H (10 %) and IOT-H (14 %) showed the shortest delays.

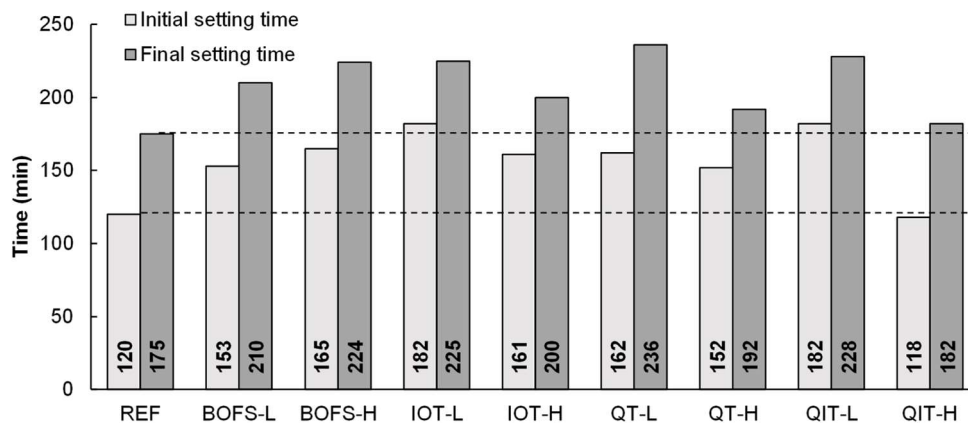


Figure 7. Results of initial and final setting times for cement-only REF paste and blended pastes.

In general, the ERMAs showed retarding effects. This behavior is related to the reduction in the amount of effective binder (dilution effect), and the slow reactivity or chemically inert properties of these powders. However, except for BOFS, the use of fine ERMAs resulted in faster setting times compared to coarse ones, with an indication of a strong influence of the chemical/mineralogical composition.

The isothermal calorimetry curves are shown in Figure 8, Figure 9, and Figure 10. In the absence of superplasticizers, the pastes showed two peaks between the acceleration and deceleration periods. The first relates to the hydration of C_3S and the second relates to the renewed hydration of C_3A (Schmidt, 2014). Sun et al. (2018) affirm that instantaneous dissolution rates of setting regulators affect hydration kinetics and mechanical strength

development. With the increase in cement alkalinity, the first peak in the isothermal profile tends to be higher, which is also related to the early formation of high-sulfate calcium hydrosulfoaluminate (AFt phase or ettringite).

The cement-only REF paste curve shows a clear separation of these peaks with the second one being higher. Pastes containing coarse ERMA s showed a longer delay between the peaks with the first being more pronounced. The paste containing IOT-H also showed the first peak more intense than the second, while the paste containing BOFS-H presented the two peaks with similar intensity. Pastes containing the quartz-based QT-H and QIT-H presented the shortest delays and the second peak more intense than the first (behavior similar to the REF paste).

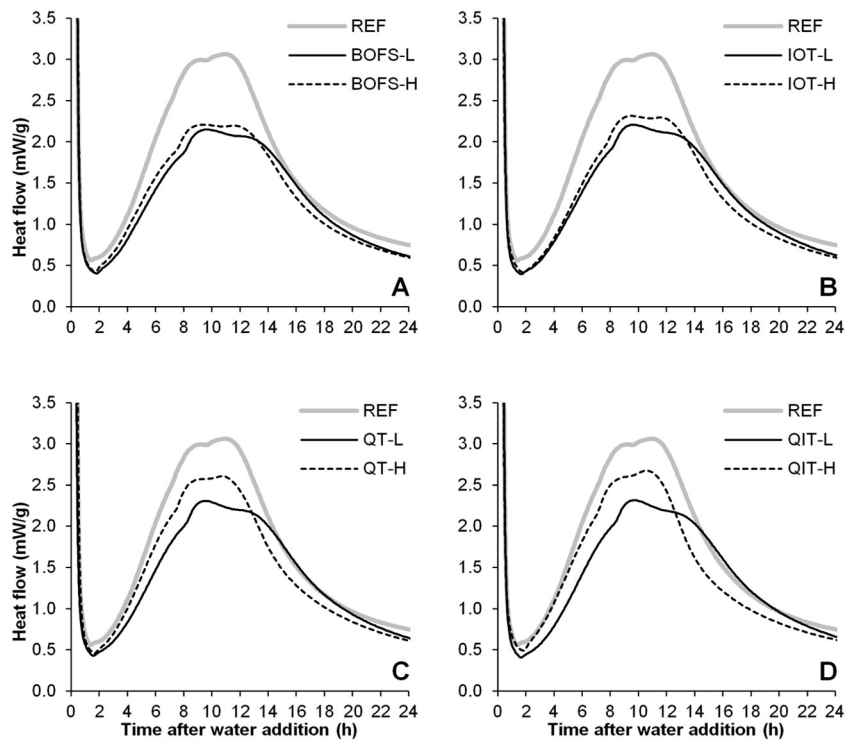


Figure 8. Isothermal calorimetry curves of cement-only paste (REF) and blended pastes (25 % cement replacement by volume) in the absence of chemical admixtures: (A) REF and BOFS blends; (B) REF and IOT blends; (C) REF and QT blends; (D) REF and QIT blends.

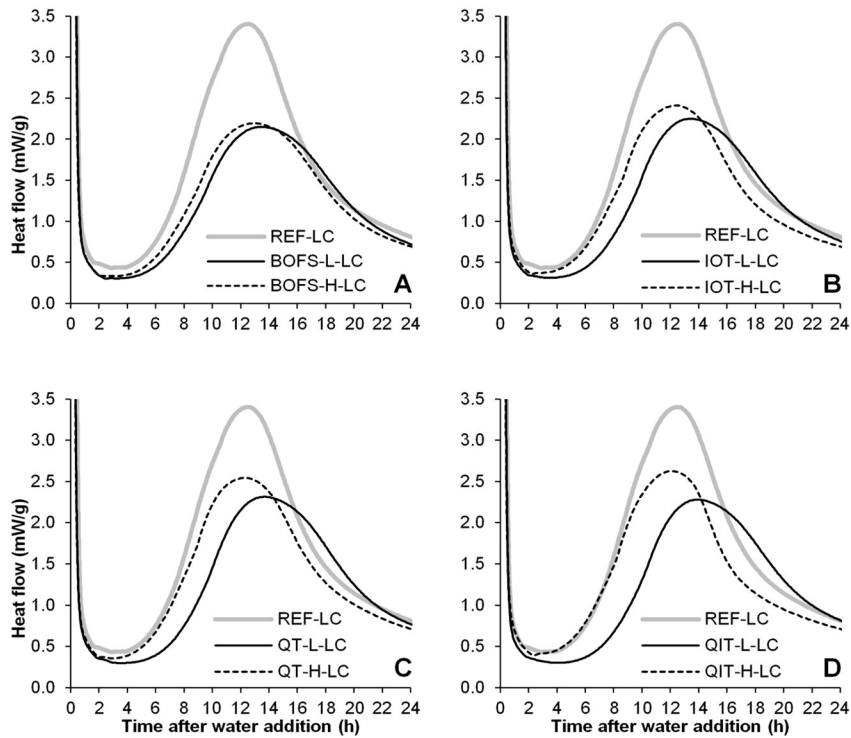


Figure 9. Isothermal calorimetry curves of cement-only paste (REF) and blended pastes (25 % cement replacement by volume) in the presence of PCE-LC: (A) REF and BOFS blends; (B) REF and IOT blends; (C) REF and QT blends; (D) REF and QIT blends.

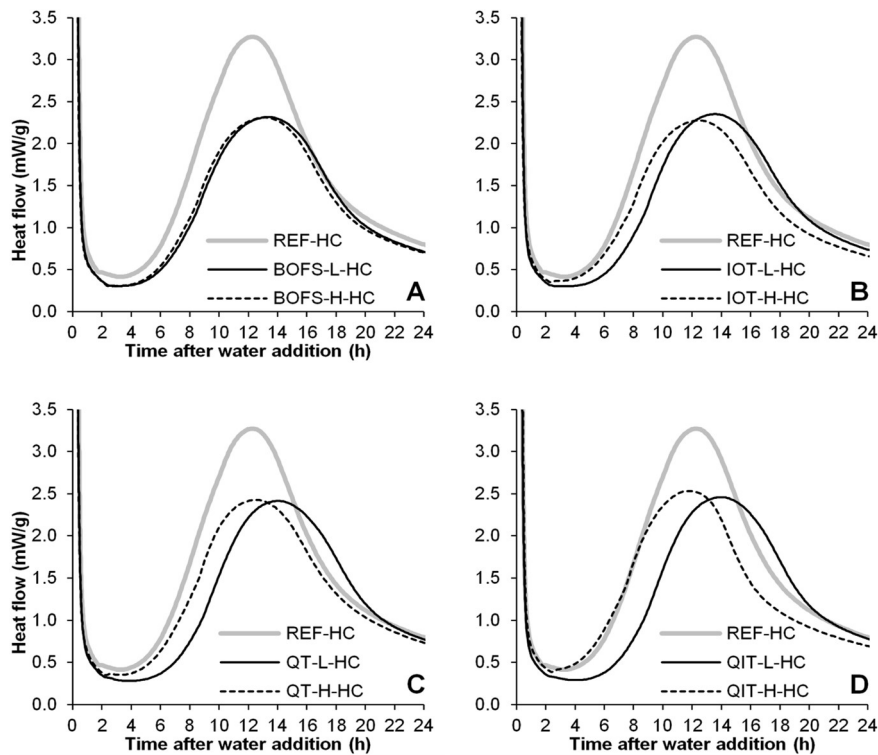


Figure 10. Isothermal calorimetry curves of cement-only paste (REF) and blended pastes (25 % cement replacement by volume) in the presence of PCE-HC: (A) REF and BOFS blends; (B) REF and IOT blends; (C) REF and QT blends; (D) REF and QIT blends.

Figure 11 shows graphics comparing the intensity of these peaks and times. It was observed that pastes containing coarse ERMAs had longer delays, mainly for reaching the second peak. Reduced delays were observed for fine ERMAs, with accelerating effects observed for QT (second peak) and mainly for QIT (two peaks).

The behaviors are closely related to the specific surface area of the ERMAs, but they are strongly influenced by the chemical/mineralogical composition. In this sense, the nucleation seed effect promoted by the quartz-based fine ERMAs (QT-H and QIT-H) was highly effective. It indicates that the high-efficiency grinding produced ultrafine quartz particles (possibly physically activating them), which contributed to the increase in the hydration degree of the cement particles. In this sense, several authors have also observed that ultrafine grinding effectively improves the reactivity of supplementary cementing materials (Mitrović & Zdujić, 2014; Souri et al., 2015; Burris & Juenger, 2016; Cordeiro et al., 2016).

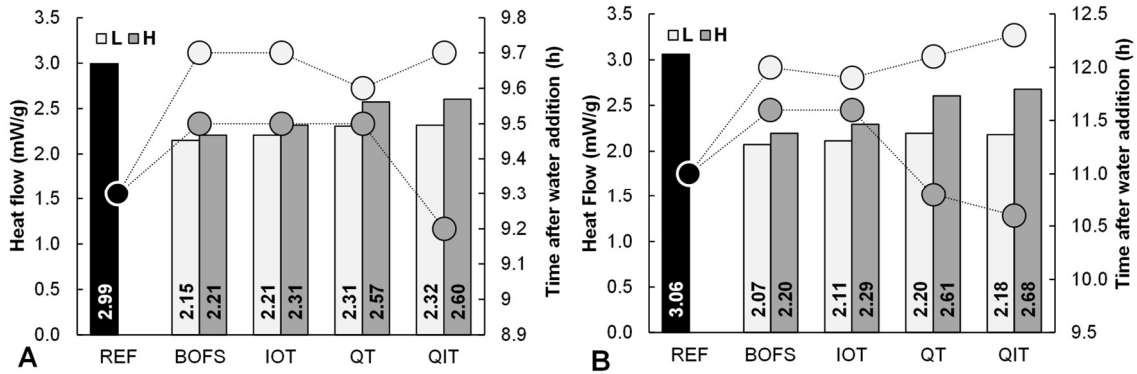


Figure 11. Results of heat flow intensity and associated time for cement-only paste (REF) and blended pastes (25 % cement replacement by volume): (A) first peak between acceleration and deceleration periods; (B) second peak between acceleration and deceleration periods.

Pastes containing PCE presented an expected strong retarding effect (Hanehara, 1999; Yamada et al., 2001; Puertas et al., 2005; Schmidt, 2014). The effect of the PCE charge density, however, was less significant. In fact, a correlation between charge density and

setting time is not clear and is strongly dependent on the total amount of polymer and temperature (Schmidt, 2014). The increase in delays, however, is associated with undesirable consequences such as segregation and postponements in construction schedules. In this sense, the coarse powders deserve special attention.

On the other hand, except for BOFS-H, consistent acceleration effects were observed in the pastes containing fine ERMA (especially QIT-H). In this sense, ternary blends containing coarse and fine ERMA can be effective strategies to mitigate the undesirable effects listed here; and QIT-H showed the best overall potential as a correction material.

The results of peak intensity and associated times are shown in Figure 12.

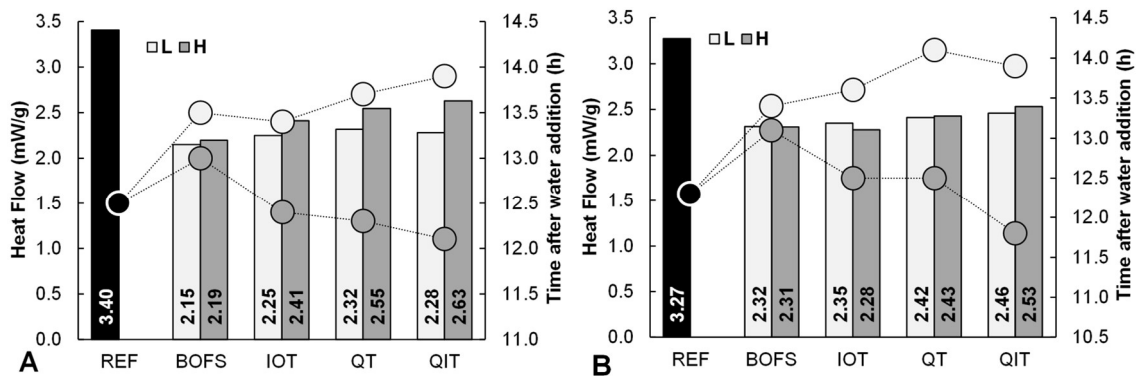


Figure 12. Results of peak intensity of the acceleration period and associated time for cement-only paste (REF) and blended pastes (25 % cement replacement by volume): (A) in the presence of PCE-LC (0.25% of the cement mass); (B) in the presence of PCE-HC (0.25% of the cement mass).

PCE affects the nucleation and growth of early Aft, which probably contributed to the presence of only one peak between the acceleration and deceleration periods. Changes in amount and total Aft surface are also dependent of the PCE type, and these changes are, thus, probably related to the stabilization of former Aft precursors due to adsorption of PCE on their surfaces (Frunz et al., 2018; Chen et al., 2018). In fact, Stroh et al. (2016) observed that the Aft formation in hydrated cement paste is strongly dependent of the

PCE type and amount, but in high concentration, both low and high charge PCEs increase the suppression.

In addition, the C-S-H structure is affected by the presence of PCE (Puertas et al., 2005; Kanchanason & Plank, 2018). However, the strong seeding effect of the delayed nanofoil-like C-S-H contributes to an early strength development (Kanchanason & Plank, 2018). This can be related to the fact that REF pastes containing PCE presented higher peaks compared to REF paste in the absence of PCE (and the highest peak was observed for the REF paste containing PCE-LC). However, in blended pastes, this effect was less significant, and the intensity of the peaks remained similar to that observed in the absence of PCE. Finally, in the presence of PCE, the fineness had a significant influence on the peak times and low influence on the peak intensities (mainly for PCE-HC).

3.3.6 Pozzolanic activity

The CH content based on the thermogravimetric curves of the cement pastes with 28, 56 and 91 days are shown in Figure 13. The use of fine ERMAs resulted in a significant reduction in CH contents compared to the REF paste. IOT-H, QT-H and QIT-H showed similar performances. These three fine ERMAs showed an average decrease of 24 % for 28 days, 31 % for 56 days and 37 % for 91 days compared to REF cement paste. The average reductions achieved by using coarse ERMAs were 9 % for 28 days, 16 % for 56 days and 19 % for 91 days. The intermediary performance of BOFS-H was probably a consequence of its intermediate particle size.

Given the dilution effect by the cement replacement, a reduction in the CH contents is expected. However, small reductions were observed in pastes containing coarse ERMAs probably as a consequence of an improved hydration degree of the cement particles. On

the other hand, the substantial differences between the results of coarse and fine ERMA pastes indicate pozzolanic activation by ultrafine grinding (Mitrović & Zdujić, 2014; Souri et al., 2015).

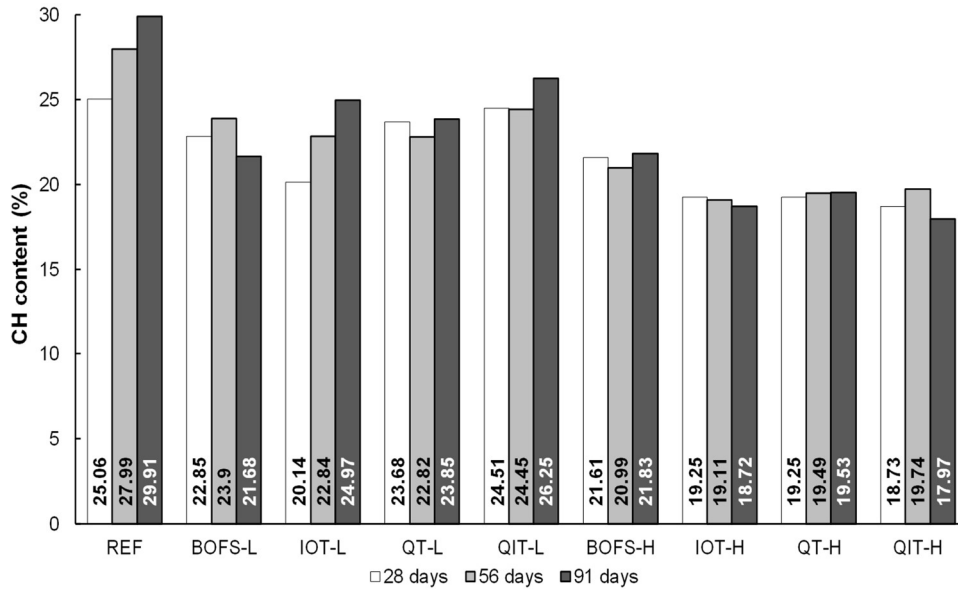


Figure 13. Results of CH content calculations in cement-only paste (REF) and blended cement pastes containing the studied ERMAs for 28, 56 and 91 days.

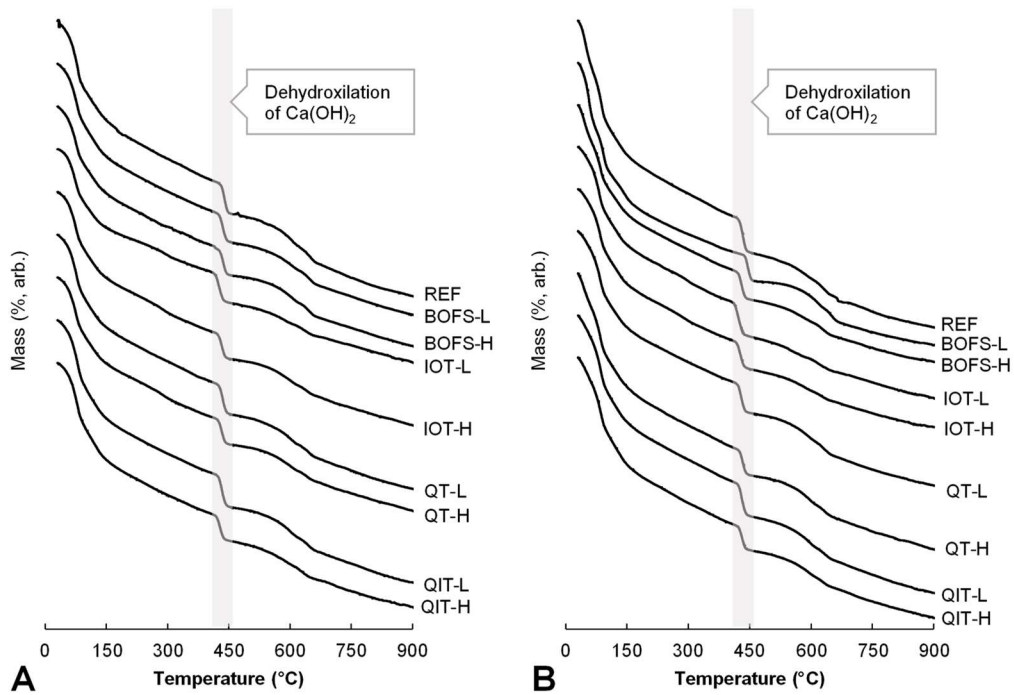


Figure 14. Thermogravimetric curves of the studied pastes: (A) aged 28 days; (B) aged 91 days.

In fact, the tendency of reduction or stabilization of the CH content along the later ages suggests that part or the CH produced in the hydration of Portland cement is being consumed in pozzolanic reactions. Among the studied ERMAs, BOFS showed an intermediate behavior since it contains in its mineralogical composition agents which are associated with pozzolanic properties (amorphous phase) and cementitious properties (e.g., larnite). The thermogravimetric curves for 28 and 91 days are shown in Figure 14.

3.3.7 Mechanical performance and durability

Figure 15 shows the results of the compressive strength tests in standard cement (REF) and blended mortars for 28 days. The IOT-L mortar presented the worst mechanical performance, achieving 68 % of REF mortar's compressive strength. Such behavior indicates an undesirable effect. In this regard, increased air entrainment and decreased mechanical performance of cement composites containing IOT have been reported (Zhao et al., 2014). However, the CH content in pastes containing IOT suggests a retarding effect with long-term gains (Figure 13). In this way, potential increases in compressive strength are expected for 56 and 91 days.

QIT-L mortar also showed low compressive strength (71 % in comparison to REF), but the CH content evaluation does not indicate a delay or decrease in hydration degree. Therefore, this result is probably a consequence of the low content of ultrafine particles (high D10), which limited the filler effect, and the worst morphological aspects of its particles, which made grain packing difficult.

QT-L and BOFS-L presented better performances among the coarse ERMAs. Their blended mortars reached 80 % and 83 % of the compressive strength of the REF mortar, respectively. These results are enough to classify QT-L and BOFS-L as pozzolans

according to the standard ASTM C618 (ASTM, 2015). It is believed that the cementing compounds of the BOFS powders and their content of the amorphous phase were effective in improving the mechanical performance of the BOFS-L mortars. The good result of the QT-L is probably due to its filler effect, enhanced by its physical and mineralogical characteristics (high purity quartz, low weathered rock, smoothed-faced volumetric-particles).

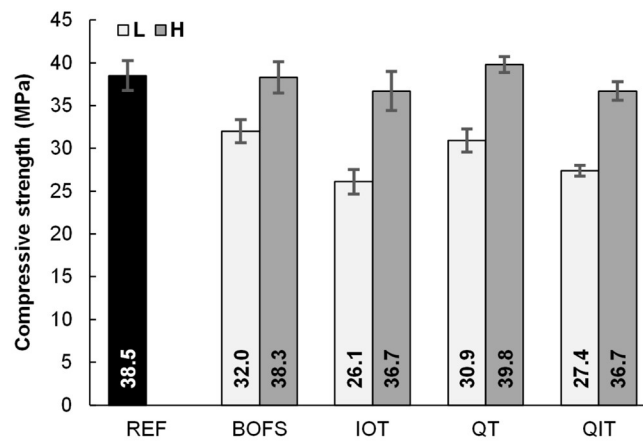


Figure 15. Compressive strength of the cement-only mortar (REF) and cement-blended mortars produced with the studied ERMA.

While the partial cement replacement by the coarse ERMA resulted in a reduction in compressive strength, all mortars containing the fine ERMA exhibited compressive strength equivalent to the REF mortar. In summary, the ratios between the compressive strength of the cement-blended mortars and the compressive strength of the REF mortar were 0.95 for the QIT-H and IOT-H; 0.99 for BOFS-H; and 1.03 for QT-H. These ratios are consistent with high-quality pozzolans according to Brazilian standard NBR 5753 (ABNT, 2016). In fact, these results are in good agreement with the pozzolanic evaluation by TG analysis in blended pastes (Figure 13).

These results also indicate that high fineness was a crucial factor in achieving high mechanical performance from different residues, regardless of the expected binder properties given by their chemical and mineralogical compositions. In addition, the high fineness was effective in equalizing the mechanical performance, promoting high gains in comparison with coarse ERMAs, as observed for QIT (+34 %) and IOT (+36 %).

Finally, the results of the autoclave expansion test are shown in Figure 16. Only the pastes containing BOFS showed expansion; however, the results were below the limit of 0.80 % prescribed by the standard ASTM C150 (ASTM, 2018). The results also suggest that the fine ERMAs have potentiated the effects (expansion or retraction) compared to the correspondent coarse ERMAs.

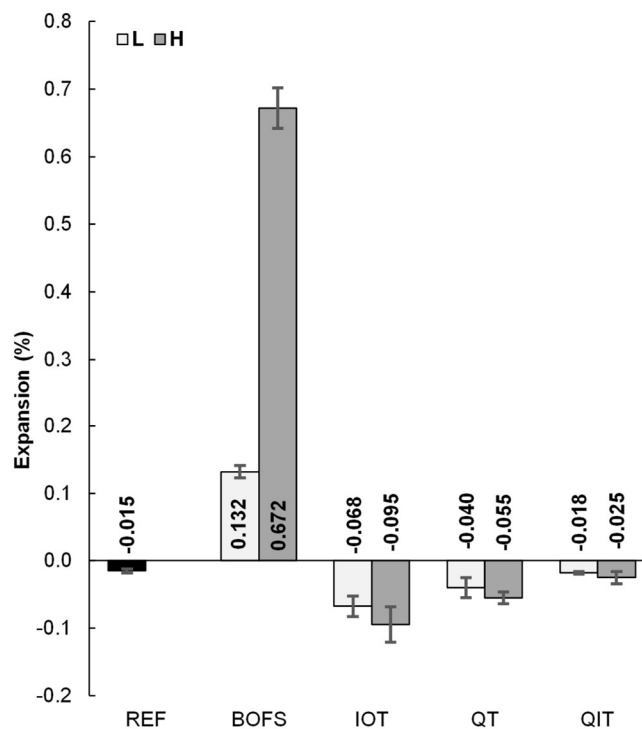


Figure 16. Results of autoclave expansibility test performed on cement-only paste (REF) and blended pastes (25 % cement replacement by volume).

Expansions in pastes containing BOFS were expected since the mineralogical characterization points to remaining expansive compounds (mainly periclase). The results

also show that the increase in fineness markedly increased the potential for expansion (BOFS-H paste showed an expansion four times greater compared to BOFS-L paste). However, even the replacement of cement by BOFS-based fine ERMAs proved to be within safe margins, despite the potentiated reactivity and the high amount used (25 % by volume).

3.4 Conclusion

Engineered recycled mineral admixtures (ERMAs) were obtained from different industrial and mining residues and evaluated individually and in blended pastes and mortars. The efficiency of their grinding programs was also analyzed. Performance tests showed that ERMAs presented high fineness and improved particle shape. Blended cement pastes presented good flowability, compatibility with PCE-based superplasticizers, no adverse effects in the hydration kinetics and acceptable results in autoclave soundness test. The finer-than-cement powders presented results compatible with pozzolanic materials in TG analysis and compressive strength tests. Mortars containing the finer powders achieved compressive strength results very close to reference cement-only mortar for a replacement rate of 25 % by volume, despite their different origin and constitution. Another contribution of the present work is the emphasis on the importance of a dedicated grinding process. All properties evaluated were significantly affected by the particle size distribution and morphology of the ERMAs produced.

3.5 Acknowledgments

The authors acknowledge the Laboratory of Electron Microscopy NANOLAB / UFOP and the Research Group on Solid Waste RECICLOS-CNPq for infrastructure use and collaboration.

Funding: This work was financed in part by the Coordenação de Aperfeiçoamento de Pessoal de Nível Superior – Brasil (CAPES) – Finance Code 001. The authors also acknowledge the financial support provided by Fundação de Amparo à Pesquisa do Estado de Minas Gerais – Brasil (FAPEMIG), and Conselho Nacional de Desenvolvimento Científico e Tecnológico – Brasil (CNPq).

3.6 References

ABNT, 1991. *NBR 5733: High early strength Portland cement - Specification*. Rio de Janeiro: Brazilian Association of Technical Standards - ABNT. (in Portuguese).

ABNT, 2003. *NBR NM 248: Aggregates - Determination of particle size distribution*. Rio de Janeiro: Associação Brasileira de Normas Técnicas - ABNT. (in Portuguese).

ABNT, 2005. *NBR 7211: Aggregates for concrete - Specification*. Rio de Janeiro: Associação Brasileira de Normas Técnicas - ABNT. (in Portuguese).

ABNT, 2015. *NBR 16372: Portland cement and other powdered materials - Determination of fineness by the air permeability method (Blaine method)*. Rio de Janeiro: Associação Brasileira de Normas Técnicas - ABNT. (in Portuguese).

ABNT, 2016. *NBR 5753: Portland cement - Pozzolanicity test for pozzolanic cements*. Rio de Janeiro: Associação Brasileira de Normas Técnicas - ABNT. (in Portuguese).

ABNT, 2017. *NBR 16605: Portland cement and other powdered material — Determination of the specific gravity*. Rio de Janeiro: Associação Brasileira de Normas Técnicas - ABNT. (in Portuguese).

Aprianti, E., 2017. A huge number of artificial waste material can be supplementary cementitious material (SCM) for concrete production – a review part II. *J. Clean. Prod.*, 142, pp.4178-94. DOI: 10.1016/j.jclepro.2015.12.115.

Arvaniti, E.C. et al., 2015a. Physical characterization methods for supplementary cementitious materials. *Mater. Struct.*, 48, pp.3675-86. DOI: 10.1617/s11527-014-0430-4.

ASTM, 2013. *C191: Standard Test Method for Time of Setting of Hydraulic Cement by Vicat Needle*. West Conshohocken: ASTM International.

ASTM, 2015. *C618: Standard Specification for Coal fly Ash and Raw or Calcined Natural Pozzolan for Use in Concrete*. West Conshohocken: ASTM International.

ASTM, 2017. *C204: Standard Test Methods for Fineness of Hydraulic Cement by Air-Permeability Apparatus*. West Conshohocken: ASTM International.

ASTM, 2018. *C150/C150-M: Standard Specification for Portland Cement*. West Conshohocken: ASTM International.

ASTM, 2018. *C151: Standard Test Method for Autoclave Expansion of Hydraulic Cement*. West Conshohocken: American Society of Testing and Materials.

Bastos, L.A.C., Silva, G.C., Mendes, J.C. & Peixoto, R.A.F., 2016. Using of iron ore tailings from tailing dams as road material. *J. Mater. Civil Eng.*, 28(10), p.04016102. DOI: 10.1061/(ASCE)MT.1943-5533.0001613.

Benezet, J.C. & Benhassaine, A., 1999. Grinding and pozzolanic reactivity of quartz powders. *Powder Technol.*, 105, pp.167-71. DOI: 10.1016/S0032-5910(99)00133-3.

Burris, L.E. & Juenger, M.C., 2016. Milling as a pretreatment method for increasing the reactivity of natural zeolites for use as supplementary cementitious materials. *Cement Concrete Comp*, 65, pp.163-70. DOI: 10.1016/j.cemconcomp.2015.09.008.

Chen, Y. et al., 2018. Impact of Different PCE Architectures on Flow Performance Depending on Precipitated Ettringite. In J. Liu et al., eds. *Superplasticizers and Other Chemical Admixtures in Concrete - Proceedings Twelfth International Conference*. Beijing: American Concrete Institute - ACI. pp.165-74.

Cordeiro, G.C., Tavares, L.M. & Toledo Filho, R.D., 2016. Improved pozzolanic activity of sugar cane bagasse ash by selective grinding and classification. *Cement Concrete Res*, 89, pp.269-75. DOI: 10.1016/j.cemconres.2016.08.020.

Da Silva, M.J. et al., 2016. Feasibility Study of Steel Slag Aggregates in Precast Concrete Pavers. *ACI Mater. J.*, 113(4), pp.439-46. DOI: 10.14359/51688986.

Damineli, B.L., 2013. *Concepts for the formulation of concretes with low binder consumption: Rheologic control, packing and particle dispersion*. São Paulo: USP. Doctoral Thesis, University of São Paulo (In Portuguese).

Dias, L.S. et al., 2016. Quartzite mining tailings for production of adhesive mortar. In Alves Jr., C., ed. *Proceedings of 22th Brazilian Congress on Material Science and Engineering - CBECIMAT*. Natal, 2016. (in Portuguese).

Diniz, D.H., Carvalho, J.M.F., Mendes, J.C. & Peixoto, R.A.F., 2017. Blast Oxygen Furnace Slag as Chemical Soil Stabilizer for Use in Roads. *J. Mater. Civil Eng.*, 29(9), p.04017118. DOI: 10.1061/(ASCE)MT.1943-5533.0001969.

Dutra, M.B. et al., 2014. Production of standard silica sand. In Alves Jr., C., ed. *Proceedings of 22th Brazilian Congress on Materials Science and Engineering - CBECIMAT*. Natal, 2014.

El-Jazairi, B. & Illston, J.M., 1980. The hydration of cement paste using the semi-isothermal method of derivative thermogravimetry. *Cement Concrete Res*, 10(3), pp.361-66. DOI: 10.1016/0008-8846(80)90111-8.

Fontes, W.C. et al., 2018. Iron ore tailings in the production of cement tiles: a value analysis on building sustainability. *Ambiente Construído (in press)*.

Fontes, W.C., Mendes, J.C., Silva, S.N. & Peixoto, R.A.F., 2016. Mortars for laying and coating produced with iron ore tailings from tailing dams. *Constr. Build. Mater.*, 112, pp.988-95. DOI: 10.1016/j.conbuildmat.2016.03.027.

Frunz, L., Juilland, P., Galloucci, E. & Zimmermann, J., 2018. Impact of Different Type of Calcium Sulfate on Early Ettringite Formation in Presence of Different PCE. In J. Liu et al., eds. *Superplasticizers and Other Chemical Admixtures in Concrete - Proceedings Twelfth International Conference*. Beijing: American Concrete Institute - ACI. pp.155-64.

García-Gusano, D. et al., 2014. Life cycle assessment of the Spanish cement industry: implementation of environmental-friendly solutions. *Clean Technol. Envir.*, 17(1), pp.59-73. DOI: 10.1007/s10098-014-0757-0.

Hanehara, S..Y.K., 1999. Interaction between cement and chemical admixture from the point of cement hydration, absorption behaviour of admixture, and paste rheology. *Cement Concrete Res*, 29, pp.1159-65.

Kajaste, R. & Hurme, M., 2016. Cement industry greenhouse gas emissions e management options and abatement cost. *J. Clean. Prod.*, (112), pp.4041-52. DOI: 10.1016/j.jclepro.2015.07.055.

Kanchanason, V. & Plank, J., 2018. Nucleation and Growth of C-S-H - PCE Used as Strength Enhancer in Cement. In J. Liu et al., eds. *Superplasticizers and Other Chemical Admixtures in Concrete - Proceedings Twelfth International Conference*. Beijing: American Concrete Institute - ACI. pp.67-75.

Land, G. & Stephan, D., 2012. The influence of nano-silica on the hydration of ordinary Portland cement. *J. Mater. Sci.*, 47(2), pp.1011-17. DOI: 10.1007/s10853-011-5881-1.

Lowell, S., Shields, J.E., Thomas, M.A. & Thommes, M., 2012. *Characterization of porous solids and powders: surface area, pore size and density*. Dordrecht: Springer Science & Business Media.

Maciel, M.H. et al., 2018. Effect of cement consumption on rendering mortars produced according the concepts of packing particles and mobility. *Ambiente Construído*, 18(1), pp.245-59. DOI: 10.1590/s1678-86212018000100219 (in Portuguese).

Malier, Y., ed., 2018. *High performance concrete: from material to structure*. CRC Press.

Marinho, A.L.B. et al., 2017. Ladle Furnace Slag as Binder for Cement-Based Composites. *J. Mater. Civil Eng.*, 29(11), p.04017207. DOI: 10.1061/(ASCE)MT.1943-5533.0002061.

Massazza, F., 1993. Pozzolanic cements. *Cement Concrete Comp.*, 15, pp.185 - 214. DOI: 10.1016/0958-9465(93)90023-3.

Mendes, J.C. et al., 2019. On the relationship between morphology and thermal conductivity of cement-based composites. *Cement Concrete Comp*, p.(in Press).

Meyers, G.D., McLeod, G. & Anbarci, M.A., 2006. An international waste convention: measures for achieving sustainable development. *Waste Manage.*, 24, pp.505-13. DOI: 10.1177/0734242X06069474.

Mitrović, A. & Zdujić, M., 2014. Preparation of pozzolanic addition by mechanical treatment of kaolin clay. *Int J Miner Process*, 132, pp.59-66. DOI: 10.1016/j.minpro.2014.09.004.

Papadakis, V. & Tsimas, S., 2002. Supplementary cementing materials in concrete Part I: efficiency and design. *Cem. Concr. Res.*, 32, pp.1525 - 1532. DOI: 10.1016/S0008-8846(02)00827-X.

Park, C.K., Noh, M.H. & Park, T.H., 2005. Rheological properties of cementitious materials containing mineral admixtures. *Cement Concrete Res*, 35, pp.842-49. DOI: 10.1016/j.cemconres.2004.11.002.

Puertas, F., Santos, H., Palacios, M. & Martínez-Ramírez, S., 2005. Polycarboxylate superplasticiser admixtures: effect on hydration, microstructure and rheological behaviour in cement pastes. *Adv Cem Res*, 17(2), pp.77-89.

Sant'ana Filho, J.N. et al., 2017. Technical and environmental feasibility of interlocking concrete pavers with iron ore tailings from tailings dams. *J. Mater. Civil Eng.*, 29(9), p.04017104. DOI: 10.1061/(ASCE)MT.1943-5533.0001937.

Schmidt, W., 2014. *Design concepts for the robustness improvement of self-compacting concrete: effects of admixtures and mixture components on the rheology and early hydration at varying temperatures*. Eindhoven: Eindhoven University of Technology. (PhD Thesis - Eindhoven University of Technology), DOI: 10.6100/IR771936.

Schober, I. & Flatt, R.J., 2006. Optimizing Polycarboxylate Polymers. *Special Publication*, 239, pp.169-84.

Scrivener, K.L. & Kirkpatrick, R.J., 2008. Innovation in use and research on cementitious material. *Cem. Concr. Res.*, 38(2), pp.128-36. DOI: 10.1016/j.cemconres.2007.09.025.

Shanahan, N., Tran, V., Williams, A. & Zayed, A., 2016. Effect of SCM combinations on paste rheology and its relationship to particle characteristics of the mixture. *Constr Build Mater*, 123, pp.745-53. DOI: 10.1016/j.conbuildmat.2016.07.094.

Shirai, H., Ikeda, M. & Tanno, K., 2011. Factors Affecting the Density and Specific Surface Area (Blaine Value) of Fly Ash from Pulverized Coal Combustion. *Energy Fuels*, 25(12), pp.5700-06. DOI: 10.1021/ef201071e.

Shi, C. et al., 2015. A review on ultra high performance concrete: Part I. Raw materials and mixture design. *Constr. Build. Mater.*, 101, pp.741-51. DOI: 10.1016/j.conbuildmat.2015.10.088.

Silva, K.D.C. et al., 2018. Rock Wool Waste as Supplementary Cementitious Material for Portland Cement-Based Composites. *ACI Mater J*, 115(5), pp.653-61.

Snellings, R., Merttens, G. & Elsen, J., 2012. Supplementary Cementitious Materials. *Rev. Mineral. Geochem.*, 74(1), pp.211-78. DOI: 10.2138/rmg.2012.74.6.

Souri, A. et al., 2015. Pozzolanic activity of mechanochemically and thermally activated. *Cem. Concr. Res.*, 77, pp.47-59. DOI: 10.1016/j.cemconres.2015.04.017.

Souri, A. et al., 2015. Pozzolanic activity of mechanochemically and thermally activated kaolins in cement. *Cement Concrete Res*, 77(November 2015), pp.47-59. DOI: 10.1016/j.cemconres.2015.04.017.

Stroh, J. et al., 2016. Time-resolved in situ investigation of Portland cement hydration. *Constr Build Mater*, 106, pp.18-26. DOI: 10.1016/j.conbuildmat.2015.12.097.

Sun, Z. et al., 2018. The Influence of Alkalinity on the Properties of the Accelerated Cement Pastes. In *Recent Advances in Concrete Technology and Sustainability Issues - Proceedings Fourteenth International Conference*. Sui, T.; Holland, T. C.; Wang, Z.; Zhao, X. ed. Beijing: American Concrete Institute - ACI. pp.11-21.

Torgal, F.P. & Jalali, S., 2010. *The Sustainability of Building Materials*. 2nd ed. Guimarães. (in Portuguese).

Vizcayno, C. et al., 2010. Pozzolan obtained by mechanochemical and thermal treatments of kaolin. *Appl. Clay Sci.*, 49, pp.405-13. DOI: 10.1016/j.clay.2009.09.008.

Wu, C. & Xin, J., 2018. Compressive Strength and Durability of Concrete Made with Combined Cementitious Materials. In T. Sui, T.C. Holland, Z. Wang & X. Zhao, eds. *Recent Advances in Concrete Technology and Sustainability Issues - Proceedings Fourteenth International Conference*. Beijing: American Concrete Institute - ACI. pp.43-54.

Yamada, K., Ogawa, S. & Hanehara, S., 2001. Controlling of the adsorption and dispersing force of polycarboxylate-type superplasticizer by sulfate ion concentration in aqueous phase. *Cement Concrete Res*, 31, pp.375-83.

Zhang, M. et al., 2016. Manifest system for management of non-hazardous industrial solid wastes: results from a Tianjin industrial park. *J. Clean. Prod.*, 133, pp.252-561. DOI: 10.1016/j.jclepro.2016.05.102.

Zhao, S., Fan, J. & Sun, W., 2014. Utilization of iron ore tailings as fine aggregate in ultra-high performance concrete. *Constr. Build. Mater.*, 50, p.540. DOI: 10.1016/j.conbuildmat.2013.10.019.

Chapter 4

More eco-efficient concrete: an approach on optimization in the production and use of waste-based supplementary cementing materials

*José Maria Franco de Carvalho, Tainá Varela de Melo, Wanna Carvalho Fontes,
Júnio Oliveira dos Santos Batista, Guilherme Jorge Brigolini, Ricardo André Fiorotti Peixoto*

Abstract

This paper presents a study that includes increase in clinker replacement and waste consumption in cement-based composites. Techniques for performance optimization of waste-based supplementary cementing materials in densely packed matrices using basic oxygen furnace slag, iron ore tailings from a tailings dam, quartz mining tailings and quartzite mining tailings were evaluated. Powders with different particle size ranges were produced and characterized. A highly-packed sand-concrete reference mix was designed and six different mixtures with 10 - 60vol% partial cement replacement were evaluated. The high binder efficiencies observed and physical-mechanical performances evidence the effectiveness of the proposal, expanding the concept of low-cost supplementary cementing materials and broadening the range of residual materials suitable for use in cement-based composites.

Keywords: Eco-efficient concrete; supplementary cementing material; particle packing; industrial waste recycling.

Construction and Building Materials, 2019, 206: 397-409

This manuscript was submitted on July 29th, 2018; received in revised form on 7 January 2019; accepted on 9 February 2019. Published on line on February 19th, 2019. DOI: <https://doi.org/10.1016/j.conbuildmat.2019.02.054>

4.1 Introduction

The growing demand for natural resources savings, reduced energy consumption, improved productivity and social responsibility in all building processes boosts the construction industry in the quest for more efficient and sustainable solutions. In this sense, impacts related to concrete production demand special attention, once it is the most consumed construction material worldwide (Mehta & Monteiro, 2006; Miller et al., 2016). The large amounts of CO₂ emitted in the production of Portland cement are pointed out as the main cause of the low environmental efficiency of conventional concrete (Hendriks et al., 1998; Huntzinger & Eatmon, 2009; Iacobescu et al., 2011; Ali & Hossain, 2011; Kajaste & Hurme, 2016), however, currently there are no feasible substitutes for this binder on a large scale. For this reason, researchers and international agencies have devoted great attention to the search for strategies to mitigate the impacts related to cement production (Salas et al., 2016; Mikulčić et al., 2016).

Among the measures proposed to promote the reduction of impacts, the clinker replacement is pointed as the most effective, since it represents 58% of the total impacts of cement production (WBCSD/IEA, 2009; Lei et al., 2011; García-Gusano et al., 2014; Kajaste & Hurme, 2016). In this sense, the use of supplementary cementing materials (SCMs), in partial replacement of Portland cement, appears as fundamental rule to obtain eco-friendly concretes. This strategy may also be accompanied by technological advantages as enhancements in mechanical performance and durability (Berndt, 2009; Nie et al., 2014; Nie et al., 2015). Additionally, the potentials and synergies of combining cement replacement and aggregate substitution must also be explored and represent even more significant gains in eco-efficiency by increasing the residue consumption (Lima et al., 2013; Faella et al., 2016).

Another mitigation route is to improve the binder efficiency in concretes and mortars, obtaining composites with the required mechanical strength and durability, accompanied by a lower binder consumption. In this regard, Damineli et al. (2010) proposed an indicator to measure concrete efficiency in terms of mechanical strength and binder consumption.

Some techniques to improve the binder efficiency include increasing the binder fineness (Alimeneti, 2015), and introducing agents such as nucleation seeds (Thomas et al., 2009), nanomaterials (Cao et al., 2015) and autogenous cure promoters (Hasholt & Jensen, 2015). However, water reduction using superplasticizers (Hartmann et al., 2011) and grain packing improvement (Castro & Pandolfelli, 2009; Damineli, 2013) pay special attention by their availability and relative simplicity of use for obtaining high and ultra-high-performance concretes.

Finally, another approach in improving the sustainability of concretes is the reduction of the consumption of non-renewable natural resources, using industrial and mineral residues, whose inadequate disposal causes environmental, social and economic impacts (Meyers et al., 2006; Zhang et al., 2016; Aprianti, 2017). In this sense, several studies have been reported, highlighting the use of rejects from the steel industry (Diniz et al., 2017; Marinho et al., 2017; Da Silva et al., 2016) as well as the mining industry (Bastos et al., 2016; Fontes et al., 2016; Sant'ana Filho et al., 2017).

This paper proposes a new approach expanding the SCM concept based on the performance of densely packed concretes containing supplementary materials in partial replacement of Portland cement. By means of binder efficiency measurements and physical properties observed, the proposed experimental program indicates that binder

properties are not necessarily mandatory and the mixing of fine and coarse powders has been effective in achieving performances consistent with efficient SCMs. Based on that is possible to expand the range of suitable waste materials for use in cement-based composites with economic advantages. Four different industrial and mining wastes were used in this research: basic oxygen furnace slag, iron ore tailings from a tailings dam, quartz mining tailings and quartzite mining tailings. The promising results were evidenced in densely packed concretes without coarse aggregates (called here sand-concretes), with replacement rates of 10-60% of Portland cement by the waste powders.

4.2 Material and methods

4.2.1 Materials

The basic oxygen furnace slag (BOFS) was obtained from a steelwork located in the city of João Monlevade, which is located in the state of Minas Gerais, Brazil. This granular material presented particle size ranging from 4.8 - 12.5mm and, in order to stabilize the expansive oxides, they were submitted to weathering for 3 years in a storage yard of the Laboratory of Civil Construction Materials (LMCC), at the Universidade Federal de Ouro Preto (Federal University of Ouro Preto - UFOP). The iron ore tailing (IOT) mud was obtained from a tailing dam located in the iron quadrilateral region (Minas Gerais, Brazil). This powdery material (particle size ranging from 0.001-1.0mm) was air-dried, smashed and stored in a sealed plastic container maintained in the LMCC/UFOP. The quartz mining tailing (referenced from this point by the acronym QT) is a granular material (particle size ranging from 2.4 -12.5mm) and was obtained from a mining facility located in the city of Sete Lagoas, in the state of Minas Gerais, Brazil. The quartzite mining tailing (referenced from this point by the acronym QIT) is a friable granular to powdery material

(particle-size ranging from 0.001 - 6.3mm) and was obtained from a mining facility located in the city of Itabirito, in the state of Minas Gerais, Brazil. These two last samples were also collected representatively and stored in sealed plastic containers in the LMCC/UFOP. Tables 1, 2 and 3 show the chemical composition, mineralogical phases and basic physical properties of the raw wastes, respectively. These data were obtained in characterization programs performed in UFOP laboratories using XRF (PANalytical Epsilon3^x), XRD (Bruker D2 Phaser2nd generation, CuK α radiation, 40 kV, 30 mA, 10 - 70° 2 θ range, 0.02° step size, 1 s/step), and standardized methods for physical characterization of building materials (specific gravity by the le Chatelier flask method and bulk density by the known-volume container method).

Table 1. Chemical composition of the raw wastes.

Compound	BOFS	IOT	QT	QIT
SiO ₂ content, %	13.4	35.5	95.5	80.0
Al ₂ O ₃ content, %	3.6	5.8	1.5	15.9
Fe ₂ O ₃ content, %	34.5	56.9	1.9	0.4
CaO content, %	36.2	0.2	0.2	-
MgO content, %	5.0	0.2	-	0.1
K ₂ O content, %	-	-	-	2.8
Na ₂ O content, %	-	-	-	-
SO ₃ content, %	0.3	-	-	-
MnO content, %	3.7	-	-	-
Cr ₂ O ₃ content, %	0.8	-	-	-
Other oxides, %	2.5	1.4	0.8	0.8
LOI, %	1.1	3.1	0.3	1.2

A high early strength Portland cement (ASTM Type III) was used in the production of the sand-concretes. This Portland cement is specified in Brazil as CPV type by the standard NBR 5733 (ABNT, 1991) and one of its characteristics is the absence of significant amounts of supplementary cementing materials (95-100% clinker + gypsum, 0 - 5% limestone filler). The characterization data of the cement were reported by the producer and are shown in Table 4.

Table 2. Mineralogical phases observed in the studied wastes.

BOFS	IOT	QT	QIT
Wuestite	Quartz	Quartz	Quartz
Larnite	Hematite		Muscovite
Brownmillerite	Goethite		
Calcite			
Helvine			
Portlandite			
Lime			
Periclase			

Table 3. Physical properties of the raw wastes.

Material	Appearance	Specific density (g/cm³)	Bulk density (g/cm³)
BOFS	Granular material, dark gray coloration	3.770	1.945
IOT	Powdery material, brown coloration	3.527	1.905
FST	Granular material, beige coloration	2.956	1.777
QT	Granular to powdery material, white coloration	2.744	1.641

Table 4. Characterization data of the Portland cement used in the research

Parameter	Value
MgO content, %	1.46
SO ₃ content, %	2.99
CO ₂ content, %	2.42
Insoluble residue, %	0.97
Loss on ignition, %	3.30
Specific surface area (Blaine), cm ² /g	4580
Density, g/cm ³	3.04
Setting time (initial / final), min.	(130 / 183)
Compressive strength (1 / 3 / 7 / 28 dias), MPa	(27.0 / 42.3 / 46.4 / 53.9)

A river quartz sand (Peixes River, city of Ponte Nova, state of Minas Gerais, Brazil) was used in the production of sand-concretes in four particle-size fractions separated by sieving, named fine-sand (particle size between 0.15 - 0.30mm); medium-fine sand (0.30 - 0.60mm); medium-coarse sand (0.60 - 1.18mm); and coarse sand (1.18 - 2.36mm). A polycarboxylate-based superplasticizer (SP) (Powerflow4000, McBauchemie) was used as dispersant.

4.2.2 Production and characterization of the powders

A preliminary comminution process was applied to the BOFS and QT samples, consisting of crushing in a Retsch BB 200 laboratory jaw crusher and sieving. The process was carried out until all samples had particle size ≤ 4.8 mm. Subsequently, the BOFS sample were subjected to a magnetic separation procedure (HF CC magnetic roll, 950 gauss, three repetitions) in order to reduce its magnetic content and consequent volumetric instability related to the oxidation of metallic iron (Toffolo, 2015).

Two powders were produced with each raw waste: a coarser-than-cement powder and a finer-than-cement one. The coarse powders were produced using a Marconi MA500 laboratory horizontal ball mill while the fine powders were also grinded in a High efficiency planetary ball mill Retsch PM100. The equipment setups are presented in Table 5 while the grinding times are shown in Table 6.

Table 5. Grinding programs and setup parameters.

Grinding program	Parameter	Information
Low-efficiency program (L)	Jar and balls (material)	Stainless steel
	Jar volume, cm ³	10,367
	Material produced per cycle, cm ³	1,740 (17%)
	Rotation speed, rpm	200
	Balls (volume, cm ³)	1,658 (16%)
	Balls (Quantity / diameter, mm)	(7/22) (17/28) (34/31) (11/38) (16/41)
High-efficiency program (H)	Jar and balls (material)	ZrO ₂
	Jar volume, cm ³	250
	Material produced per cycle, cm ³	80 (32%)
	Rotation speed, rpm	400
	Balls (volume, cm ³)	64,3 (26%)
	Balls (Quantity / diameter, mm)	(99/10) (191/5)

Table 6. Powders produced, grinding programs and grinding times.

Fine	Grinding programs	Grinding times (min.)
BOFS-L	L	180
IOT-L	L	30
QT-L	L	120
QIT-L	L	30
BOFS-H	(L / H)	(180 / 45)
IOT-H	(L / H)	(180 / 45)
QT-H	(L / H)	(180 / 45)
QIT-H	(L / H)	(180 / 45)

The particle size distributions of the produced powders were obtained using the laser diffraction technique (Bettersize2000) and the specific surface areas were obtained using the Blaine air permeability method [C204 (ASTM, 2017), NBR 16372 (ABNT, 2015)]. Scanning electron microscopy images (SEM, Tescan Vega 3 microscope, high vacuum, SE images, 20kV) obtained from gold coated powder samples (Quorum Q150) were used for the morphological evaluation.

2.3 Mixing design of the densely-packed sand-concretes

The dry mixture of the reference sand-concrete was designed using the modified Andreassen particle size distribution method (Funk & Dinger, 1994). The calculations were performed according to Equation 1 where: $CPFD$ is the cumulative volume of particles with particle size smaller than D ; D_L is the diameter of the largest particle; D_S is the diameter of the smallest particle; and q is the distribution coefficient (adopted 0.3 for a compact mixture with good workability). Based on the reference sand-concrete, six different mixtures with partial replacement of Portland cement by waste powders were designed (10 - 60vol.%). Table 7 shows the sand-concrete mixtures with the proportions in volume.

Equation 1
$$CPFT(\%) = 100 \left(\frac{D^q - D_S^q}{D_L^q - D_S^q} \right)$$

Table 7. Identification of the sand-concretes produced in this research, constituent materials and proportions of the dry mixtures.

Blend	Powders % total volume (% powder volume)			Aggregates % total volume			
	Coarse powder (C)	Portland cement (PC)	Fine powder (R)	Fine sand	Medium-fine sand	Medium-Coarse sand	Coarse sand
Ref.	0.0 (0)	33.3 (100)	0.0 (0)	16.7	16.7	16.7	16.7
00-90-10	0.0 (0)	29.9 (90)	3.3 (10)	16.7	16.7	16.7	16.7
00-80-20	0.0 (0)	26.6 (80)	6.6 (20)	16.7	16.7	16.7	16.7
20-70-10	6.6 (20)	23.2 (70)	3.3 (10)	16.7	16.7	16.7	16.7
20-60-20	6.6 (20)	19.9 (60)	6.6 (20)	16.7	16.7	16.7	16.7
40-50-10	13.3 (40)	16.6 (50)	3.3 (10)	16.7	16.7	16.7	16.7
40-40-20	13.3 (40)	13.3 (60)	6.6 (20)	16.7	16.7	16.7	16.7

4.2.3 Dosing of superplasticizer

The sand-concretes were produced using the optimal content of SP given by its saturation point. The SP saturation point was determined experimentally in the blends of cement and the studied powders using a method based on that proposed by Aitcin (2000). The tests were performed in fluid pastes using a Ford viscometer cup (105.7 cm³ stainless steel cup, Ø4.0 mm brass orifice). The flow times of the pastes produced with different SP contents for a given water/fines (w/f) ratio (w/f = 0.35, 25°C) were taken and curves flow time vs. SP content were plotted.

4.2.4 Determination of the maximum experimental packing density

The sand-concretes were produced for the w/f ratios given by the maximum experimental packing densities obtained accordingly to a method based on that proposed by Wong and

Kwan (Wong & Kwan, 2008; Kwan & Wong, 2008). The procedure is described as follows.

- The amount of the dry blend was taken.
- The specified amount of water was taken according to the w/f ratios defined in the study (0.5, 0.4, 0.35, 0.3, 0.25, and 0.2 by mass).
- The amount of water and half amount of the dry blend were placed in the mixer vessel.
- The content was mixed for three minutes.
- The other half of the dry blend was taken in three equal parts.
- Each part was added to the mixer vessel and mixed for additional three minutes.
- A rigid known-volume cylindrical-vessel was filled with the fresh mixture in three layers compacted with 30 blows each one using a standard hammer.
- The mass of the fresh mixture in the known-volume vessel was determined.

The mixing process was done in a standard mixer (Fortest, VC 370, 62rpm in planetary motion, blade rotation 140rpm). Equations 2, 3 and 4 were used for calculations (V_s is the volume of solids; M is the mass of the material in the vessel with known volume V ; ρ_w is the water density; u_w is the volumetric water/fines ratio; ρ_i is the density of the i -th material; R_i is the volumetric ratio of the i -th material in the blend; u is the void index; and ϕ is the packing density).

Equation 2

$$V_s = \frac{M}{\rho_w u_w + \sum_{i=1}^n \rho_i R_i}$$

Equation 3

$$u = \frac{V - V_s}{V_s}$$

Equation 4

$$\phi = \frac{V_s}{V}$$

4.2.5 *Characterization of the sand-concretes*

The characterization program performed in the sand-concretes comprised the following methods.

- Tensile and compressive strength in prismatic 40x40x160mm specimens (7 and 28 days old) as prescribed in the standards ASTM C348 (ASTM, 2014), ASTM C349 (ASTM, 2014) and NBR 13279 (ABNT, 2005) (EMIC DL20000 universal testing machine, 20kN load cell, 50N/s load step for bending tests and 500N/s load step for compressive test).
- Density, porosity and void index in 28 days old Ø50x100mm cylindrical specimens, based on NBR 9778 method (ABNT, 2005), comprising weighing of oven dried specimens (105± 5°C, 168 h) and weighing of saturated surface-dry specimens (168h immersion in room temperature water and additional 5h immersion in boiling water).
- Ultrasonic pulse velocity in the same cylindrical specimens Ø50x100mm, oven dried at 105± 5°C for 168 h (Proceq TICO). All specimens were demolded and maintained in wet chamber until the test (Equilam SS600UM, 98 ± 2% relative humidity, 40°C). Three specimens were used in each determination.

In order to evaluate the characteristics of the trapped air bubbles observed in the hardened samples, a complementary macroporosity study was carried out in some of the tested sand-concretes chosen accordingly their strength, porosity and waste consumption (concretes 00-90-10, 00-80-20 and 40-40-20). The evaluation comprised the measurement of the pore-sizes and pore-distributions using the software developed by Rabbani et al. (Rabbani & Jamshidi, 2014). The images used in these analyzes were obtained from the sample cross-sections using an optical scanner (Scanjet G4050 hp, 1200 dpi resolution). In order to provide a good contrast between the pores and the solid, the technique proposed by Mendes et al. (Mendes et al., 2017) was implemented. The method consists on painting the cross-section with a dark colored paint (whiteboard marker) and filling the voids with a white powder (corn starch).

The macro and microstructure were also observed using SEM images of gold coated (Quorum Q150) fractured surfaces with 90+ days of age (Tescan Vega 3 microscope, high vacuum, SE images, 20kV). For this, fragments of sound parts of some samples submitted to the mechanical tests were taken. The samples chosen were the same used in the macrostructure evaluations.

4.2.6 Eco-efficiency evaluation

The waste consumption and binder intensity bi (Damineli et al., 2010) were used in the sand-concrete eco-efficiency evaluation. Equation 5 was used for bi calculation [b is the total binder consumption in kg/m^3 (Portland cement) and p is the performance achieved (considered here the compressive strength at 28 days)].

Equation 5

$$bi = \frac{b}{p}$$

4.2.7 Durability

This work does not comprise a deeply durability evaluation of the proposed composites, however, autoclave expansibility tests ASTM C151 (ASTM, 2016) were performed in blended pastes produced with cement and BOFS powders (40vol.% cement, 40vol% BOFS-L, 20vol% BOFS-H, water/fines ratio 0.88 by volume). For this purpose, prismatic specimens 25x25x285mm were produced. The blends were mixed in a Fortest, VC 370 standard mixer (30 seconds in low velocity and 60s in high velocity) and the molds were filled and compacted by hand. The specimens were kept in a humid chamber for 24h (25°C, 99% RH), demolded and placed in the autoclave (Matest E070). The specimens were submitted to a hot and pressurized environment for 180 min (295psi; ~215°C). Measurements were performed before and after the test (25°C).

4.3 Results and discussion

4.3.1 Production and characterization of the powders

The fineness of the powders reached the objective of this study and, for all tested wastes, a coarser-than-cement powder and a finer-than-cement one were obtained. The coarse powders presented fineness almost similar with close values for the parameters D90, D50 and D10 (where D is the diameter of the particles corresponding to the N% of the cumulative volume in the particle-size distribution). In addition, the particle size distribution curves were approximately coincident. The fine powders were produced in a unique grinding protocol and their particle size distribution curves showed different aspects accordingly the grindability of the different wastes. The particle size distribution curves of QT-H and QIT-H were almost similar due to the proximity of their mineralogical composition. The IOT-H curve presented less uniform than these lasts and

the BOFS-H curve was the least uniform of all. The worst grindability presented by the BOFS waste limited its fineness and BOFS-H was the coarser fine powder, with not so different particle size distribution compared to cement. Table 8 shows the fineness parameters of the produced powders. The particle size distribution curves of the powders are shown in Figure 1.

Table 8. Fineness parameters of the produced powders.

Powder	Fineness parameters			
	D90 (μm)	D50 (μm)	D10 (μm)	Spec. surf. area (cm ² /g)
BOFS-L	118.0	27.23	1.704	2,635
BOFS-H	39.59	8.550	1.109	5,416
IOT-L	139.5	40.25	2.347	2,202
IOT-H	21.11	3.406	0.859	6,442
QT-L	108.5	29.78	2.445	3,100
QT-H	10.36	2.750	0.849	11,818
QIT-L	129.5	33.77	5.458	2,386
QIT-H	13.03	3.217	0.886	11,519
PC	36.91	10.95	1.743	4,572

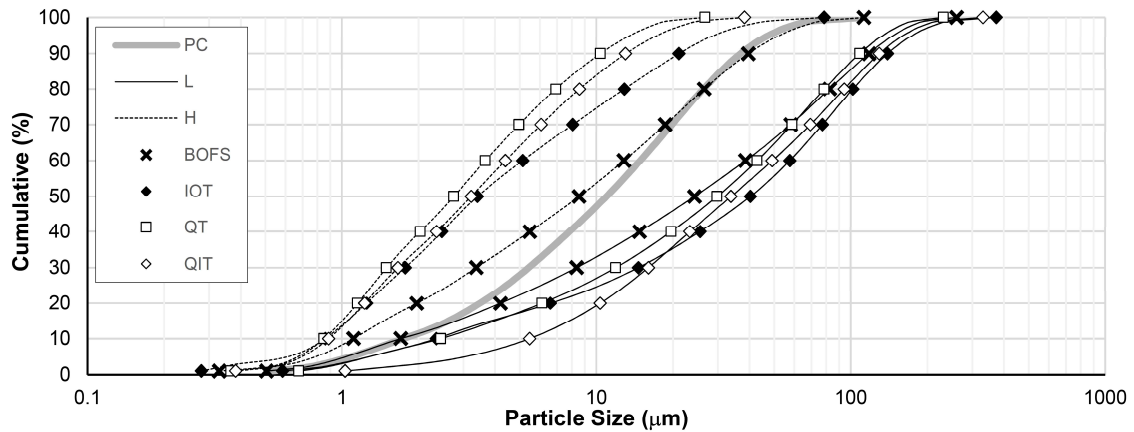


Figure 1. Particle size distributions of the produced powders.

Among the coarse powders, QT-L presented the highest specific surface area (3,100cm²/g) and IOT presented the lowest (2,202 cm²/g). Differences in the particle shapes explain the differences between the specific surface areas measured and the

expectations considering the particle size distributions. Among the fine powders, QT-H and QIT-H showed the highest values (11,818 and 11,519 cm²/g, respectively), while the BOFS presented the lowest (5,416 cm²/g). For these, the results are in good fit with the particle size distributions.

The grinding process requires energy, which reduces the eco-efficiency of the products. However, grinding is also a process in cement production, whose impacts add to the other intrinsic impacts not observed in the production of the proposed SCMs (e.g., carbon dioxide emissions from limestone decarbonation). Furthermore, the impacts related to the grinding process are highly dependent of the energy source. In this sense, developments in the green energy field has direct and more sensitive positive impacts in the production of fines with promising prospects (Midilli et al., 2006; Dincer & Acar, 2015; Dincer & Acar, 2017). Additionally, impacts can be mitigated using low amounts of high-energy ground powders and high amounts of low-energy ground powders in blends containing Portland cement.

Micrographs of the powders showed that the quartz particles of QT-L, QIT-L and IOT-L are predominantly angular with sharp edges, although, QT-L has more volumetric and less rough particles. Large number of small particles adhered into large ones are observed in IOT-L samples. The QIT-L particles presented the worst morphology, with highly fractured and less volumetric particles due to high weathering and low grinding time. The BOFS-L particles are predominantly volumetric, moderately rough but with rounded edges. All fine powders involved in this study presented better shape with less roughness and smoothed edges. Figure 2 shows some SEM images of the powders.

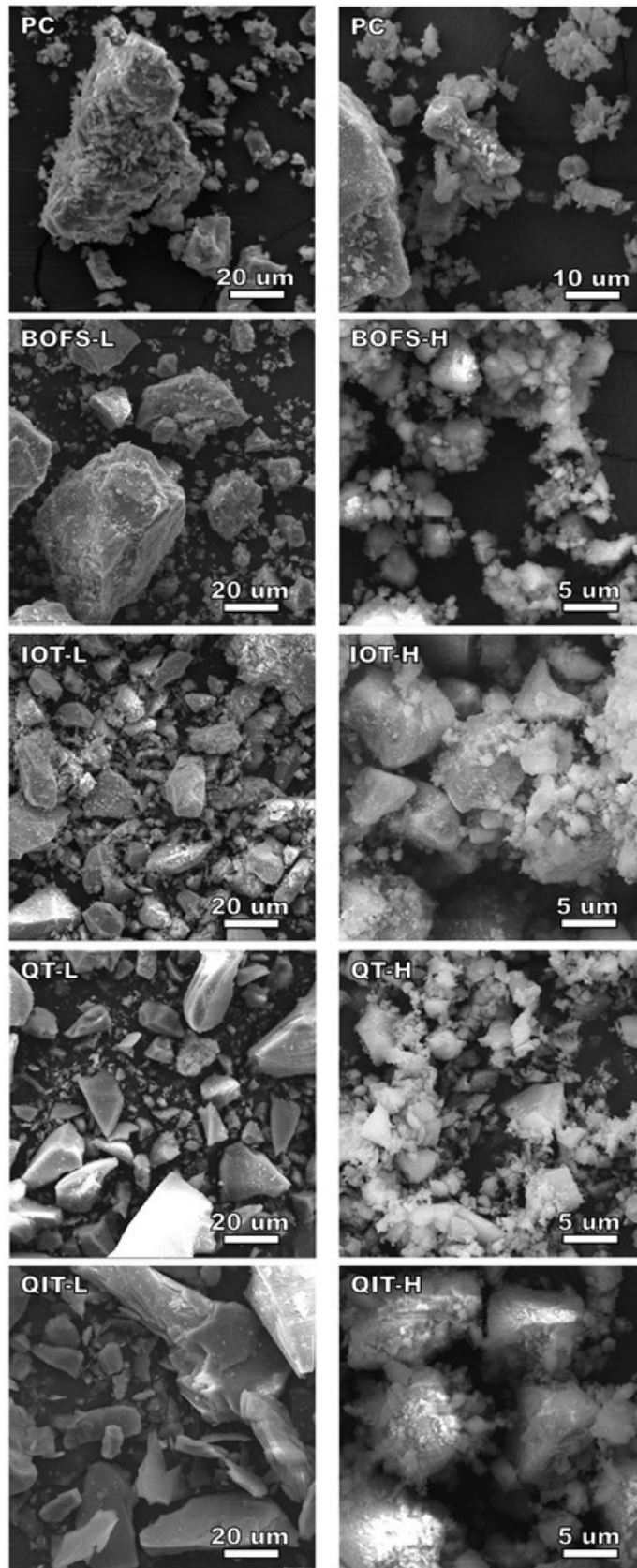


Figure 2. SEM images of the produced powders

4.3.2 Performance of the powders as SCMs in densely packed sand-concretes

4.3.2.1 Rheological performance and packing density

The powders presented good compatibility with the superplasticizer, so that in all the mixtures the flow times were smaller for those with replacement of cement by the powders. It suggests that the adsorption of the superplasticizer by the powder particles showed good efficiency and the steric repulsion effect contributed to a better dispersion of all fines in the system. The best results were observed in the mixtures with BOFS due to the lowest fineness and also to the improved shape of its particles. The behaviors of the mixtures with QT and QIT were consistently good and quite similar. IOT mixtures showed the worst results, mainly for the lowest admixture contents. The results of the superplasticizer saturation point tests are shown in Figure 3.

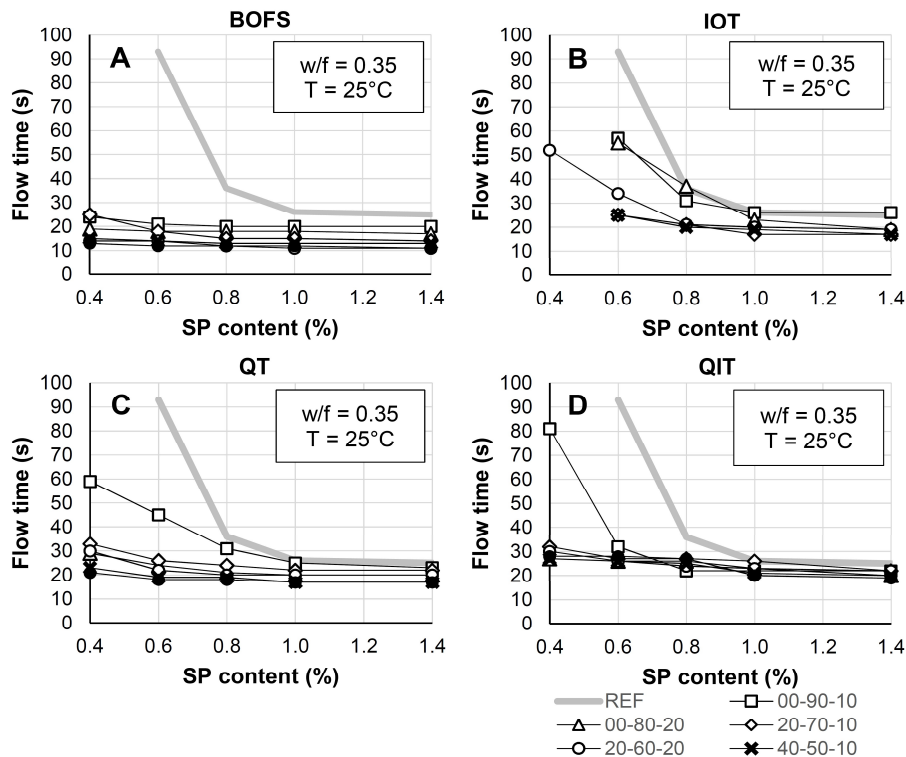


Figure 3. Flow time curves of the reference paste (Portland cement) and blended pastes (Portland cement + waste powders) obtained from the superplasticizer saturation point tests [(A) BOFS; (B) IOT; (C) QT; (D) QIT].

The reference mixture presented good fit with the particle size distribution curve of the modified Andreassen method (Funk & Dinger, 1994) as shown in Figure 4. The criterion of using the four fractions of the sand in equal proportions, however, affected the fit in the region of particle size of 150 μm . The particle size distribution of the cement was another source of distortion, which was expected. In this sense, the use of a fine powder associated with a coarse powder was effective in the adjustments of the cement curve ends. In this sense, the coarse powders were more effective. Relating to the fine powders, however, the use of these did not lead to major changes in the grain size curve, suggesting that better results would be achieved if this material had reached a higher fineness (D50 values close to 1 μm). Figure 4 also shows the curves for the mixtures with QT fines.

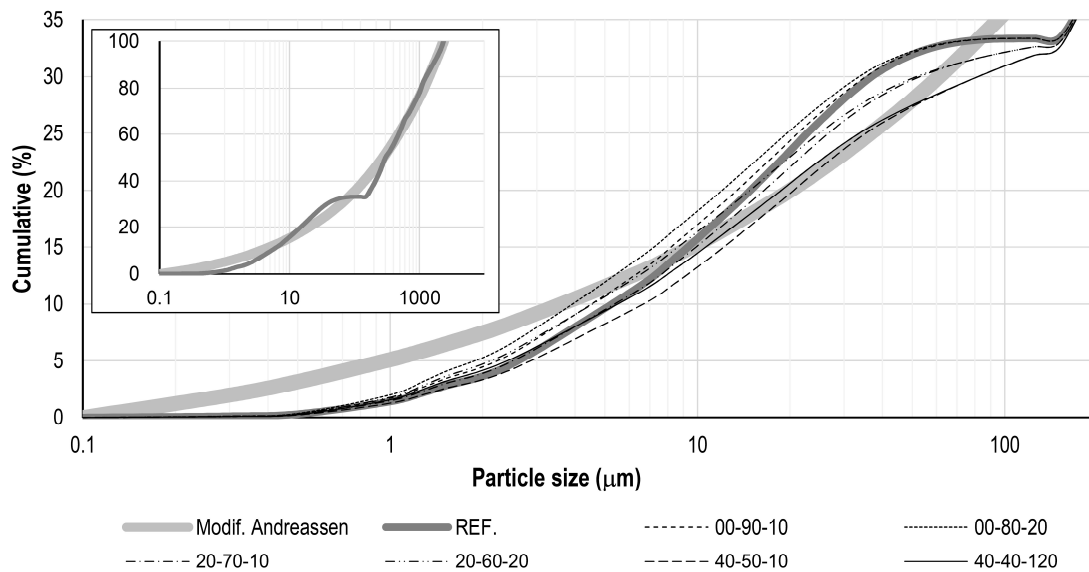


Figure 4. Particle size distributions of designed sand-concrete mixtures and modified Andreassen distribution for $D_L = 2360 \mu\text{m}$, $D_S = 0.1 \mu\text{m}$, and $q = 0.3$.

The results of the experimental packing density tests (Table 9) showed that, except for the mixtures IOT 00-90-10 and IOT 00-80-20, all the others reached the highest packing density at water/fines ratios lower than that obtained for the reference sand-concrete,

which is in good agreement with the results of the flow time test. It is explained by the efficient action of the admixture on the powder particles and their shape, improving the system rheology (which is a behavior of interest for SCMs). The best experimental packing performance was observed for the mixtures containing no coarse powders (BOFS, QT and QIT), or containing them in small quantities (IOT and QIT). These observations indicate that the better morphology of the particles of refined powders comparing to the coarse ones played a decisive role in the packing performance. Additionally, for all mixtures, the best packing density results were presented by those containing higher amounts (20%) of fine powder (BOFS 00-80-20, IOT 20-60-20, QT 00-80-20, QIT 00-80-20 and QIT 20-60-20), the only exception was the mixture QIT 20-70-10, whose performance was the same observed in the mixtures QIT 00-80-20 and QIT 20-60-20.

4.3.2.2 Physical and mechanical performance

The physical characterization of the hardened sand-concretes comprised density, void index, and ultrasonic pulse velocity. These tests were performed in 28-day-old cylindrical specimens ($\text{\O}50 \times 100 \text{mm}$), and the results are shown in Fig. 5A, B and C respectively.

The BOFS sand-concretes presented the highest densities, followed by the IOT sand-concretes. This behavior was expected given the higher densities of these two materials. The lighter sand-concretes were those produced with QT and QIT.

Table 9. Results of the experimental packing density test.

Mixture	Water/fines ratio		Experimental packing density
	(wt%)	(vol%)	
REF.	0.30	0.91	0.72
BOFS 00-90-10	0.25	0.78	0.73
BOFS 00-80-20	0.25	0.79	0.74
BOFS 20-70-10	0.25	0.81	0.70
BOFS 20-60-20	0.25	0.82	0.70
BOFS 40-50-10	0.26	0.88	0.73
BOFS 40-40-20	0.23	0.79	0.71
IOT 00-90-10	0.30	0.92	0.73
IOT 00-80-20	0.30	0.94	0.73
IOT 20-70-10	0.26	0.82	0.74
IOT 20-60-20	0.26	0.84	0.75
IOT 40-50-10	0.26	0.85	0.74
IOT 40-40-20	0.26	0.86	0.73
QT 00-90-10	0.25	0.76	0.74
QT 00-80-20	0.25	0.76	0.75
QT 20-70-10	0.25	0.75	0.73
QT 20-60-20	0.24	0.72	0.73
QT 40-50-10	0.24	0.72	0.72
QT 40-40-20	0.23	0.69	0.72
QIT 00-90-10	0.24	0.72	0.72
QIT 00-80-20	0.24	0.71	0.75
QIT 20-70-10	0.23	0.68	0.75
QIT 20-60-20	0.25	0.73	0.75
QIT 40-50-10	0.24	0.69	0.73
QIT 40-40-20	0.25	0.71	0.73

Bold values indicate the best results

The void index results (Fig. 6B) showed that the incorporation of the powders promoted the achievement of more compact and less porous composites compared to reference sand-concrete. The exceptions were the IOT mixtures, the BOFS 40-50-10 mixture and the QIT 40-40-20 mixture. Zhao et al. (2014) studied iron ore tailings in cement-based composites and also observed increased contents of entrapped air in composites containing iron ore tailings. The coarsest particles of the BOFS refined powders are responsible for both low packing density and higher porosity. The QT and QIT sand-concretes presented the lowest void indexes for the 00-80-20 mixture, and the value

presented by the QIT 00-80-20 was the lowest of all sand-concretes tested. This observation is also in good agreement with the packing density values presented for these two mixtures. With the increase in the replacement contents and consequent reduction in the cement contents, the pore filling ability by cement hydration products is also reduced, and a greater porosity was expected due to the increasing in the water/cement ratio. However, the grain packing and the improvement in the degree of hydration mitigated this effect, so that the composites became less porous in most cases.

Good agreements were observed between ultrasonic pulse velocity and porosity (void index), which was expected. In this sense, the behavior of the BOFS, QT and QIT samples presented better adjustment. The behavior of the IOT samples, however, showed an interesting trend: while the void indices were almost similar, the samples with low IOT content showed a significant reduction in the ultrasonic pulse velocity when compared to the samples with higher IOT contents. These distortions are related with the microporosity inaccessible by water, result of the ability of the IOT fines as air entraining agents (micropores between lamellar clay particles). This distortion is reduced in the samples with higher IOT contents because of the reduction in the content of inaccessible voids. The same can be stated for the reference samples, but in this case the cause of that inaccessible microporosity is related to the absence of filler particles.

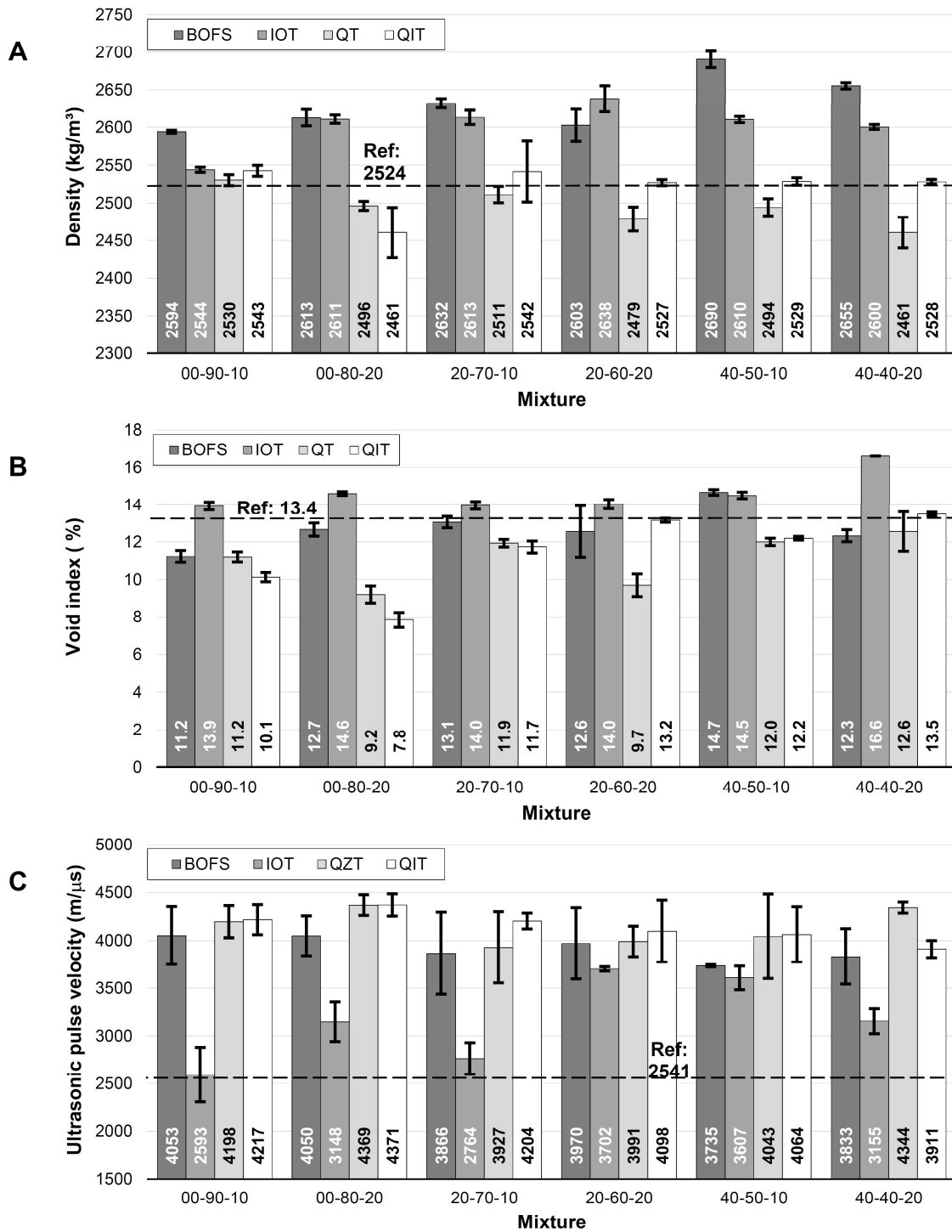


Figure 5. Results of physical characterization of the sand-concretes: (A) density; (B) void index; and (C) ultrasonic pulse velocity.

The best overall mechanical performance was presented by the BOFS sand-concretes and they are shown in Fig. 6A and 6B. At 28 days, the sand-concrete BOFS 00-80-20 presented compressive strength 16.4% higher than that presented by the reference sand-

concrete (109.14 MPa vs. 93.81 MPa). Four sand-concretes presented better results compared to reference, highlighting the BOFS 20-60-20, whose compressive strength at 28 days was 103.08 MPa, despite its 40vol.% cement replacement. Even the least strength sand-concretes reached values considered high for the applied replacement levels. The worst result (87.73 MPa) was obtained by the sand-concrete BOFS 40-40-20 (60vol.% cement replacement), which represents only -6.48% in comparison with the reference sand-concrete strength. Despite the reduced age for mobilization of the all BOFS cementing potential it has contributed to the good performance presented (Diniz et al., 2017). The particles shape also played an important role, especially the coarsest fraction, which is evidenced by the good results of voids index presented by the composites rich in coarse powders. The best overall tensile strength in flexure was also observed for the sand-concrete BOFS 00-80-20 (17.43 MPa), however, only two BOFS sand-concretes presented better results than the reference. On average, the results of flexure tensile strength of the BOFS sand-concretes corresponded to 12.9% of the compressive strength, implying a small decrease in ductility compared to the reference sand-concrete (14.3%).

The QT sand-concretes achieved mechanical performance comparable to BOFS (Figures 6E and 6F), even without a probable chemical binding action. Four QT sand-concretes also reached compressive strengths higher than the reference, highlighting the QT 20-60-20, whose strength was 18.07% higher than the reference (110.76 MPa vs. 93.81 MPa) even at a 40vol.% cement replacement. The best result was obtained by QT 00-90-10 (114.2MPa) and the worst result (82.69MPa) is only 11.86% smaller than the reference and it was obtained by the QT 40-50-10 sand-concrete. The good performances of the QT 20-60-20 and QT 40-40-20 compared to the previous ones are related to the lowest water / fines ratio of these mixtures, which in turn, is a consequence of a good lubrication of the system obtained by the interaction of the small and more rounded particles (fine powder)

with larger and smooth ones (coarse powder). Regarding the flexural tensile performance, the results obtained by the QT sand-concrete were also as good as those presented by the BOFS sand-concretes, highlighting the QT 00-80-20, whose result reached 17.09 MPa. The tensile strength, on average, corresponded to 13.7% of the compressive strength.

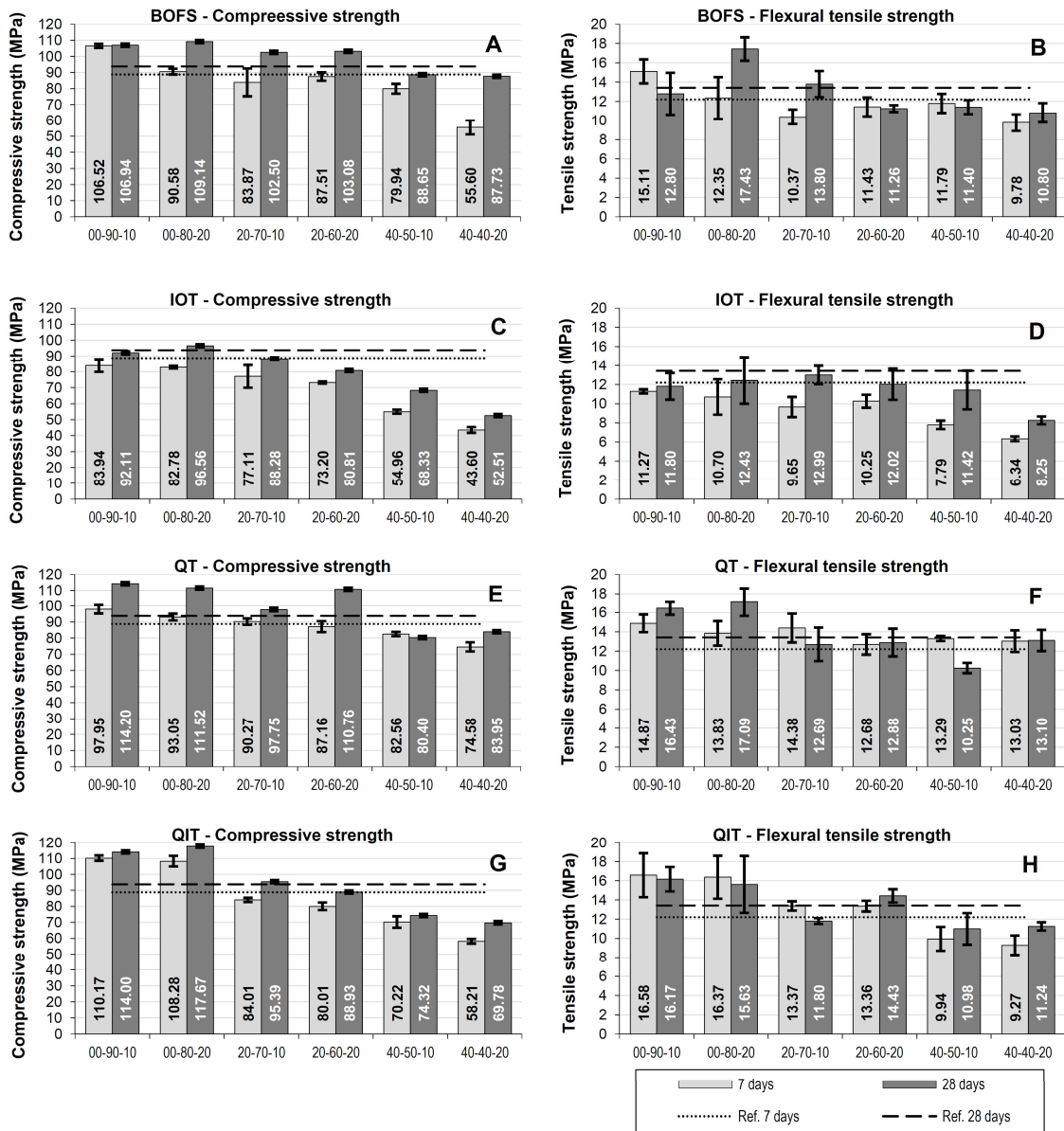


Figure 6. Results of the mechanical characterization of the sand-concretes: (A) compressive strength of the BOFS sand-concretes; (B) flexural tensile strength of the BOFS sand-concretes; (C) compressive strength of the IOT sand-concretes; (D) flexural tensile strength of the IOT sand-concretes; (E) compressive strength of the QT sand-concretes; (F) flexural tensile strength of the QT sand-concretes; (G) compressive strength of the QIT sand-concretes; (H) flexural tensile strength of the QIT sand-concretes.

The QIT sand-concretes with cement replacement by only refined powders presented the best overall results, reaching 117.67 MPa for the QIT 00-80-20 (25.44% higher than reference). The performance of the mixtures with coarse powder, however, has dropped significantly due to the worst morphological characteristics of its particles. The worst result was presented by the QIT 40-40-20 (69.78 MPa). The results of tensile strength were also satisfactory, with the best performance presented by the QIT 00-90-10 sand-concrete (16.17 MPa). Mechanical result of QIT sand-concretes are shown in Figures 6G and 6H.

The lower overall mechanical performances were presented by the IOT sand-concretes (Figures 6C and 6D), which is in good agreement with their highest void indices and water / fines ratios. However, even without a chemical binding action expected for the IOT fines and with the worse performance of the IOT sand-concretes, the IOT 00-80-20 achieved 2.93% higher compressive strength compared to reference sample at 28 days. In addition, the observed reductions in compressive strength of the IOT 00-90-10 and IOT 20-70-10 sand-concretes, compared to the reference, are considered small (-1.81% and -5.90%, respectively). This good performance, however, was overshadowed by the better results reached by the other sand-concretes. The worst overall result was presented by the sand-concrete IOT 40-40-20 (52 MPa). The flexural tensile strengths are in good agreement with the compressive strengths, and the sand-concretes with higher cement replacement rates presented increased ductility, reaching 16.7% of the compressive strength in the IOT 40-50-10 sand-concrete.

4.3.2.3 Macro and Microstructural evaluation

The macrostructure images show dense composites with good involvement of the aggregates into the paste and absence of defects. However, the presence of macropores is evident in all samples, caused by entrapped air due to the mixing and molding processes. These pores have characteristic spherical shape and almost similar distribution in all mixtures. A macroporosity evaluation showed these macropores represent, in average, 7.0% of the sample volume, with standard deviation of 1.6%. Figure 7 shows the distribution of the macropores. Images of the cross-section of some samples are shown in Figure 8.

SEM images of the concretes also show the integrity of the matrices at microstructural level. It was also observed reduced presence of portlandite within entrapped air pores in blended matrices compared with the reference sample. Some SEM images are shown in Figure 9.

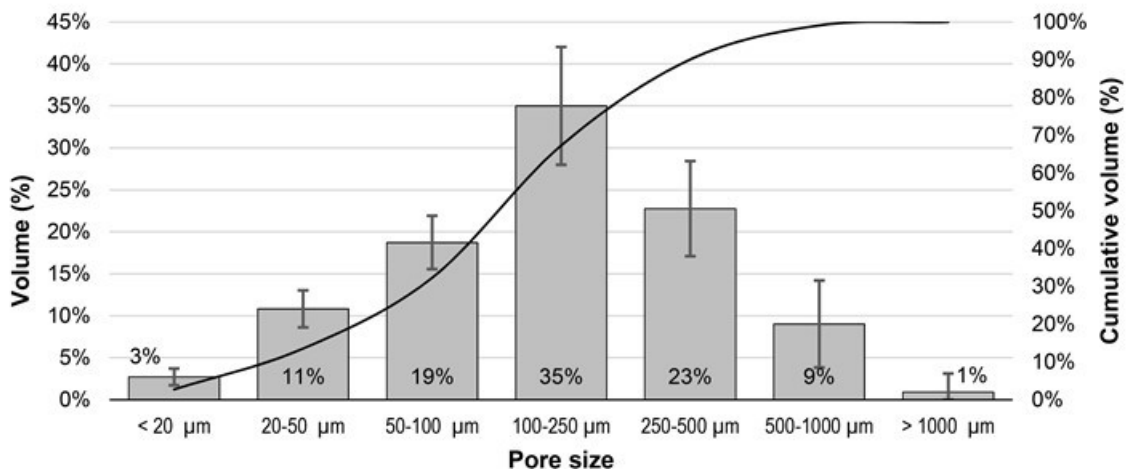


Figure 7. Macroporosimetry of the sand-concretes.

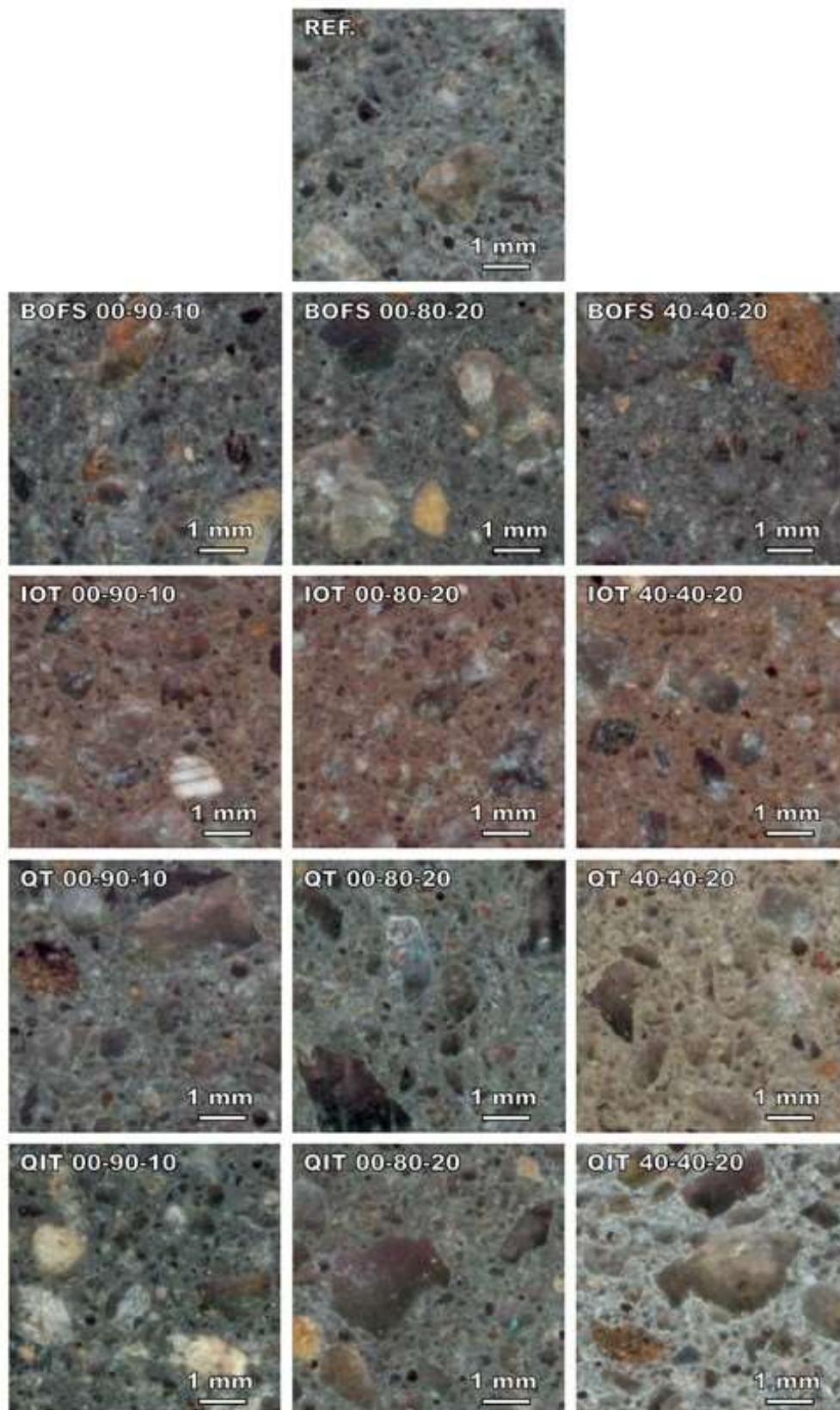


Figure 8. Macrostructural images of sand-concretes.

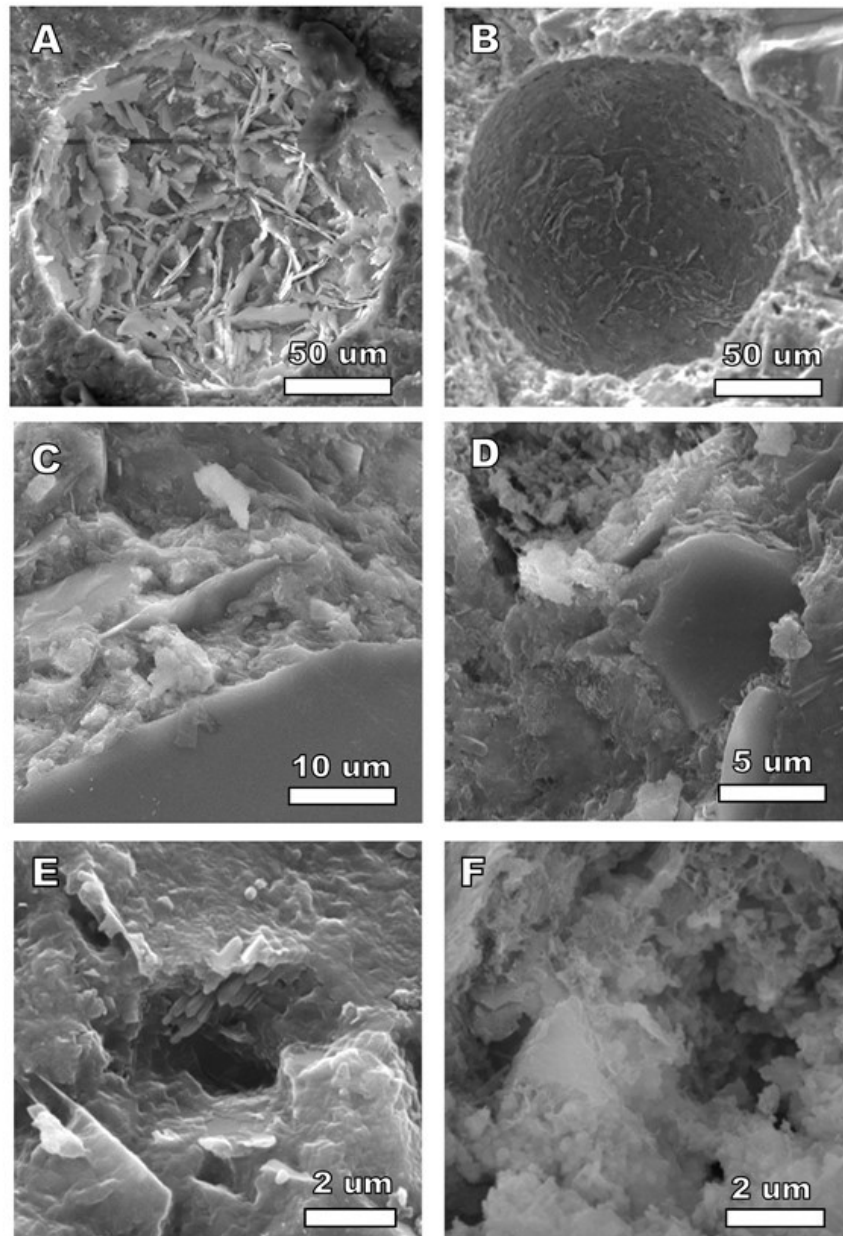


Figure 9. SEM images of the sand-concretes: (A) entrapped air pore in the REF sample; (B) entrapped air pore in the sample QT 40-40-20; (C) interface between aggregate and paste in the sample BOFS 40-40-20; (D) aspects of the microstructure of the sample QIT 40-40-20 showing particles of powder involved by hydration products; (E) aspects of the microstructure and microporosity of the sample QT 00-80-20; (F) aspects of the microstructure and microporosity of the sample IOT 40-40-20.

3.2.4 Eco-efficiency evaluation

The reference sand-concrete presented cement consumption of 771.5 kg/m³ and compressive strength of 93.81 MPa, which implies a binder intensity of 8.22 kg/m³/MPa.

Damineli et al. (2010) investigated 1,583 literature data related to compressive strength, binder consumption and composition of concretes. They observed that the vast majority of the data obtained were in the range of 5 - 20 kg/m³/MPa. Thus, the eco-efficiency of the reference sand-concrete can be considered intermediate to good, showing that the mixing design achieved a good performance.

Table 10 shows that all sand-concretes with cement replacement by waste powders achieved better eco-efficiency results compared to the reference. With few exceptions, the sand-concretes showed improvements in binder intensity as cement replacement content increased. This shows that, even with a decrease in mechanical performance, the use of blends of powders and cement in the proposed particle size distributions improved the binder efficiency. The best overall result was observed for the sand-concrete BOFS 40-40-20, with cement consumption of only 317.9 kg/m³ and binder intensity of 3.62 kg/m³/MPa. This result is better than the best result reported by Damineli et al. (2010) in their survey (4.3 kg/m³/MPa), even without using silica fume or very fine fly ash (pointed by the authors as key factors to obtain concretes with binder intensity below 5 kg/m³/MPa). The finer-than-cement powders were effective in improve the mechanical performance as evidenced in the results of the mixtures 00-90-10 and 00-80-20. The improved binder intensity performance of the mixtures with high waste consumption, however, show that the coarse powders played an important role in waste consumption and consequent eco-efficiency performance.

Table 10. Eco-efficiency indicators of the studied sand-concretes: Cement consumption, binder intensity and waste consumption.

Sand-concrete	Cement consumption (kg/m³)	Binder intensity - <i>bi</i> (kg/m³/MPa)	Waste consumption (kg/m³)
REF.	771.5	8.22	0
BOFS 00-90-10	719.8	6.76	99.1
BOFS 00-80-20	636.8	5.83	197.5
BOFS 20-70-10	554.4	5.41	294.7
BOFS 20-60-20	473.0	4.59	391.1
BOFS 40-50-10	388.9	4.39	481.9
BOFS 40-40-20	317.9	3.62	591.4
IOT 00-90-10	693.9	7.53	89.4
IOT 00-80-20	614.3	6.36	178.3
IOT 20-70-10	556.2	6.30	276.9
IOT 20-60-20	472.7	5.85	365.5
IOT 40-50-10	392.5	5.74	455.5
IOT 40-40-20	313.0	5.96	544.7
QT 00-90-10	722.9	6.33	78.1
QT 00-80-20	669.5	6.00	162.8
QT 20-70-10	562.8	5.76	234.7
QT 20-60-20	502.8	4.54	325.7
QT 40-50-10	419.2	5.21	407.7
QT 40-40-20	330.0	3.93	481.4
QIT 00-90-10	724.0	6.35	72.6
QIT 00-80-20	649.8	5.52	146.7
QIT 20-70-10	574.4	6.02	222.1
QIT 20-60-20	481.8	5.42	289.9
QIT 40-50-10	408.9	5.50	368.8
QIT 40-40-20	325.0	4.66	440.1

Finally, the waste consumption (increasing with the cement replacement) achieved the maximum value (591.4 kg/m³) in the sand-concrete BOFS 40-40-20. This way, this sand-concrete presented the best eco-efficiency performance in both criteria: binder intensity and waste consumption. However, in this case, the density of the material was determinant, once the mixtures were designed in volume. Thus, all sand-concretes presented the same consumption of dry components, in volume, for the same mixture, and the water consumption (given by the experimental packing density performance) was the real variable.

Natural river sand was used in this research as aggregate, but studies with recycled aggregates have been carried out indicating, in some cases, similar and even superior performance in cement-based composites (Fontes et al., 2016). This way, using recycled aggregates, the waste consumption should be improved about three times. Additionally, using more eco-efficient cements (e.g., pozzolanic or ground granulated blast furnace slag cements), the sand-concretes could reach even better environmental performances.

4.3.2.4 Durability

The specimens produced with the paste BOFS 40-40-20 presented an expansion of 1.01% with a standard deviation of 0.092%. The prescribed limit of 0.80% given by the standard C150 (ASTM, 2018) was exceeded, but the samples remained intact, with no visible damages. The result is considered satisfactory and encouraging, once the amount of cement replacement was the highest studied (60%). Furthermore, expansibility tests in pastes with 25vol.% replacement by BOFS-L and BOFS-H, separately, were also conducted and the results showed that the fine powder is the main responsible for the high expansion presented. In these tests, the paste with BOFS-L presented expansion of 0.132% with a standard deviation of 0.009% while the paste with BOFS-H presented an expansion five times greater (0.672% with a standard deviation of 0.03%). In this way, the use of coarse BOFS powder has proved to be safe in this aspect, as well as the moderate use of BOFS fine powder. The combination of these two, however, must be conducted carefully.

4.4 Conclusion

The use of different waste-based powders in two different particle-size ranges associated with Portland cement (in an intermediate fineness condition) in densely packed mixtures

was proposed in this study as a strategy to improve the SCM performance, and the main findings are listed below.

- The grinding programs used in the production of the proposed SCMs were effective in obtaining coarser-than-cement and finer-than-cement powders compatible with the objectives of this research. Their good particle morphology and interaction with the polycarboxylate-based superplasticizer improved the flow performances in the proposed blends permitting important reductions in the w/f ratios.
- The proposed sand-concrete mix proportion based on the Modified Andreassen packing model was effective in obtaining matrices with low water consumption, reflecting in high experimental packing densities.
- With few exceptions, the sand-concretes presented lower void indices in comparison with reference cement-only mortars even for high cement replacement due to the improved particle packing. The blended sand-concretes also showed higher ultrasonic pulse velocities as a result of dense and sound matrices, which was confirmed by the macro and microstructural evaluations.
- All blended sand-concretes presented high mechanical and eco-efficiency performances. The fine SCMs were highly effective to improve the compressive strength as observed in sand-concretes with cement replacement rates of 10% and 20%. On the other hand, the coarse SCMs represent economic advantages (less expensive grinding) and were highly effective in improving the eco-efficiency (reducing the binder intensities) even in sand concretes presenting lower compressive strengths.

The results emphasize a great potential in obtaining highly effective SCMs from different residues. Moreover, the great potential for consumption of larger quantities of waste from different production chains broadens the prospects of obtaining more sustainable products, meeting the needs and economic interests of different sectors.

4.5 Acknowledgments

Authors acknowledge the financial support provided by CAPES, FAPEMIG, CNPq, UFOP, UFV and Fundação Gorceix. Equipment and technical support provided by the following laboratories are gratefully appreciated: Laboratory of Electronic Microscopy - NANOLAB - Redemat - UFOP; Laboratory of Construction Materials - Department of Civil Engineering – UFOP; and Laboratory of Construction Materials – Department of Civil Engineering - UFV. Thanks are also due to the Research Group on Solid Wastes RECICLOS–CNPq for infrastructure use and collaboration.

4.6 References

ABNT, 1991. *NBR 5733: High early strength Portland cement - Specification*. Rio de Janeiro: Associação Brasileira de Normas Técnicas. (in Portuguese).

ABNT, 2005. *NBR 13279: Mortars applied in walls and ceilings - Determination of the flexural and the compressive strength in the hardened stage*. Rio de Janeiro: Associação Brasileira de Normas Técnicas. (in Portuguese).

ABNT, 2005. *NBR 9778: Hardened mortar and concrete - Determination of absorption, voids and specific gravity*. Rio de Janeiro: Associação Brasileira de Normas Técnicas. (in Portuguese).

ABNT, 2015. *NBR 16372: Portland cement and other powdered materials - Determination of fineness by the air permeability method (Blaine method)*. Rio de Janeiro: Associação Brasileira de Normas Técnicas - ABNT.

Aitcin, P.C., 2000. *High performance concrete*. São Paulo: PINI.

Ali, M.B. & Hossain, M.S., 2011. A review on emission analysis in cement industries. *Renew. Sust. Energ. Rev.*, (15), pp.2252-61. DOI: 10.1016/j.rser.2011.02.014.

Alimeneti, N.R., 2015. *Properties of Microcement mortar with nanoparticles*. Arlington: University of Texas at Arlington. Available at: <http://hdl.handle.net/10106/25403>.
Master's thesis.

Aprianti, E., 2017. A huge number of artificial waste material can be supplementary cementitious material (SCM) for concrete production – a review part II. *Journal of cleaner production*, 142, pp.4178-94. DOI 10.1016/j.jclepro.2015.12.115.

ASTM, 2014. *C348-14: Standard Test Method for Flexural Strength of Hydraulic-Cement Mortars*. West Conshohocken: American Society of Testing and Materials.

ASTM, 2014. *C349-14: Standard Test Method for Compressive Strength of Hydraulic-Cement Mortars (Using Portions of Prisms Broken in Flexure)*. West Conshohocken: American Society of Testing and Materials.

ASTM, 2016. *Standard Test Method for Autoclave Expansion of Hydraulic Cement*. West Conshohocken: American Society of Testing and Materials - ASTM.

ASTM, 2017. *Standard test methods for fineness of hydraulic cement by air-permeability apparatus*. West Conshohocken: American Society for Testing and Materials.

ASTM, 2018. *C150/C150-M: Standards Specification for Portland Cement*. West Conshohocken: ASTM International.

Bastos, L.A.C., Silva, G.C., Mendes, J.C. & Peixoto, R.A.F., 2016. Using of iron ore tailings from tailing dams as road material. *J. Mater. Civil Eng.*, 28(10), p.04016102. DOI: 10.1061/(ASCE)MT.1943-5533.0001613.

Berndt, M.L., 2009. Properties of sustainable concrete containing fly ash, slag and recycled concrete aggregates. *Constr. Build. Mater.*, 23, pp.2606-13. DOI: 10.1016/j.conbuildmat.2009.02.011.

Cao, Y. et al., 2015. The influence of cellulose nanocrystal additions on the performance of cement paste. *Cement & Concrete Composites* 56, pp.73-83. DOI 10.1016/j.cemconcomp.2014.11.008.

Castro, A.L. & Pandolfelli, V.C., 2009. Review: Concepts of particle dispersion and packing for special concrete production. *Cerâmica*, 55, pp.18-32. DOI: 10.1590/S0366-69132009000100003 (in Portuguese).

Da Silva, M.J. et al., 2016. Feasibility Study of Steel Slag Aggregates in Precast Concrete Pavers. *ACI Mater. J.*, 113(4), pp.439-46. DOI: 10.14359/51688986.

Damineli, B.L., 2013. *Concepts for the formulation of concretes with low binder consumption: Rheologic control, packing and particle dispersion*. São Paulo: USP. Doctoral Thesis, University of São Paulo (In Portuguese).

Damineli, B.L., Kemeid, F.M., Aguiar, P.S. & John, V.M., 2010. Measuring the eco-efficiency of cement use. *Cement Concrete Comp.*, 32, pp.555-62. DOI: 10.1016/j.cemconcomp.2010.07.009.

Dincer, I. & Acar, C., 2015. A review on clean energy solutions for better sustainability. *Int J Energ Res*, 39(5), pp.585-606. DOI: 10.1002/er.3329.

Dincer, I. & Acar, C., 2017. Smart energy systems for a sustainable future. *Appl Energ*, 194, pp.225-35. DOI: 10.1016/j.apenergy.2016.12.058.

Diniz, D.H., Carvalho, J.M.F., Mendes, J.C. & Peixoto, R.A.F., 2017. Blast Oxygen Furnace Slag as Chemical Soil Stabilizer for Use in Roads. *J. Mater. Civil Eng.*, 29(9), p.04017118. DOI: 10.1061/(ASCE)MT.1943-5533.0001969.

Faella, C. et al., 2016. Mechanical and durability performance of sustainable structural concretes: An experimental study. *Cement Concrete Comp*, 71, pp.85-96. DOI: 10.1016/j.cemconcomp.2016.05.009.

Fontes, W.C., Mendes, J.C., Silva, S.N. & Peixoto, R.A.F., 2016. Mortars for laying and coating produced with iron ore tailings from tailing dams. *Constr. Build. Mater.*, 112, pp.988-95. DOI: 10.1016/j.conbuildmat.2016.03.027.

Funk, J.E. & Dinger, D.A., 1994. Particle size control for high-solids castable refractories. *Am. Ceram. Soc. Bull.*, 73(10), pp.66-69.

García-Gusano, D. et al., 2014. Life cycle assessment of the Spanish cement industry: implementation of environmental-friendly solutions. *Clean. Technol. Envir.*, 17(1), pp.59-73. DOI: 10.1007/s10098-014-0757-0.

Hartmann, C., Jeknavorian, A., Silva, D. & Benini, H., 2011. Chemical admixtures for cement and concretes. In G.C. Isaia, ed. *Concrete Science and Technology*. São Paulo: IBRACON. pp.347-80. (in Portuguese).

Hasholt, M.T. & Jensen, O.M., 2015. Chloride migration in concrete with superabsorbent polymers. *Cement and Concrete Composites*, 55, pp.290-97. DOI 10.1016/j.cemconcomp.2014.09.023.

Hendriks, C.A. et al., 1998. Emission reduction of greenhouse gases from the cement industry. In *Proceedings of the fourth international conference on greenhouse gas control technologies*. pp.939-44.

Huntzinger, D.N. & Eatmon, T.D., 2009. A life-cycle assessment of Portland cement manufacturing: comparing the traditional process with alternative technologies. *J. Clean. Prod.*, 17(7), pp.668-75. DOI: 10.1016/j.jclepro.2008.04.007.

Iacobescu, R.I. et al., 2011. Valorisation of electric arc furnace steel slag as raw material for low energy belite cements. *J. Hazard. Mater.*, pp.287-94. DOI: 10.1016/j.jhazmat.2011.09.024.

Kajaste, R. & Hurme, M., 2016. Cement industry greenhouse gas emissions e management options and abatement cost. *J. Clean. Prod.*, (112), pp.4041-52. DOI: 10.1016/j.jclepro.2015.07.055.

Kwan, A.K.H. & Wong, H.H.C., 2008. Packing density of cementitious materials: part 2 - packing and flow of OPC + PFA + CSF. *Mater. Struct.*, 41, pp.773-84. DOI: 10.1617/s11527-007-9281-6.

Lei, Y., Zhang, Q., Nielsen, C. & He, K., 2011. An inventory of primary air pollutants and CO₂ emissions from cement production in China. *Atmos. Environ.*, 45(1), pp.147-54. DOI: 10.1016/j.atmosenv.2010.11.027.

Lima, C. et al., 2013. Physical properties and mechanical behaviour of concrete made with recycled aggregates and fly ash. *Constr Build Mater*, 47, pp.547-59. DOI: 10.1016/j.conbuildmat.2013.04.051.

Marinho, A.L.B. et al., 2017. Ladle Furnace Slag as Binder for Cement-Based Composites. *J. Mater. Civil Eng.*, 29(11), p.04017207. DOI: 10.1061/(ASCE)MT.1943-5533.0002061.

Mehta, P.K. & Monteiro, P.J.M., 2006. *Concrete - microstructure, properties, and materials*. New York: McGraw-Hill.

Mendes, J.C. et al., 2017. Mechanical, rheological and morphological analysis of cement-based composites with a new LAS-based air entraining agent. *Constr. Build. Mater.*, 145, pp.648-61.

Meyers, G.D., McLeod, G. & Anbarci, M.A., 2006. An international waste convention: measures for achieving sustainable development. *Waste Management*, 24, pp.505-13. DOI 10.1016/j.wasman.2005.08.003.

Midilli, A., Dincer, I. & Ay, M., 2006. Green energy strategies for sustainable development. *Energy Policy*, 34(18), pp.3623-33. DOI: 10.1016/j.enpol.2005.08.003.

Mikulčić, H. et al., 2016. Reducing greenhouse gasses emissions by fostering the deployment of alternative raw materials and energy sources in the cleaner cement

manufacturing process. *J. Clean. Prod.*, 136, pp.119-32. DOI: 10.1016/j.jclepro.2016.04.145.

Miller, S.A., Monteiro, P.J.M., Ostertag, C.P. & Horvath, A., 2016. Comparison indices for design and proportioning of concrete mixtures taking environmental impacts account. *Cement Concrete Comp.*, (68), pp.131-43. DOI: 10.1016/j.cemconcomp.2016.02.002.

Nie, Q. et al., 2015. Numerical simulation of fly ash concrete under sulfate attack. *Constr Build Mater*, 84, pp.261-68. DOI: 10.1016/j.conbuildmat.2015.02.088.

Nie, Q. et al., 2014. Chemical, Mechanical, and Durability Properties of Concrete with Local Mineral Admixtures under Sulfate Environment in Northwest China. *Materials*, 7(5), pp.3772-85. DOI: 10.3390/ma7053772.

Rabbani, A. & Jamshidi, S.S.S., 2014. An automated simple algorithm for realistic pore network extraction from micro-tomography images. *J. Pet. Sci. Eng.*, 123, pp.164-71.

Salas, D.A. et al., 2016. Environmental impacts, life cycle assessment and potential improvement measures for cement production: a literature review. *J. Clean. Prod.*, 113, pp.114-22. DOI: 10.1016/j.jclepro.2015.11.078.

Sant'ana Filho, J.N. et al., 2017. Technical and environmental feasibility of interlocking concrete pavers with iron ore tailings from tailings dams. *J. Mater. Civil Eng.*, 29(9), p.04017104. DOI: 10.1061/(ASCE)MT.1943-5533.0001937.

Thomas, J.J., Jennings, H.M. & Chen, J.J., 2009. Influence of nucleation seeding on the hydration Mechanisms of Tricalcium Silicate and Cement. *The Journal of Physical Chemistry C* 113, pp.4327-34. DOI 10.1021/jp809811w.

Toffolo, R.V.M., 2015. *Sustainable pavements*. Ouro Preto: UFOP. (Master's Thesis - Federal University of Ouro Preto) (in Portuguese).

WBCSD/IEA, 2009. *Cement Technology Roadmap 2009*. OECD/IEA and World Business Council for Sustainable Development.

Wong, H.H.C. & Kwan, A.K.H., 2008. Packing density of cementitious materials: part 1 - measurement using a wet packing method. *Mater. Struct.*, 41, pp.689-701. DOI: 10.1617/s11527-007-9274-5.

Zhang, M. et al., 2016. Manifest system for management of non-hazardous industrial solid wastes: results from a Tianjin industrial park. *Journal of Cleaner Production*, 133, pp.252-561. DOI 10.1016/j.jclepro.2016.05.102.

Zhao, S., Fan, J. & Sun, W., 2014. Utilization of iron ore tailings as fine aggregate in ultra-high performance concrete. *Constr. Build. Mater.*, 50, p.540. DOI: 10.1016/j.conbuildmat.2013.10.019.

Chapter 5

Reaction speed and rheological behavior of cement-blended pastes containing engineered recycled mineral admixtures obtained from steel slag, iron ore tailings, quartz tailings and quartzite tailings

José Maria Franco de Carvalho, Wolfram Schmidt, Hans-Carsten Kühne, Ricardo André Fiorotti Peixoto

Abstract

The influence of particle size and polycarboxylate-based superplasticizers on rheological properties and reaction speed of cement-blended pastes containing engineered recycled mineral admixtures obtained from steel slag, iron ore tailings, quartz tailings and quartzite tailings were evaluated in this work. The experimental program comprised zeta potential measurements, spread in the flow table, rheological tests in a Couette type rheometer, and measurements of Vicat needle penetration depths along the time. Similar or meliorated flow properties were observed in cement-blended pastes in comparison to reference cement-only pastes. PCE type and particle size exerted great influence in the stability of the mixtures and reaction speed.

Keywords: Engineered recycled mineral admixture, rheology, hydration, steel slag, mining tailings, PCE-based superplasticizer.

Construction and Building Materials

This manuscript was submitted on February 14th, 2019.

Current status: in review.

5.1 Introduction

The scientific community has largely discussed the low environmental performance of conventional concrete due to the high CO₂ emissions in the production of Portland cement (Hendriks, et al., 1998; Huntzinger & Eatmon, 2009; Iacobescu, et al., 2011; Ali & Hossain, 2011; Kajaste & Hurme, 2016). In this sense, mitigation routes have been pointed, and their application has become mandatory. The partial replacement of Portland cement by low impact supplementary cementing materials (SCM) is the most effective measure among the alternatives proposed by the literature (WBCSD/IEA, 2009; Lei, et al., 2011; García-Gusano, et al., 2014; Kajaste & Hurme, 2016; Salas, et al., 2016; Mikulčić, et al., 2016). This route is even more effective considering SCMs obtained from residues, in a strategy able save natural resources at the same time that provides an adequate destination to environmental liabilities (Meyers, et al., 2006; Zhang, et al., 2016; Aprianti, 2017).

Steelmaking slags are by-products of the refining process of the steel production generated in large amounts (Diniz, et al., 2017; Da Silva, et al., 2016). Despite their cementing properties and adequate characteristics for use in cement composites as aggregates or supplementary cementitious material, their use is yet small once the presence of expansive oxides and high content of metallic iron cause concern (Diniz, et al., 2017). However, studies demonstrated the effectiveness and profitability of processing these materials. Also, cement-based products using steel slag as aggregates or powders have proved to be technically feasible (Da Silva, et al., 2016; Diniz, et al., 2017; Gonçalves, et al., 2016; Carvalho, et al., 2018; Andrade, 2018).

The mining industry is also responsible for the generation and disposal of large amounts of residues. One of the remarkable examples is iron ore mining. In Brazil this residue is generated in large amounts and commonly disposed of in tailings dams, implying in high environmental impacts with increased risk for the environment and human life in case of collapse, as observed recently in Mariana and Brumadinho, Minas Gerais State, Brazil (Fontes, et al., 2016; do Carmo, et al., 2017; Silva, et al., 2019). The feasibility in using this material in cement-based composites in different ways is also demonstrated (Bastos, et al., 2016; Fontes, et al., 2016; Sant'ana Filho, et al., 2017; Galvão, et al., 2018). Other residues from different mining industries as low-quality fractions and sterile have also been studied with promising results (Dutra, et al., 2014; Dias, et al., 2016; Carvalho, et al., 2019).

Polymers based on Polycarboxylate-ether (PCEs) are high range water reducing admixtures used in concretes. These comb-like polymers consist of a backbone where are attached ionic carboxylic or sulfonic groups, and non-ionic side chains commonly based on polyalkyleneoxide or polyethylene glycol (Schober & Mäder, 2003; Kanchanason & Plank, 2018). The PCE molecules are adsorbed onto the positively charged surface sites of cement particles, but also positive sites of other supplementary particles and hydration products like ettringite (AFt) (Schmidt, 2014; Kanchanason & Plank, 2018). Induced electrostatic repulsion and steric hindrance are the dispersion mechanisms of PCE molecules, and the proportions vary depending on the ionic strength of the solution, molecular structure and molar mass of the polymers (Schober & Mäder, 2003). Modifications of these polymers are possible varying the length of the backbone, the content of ionic groups, and the length, amount and type of the side chains. In this concern, the influence of these parameters on the performance has been reported (Ohta, et al., 1997; Plank, et al., 2006; Sakai, et al., 2003).

However, the charge density is the main practical characteristic that effectively exerts significant influence in the adsorption properties (Schober & Mäder, 2003; Schober & Flatt, 2006; Winnefeld, et al., 2007; Shin, et al., 2008). In a summarized way, the charge density increases with the reduction in the number and length of the side chains, as well as, with the increase in the backbone length (Schmidt, 2014). High charge PCEs provide a fast and higher flow in cement pastes (Schober & Mäder, 2003). Nevertheless, due to the fast consumption of available PCE molecules by the continuing hydration process, the retention is poor. In this sense, low charge PCEs are more effective, once they adsorb with retardation, and increased amounts of molecules remain available in the pore solution for a longer time. As a consequence, they present a limited effect on yield stress once they do not provide an ultimate flowability (Schober & Mäder, 2003). Besides, the flow performance of cementitious systems in the presence of PCE is affected for interactions between polymers and ions available in pore solution and competitive adsorption with sulfate ions (Yamada, et al., 2001). Furthermore, the formation of phases in the pore solution and morphology changes provide new adsorption sites along the hydration process (Schmidt, 2014; Schmidt, et al., 2014; Schmidt, et al., 2018).

PCE-based admixtures promote a remarkable effect in the hydration kinetics. In this sense, noticeable retarding effects are observed (Hanehara, 1999; Yamada, et al., 2001; Puertas, et al., 2005). This effect is also strongly affected by the charge density. With the increase in PCE adsorption, the delays also increase (Schmidt, et al., 2014). The presence of PCE admixtures induces changes on the C-S-H structure (Puertas, et al., 2005; Kanchanason & Plank, 2018). The C-S-H surface can exhibit a slightly positive charge in an alkaline medium, facilitating the adsorption of ionic PCE. As a result, the conversion of the globular for nanofoil-like form is retarded, but after that, they can exhibit strong seeding effect contributing to early strength development (Kanchanason & Plank, 2018).

The use of mineral admixtures in cement blends may remarkably modify the flow properties of the cementitious system (Park, et al., 2005; Shanahan, et al., 2016). The total specific surface area (SSA) of the fines can be mostly altered depending on the SSA of the admixture and replacement rate. In this sense, a good correlation between SSA and yield stress has been reported (Shanahan, et al., 2016). Nevertheless, the morphological characteristics play an important role, once rounded particles improve the “ball bearing effect” (Park, et al., 2005), In this sense, even particles with high SSA can present good envelop shape and consequent good flow performance. Finally, good interaction with anionic superplasticizers is expected for particles presenting high positive values of ζ -potential.

The physical, chemical and mineralogical properties of the particles will affect both rheological properties and hydration kinetics. The increase in fineness is related to an acceleration in the hydration reactions by providing increased C-S-H nucleation sites. Ultrafine grinding is also related to the development of pozzolanic properties and increased reactivity of cementitious materials. The potentiated dissolution, however, will interfere in the type and quantity of ions available in the pore solution, with implications in the hydration kinetics and superplasticizer interaction with early hydration phases (e.g., AFt and AFm) (Schmidt, 2014).

The production and use of engineered recycled mineral admixtures (ERMAs) obtained from steel slags, iron ore tailings, quartz mining tailings, and quartzite mining tailings have been proposed by the author’s research group. These materials are designed aiming to gain packing improvement in cementitious composites, and promising mechanical and eco-efficiency results has been demonstrated (Carvalho, et al., 2018; Carvalho, et al., 2019). In this work, an investigation on the rheologic performance of cement pastes

containing these products is presented. Tests were performed in absence of chemical admixtures and in the presence of different PCE-based superplasticizers. An investigation on the reaction speed is also provided.

5.2 Material and methods

5.2.1 Materials

The materials used in this study comprised of samples of steel slag and three mining tailings. The granular basic oxygen furnace slag (BOFS) was provided by a steelmaker located in Minas Gerais State, Brazil. The material was stored in a stockyard outdoors and subject to weathering for approximately three years. The sample of iron ore tailings (IOT) was collected in a tailings dam located in the central region of the Minas Gerais State and was stored in sealed plastic containers. The sample of the granular quartz mining tailings (QT) was provided by a mining plant located in Sete Lagoas, state of Minas Gerais. Finally, the sample of quartzite mining tailing (QIT) was provided by a mine located in the city of Itabirito, Minas Gerais. Some of the physical properties and the mineralogical composition of the raw materials are listed in Table 1. Table 2 shows the oxide composition from XRF.

Ordinary Portland cement, specified as CEM I 42.5 R according to EN 197-1, 2011 (DIN, 2011) was used for the experiments. The specific gravity is 3.125 and the Blaine value is 4100 cm²/g.

Two powder type polycarboxylate based superplasticizers (PCE) were used in this study. One PCE provides a lower charge density and longer side chains relative to the second

polymer. Therefore, the lower charge polymer and the higher charge polymer are named PCE-LC and PCE-HC, respectively.

Table 1. Some physical properties and mineralogical composition of the raw materials.

Property	BOFS	IOT	QT	QIT
Aspect	Granular, dark grey coloration	Powdery (mud), red to brown coloration	Granular, beige coloration	Powdery to granular, white to grey coloration
Particle size range	2 - 15 mm	0.0004 - 0.1 mm	0.5 – 40 mm	0.0006 – 5 mm
Bulk density	1.945 g/cm ³	1.905 g/cm ³	1.777 g/cm ³	1.641 g/cm ³
Mineralogical composition	Larnite Brownmillerite Periclase Wuestite Calcite Helvine Lime Amorphous	Quartz Hematite Goethite	Quartz	Quartz Muscovite

Table 2. Chemical composition of the studied materials

Compound	Content (%)			
	BOFS	IOT	QT	QIT
SiO ₂	15.6	35.5	95.5	80.0
Al ₂ O ₃	4.4	5.8	1.5	15.9
Fe ₂ O ₃	31.2	56.9	1.9	0.4
CaO	36.8	0.2	0.2	-
MgO	5.0	0.2	-	0.1
K ₂ O	-	-	-	2.8
Na ₂ O	-	-	-	-
SO ₃	0.4	-	-	-
MnO	3.5	-	-	-
Cr ₂ O ₃	0.8	-	-	-
V ₂ O ₅	0.1	-	-	-
P ₂ O ₅	1.5	-	-	-
TiO ₂	0.5	-	-	-
Other	0.2	1.4	0.9	0.8
LOI	1.1	3.1	0.3	1.2

5.2.2 *Processing of the raw wastes and production of the mineral admixtures (powders)*

The powders were produced from particles with a maximum size of 5.0 mm. For this, the BOFS and QT samples were given to a preliminary comminution process comprising crushing in a laboratory jaw crusher (BB200, Retsch).

Based on preliminary studies, two powders were produced from each raw waste: one powder was coarser than cement, while the other one was finer. The objective is to evaluate the influence of the fineness on the rheology and the hydration kinetics of blended pastes with partial replacement of cement by the studied powders. The grinding programs were performed in a laboratory horizontal ball mill and a high-efficiency planetary ball mill. Table 3 and Table 4 show the grinding conditions and specifications, respectively.

Table 3. Characteristics of the grinding programs and mills used in the production of the studied powders.

Grinding program	Parameter / characteristic	Specification
L	Mill (rotational speed)	Marconi MA 500 (200 rpm)
	Constituent material (jar and balls)	Stainless steel
	Jar volume, cm ³	10,360
	Balls volume, cm ³ (% jar volume)	1,658 (16 %)
	Material volume, cm ³ (% jar volume)	1,740 (17 %)
H	Mill (rotational speed)	Retsch PM 100 (400 rpm)
	Constituent material (jar and balls)	Zirconia (ZrO ₂)
	Jar volume, cm ³	250
	Balls volume, cm ³ (% jar volume)	64.3 (26 %)
	Material volume, cm ³ (% jar volume)	80 (32 %)

The basic characterization comprised of the determination of the specific density by helium pycnometry (Porotec Pycnomatic ATC), the specific surface area (SSA) using the BET method (Micrometrics TriStar II), and the particle size distribution (PSD) by laser

diffraction (Bettersize2000). SEM images (Tescan VEGA3) were used to evaluate the particles' morphology.

Table 4. Identification of the powders produced comprising the grinding programs and times.

Powder	Grinding program	Grinding time (min)
BOFS-L	L	180
IOT-L	L	30
QT-L	L	120
QIT-L	L	30
BOFS-H	L / H	180 / 15
IOT-H	L / H	180 / 45
QT-H	L / H	180 / 45
QIT-H	L / H	180 / 45

5.2.3 Evaluation of the ζ -potential

The zeta potential was determined via the electrophoretic mobility using a light scatter device (Malvern, Zetasizer Nano ZS). For this, the U-shaped measurement cells with electrodes are filled with the suspensions to be measured, and then an electric field of known strength was applied. Depending upon their charges, particles are moved towards the oppositely charged electrode, while the ions beyond the shear plane stay behind. The remaining excess charge of the particle upon motion is the zeta potential and can be derived by the particles' velocity depending on the current. The tests were performed in samples of the studied waste powders in two different media: deionized water and saturated Ca(OH)₂ solution. The preparation of the samples comprised of the dispersion of approximately 0.1 mg of the respective material in the liquid medium (10 mL) with the aid of a laboratory ultrasonic agitator (Bandelin RK 106). After that, part of the medium containing the dispersed particles was transferred to the measuring cell using a PTFE filter to ensure that only particles with a diameter less than 1 μ m were evaluated. In

parallel, a sample of the medium containing the dispersed particles was taken, and the pH was measured for each determination. The zeta potentials were calculated by software using Equation 1, where ζ is the zeta potential, η is the solution viscosity, D is the dielectric constant and E is the electrical potential.

Equation 1
$$\zeta = \frac{4\pi\eta\nu}{DE}$$

5.2.4 Rheology

The rheological tests were performed on cement pastes using a Couette type rheometer (Schleibinger, Viskomat NT). One reference paste (REF, cement-only) and eight blended pastes were evaluated for each studied PCE and dosage. The blends were produced for a replacement rate of 10% by volume of the cement by the studied powders. The solids volume fraction ϕ was 0.5 and demineralized water at 20 ± 2 °C was used.

The mixing was conducted in a kitchen mixer Kenwood Chef Classic Platin KM 416. This mixer shows excellent homogenization performance at small mixing volumes (Schmidt, 2014). Initially, a dry mixing step was performed for 60 s at low velocity. After that, water was added over the course of approximately 30 s, after which the sample was mixed for 60 s at high speed. This was followed by a 30 s resting period in which any possible powder remainders were scraped off the paddle and the bowl's wall. Eventually, the mixture was mixed for another 60 s at high speed.

In order to determine the consistency with and without PCE the flow table test after EN 1015-3, (DIN, 2007) was used. The so-called Haegermann conus with upper and lower diameters of 70 mm and 100 mm, respectively, and a height of 80 mm is filled with paste or mortar, compacted and lifted. Then the flow table is lifted for 10 mm and dropped

15 times. The average of two perpendicular diameters is defined as the flow spread diameter.

For the torque measurements using the rheometer, a wing stirrer probe for cement paste V0013 was used. This probe is indicated for particle sizes less than 0.5 mm. It is used for relative measurements of fluids. At high shear velocities, the cell ensures that no segregation take place (Vasiliou, et al., 2017). The volume of paste used for the determinations was 375 mL. The maximum PCE content was fixed at 0.25 % by mass of cement. This amount was divided into seven equal portions to be added along the test.

The measuring profile is shown in Figure 1 and consists of 8 equal ramps and plateaus phases over a period of 300 s. For each ramp the torque was increased from 0 to 240 rpm in 30 s, then the plateau was held at 240 rpm for 240 seconds after which the speed was decreased again to 0 over a time of 30 s. The first cycle was performed without PCE addition. Then, at the beginning of each ramp, following portions of 0.0357% PCE by mass of cement were added to the mixture. Hence, the total amount of PCE added after the last addition during the 8th ramp added up to 0.25% by mass of cement.

The evaluation of the flow properties was made using the Bingham model, where after exceeding a stress value that initiates flow, the so-called yield stress τ_0 , shear rate and shear stress are proportional (Bingham, 1922). However, with the applied cell, where flow and shear areas are unknown, the conversion of torque to stress and rotational speed to shear rate is impossible (Vasiliou, et al., 2017). However, both stress and shear rate values are qualitatively linked to torque and rotational speed, respectively. This way, qualitative correlations between torque and shear stress and rotational velocity and shear rate can be made to observe influences of additions (Schmidt, 2014; Vasiliou, et al., 2017). Equation

2 describes the Bingham model, where τ is the shear stress [Pa]; η_{pl} is the plastic viscosity [Pa·s]; and $\dot{\gamma}$ is the shear rate [1/s].

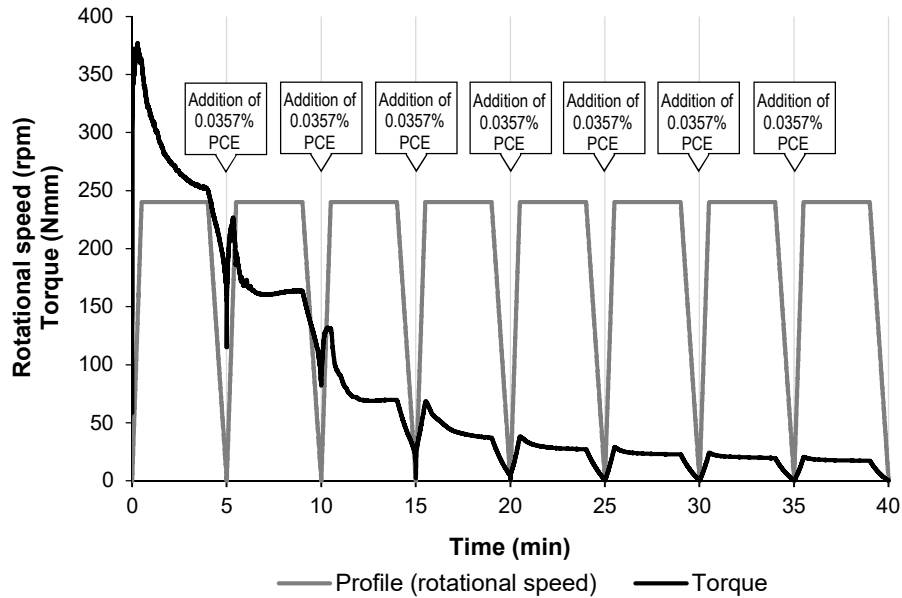


Figure 1. Measuring profile adopted in the rheological tests and torque measurement curve for REF paste with the addition of PCE-HC.

Equation 2
$$\tau = \tau_0 + \eta_{pl} \cdot \dot{\gamma}$$

Measurements performed in the third stage of the measuring profile presented in Figure 1 were taken and flow curves torque versus rotational speed were adjusted. The slopes and ordinate intercept of the curves were used in the qualitative evaluations of the viscosity and yield stress respectively.

5.2.5 Reaction speed

The influence of the powders and SPs in the reaction speed was qualitatively evaluated using an adapted method based on the Vicat needle test EN 196-3 (DIN, 2016) (Schmidt, 2014). For this, an automatic 11-slot Vicat device (Toni Technik) was used, and the tests

were performed in samples immersed in water in a temperature-controlled room (22 ± 2 °C). However, the tests were not performed in standard consistency pastes, but in the same pastes evaluated in the consistency tests (without SP) and rheologic tests (with SP). In all cases, the solids volume fraction ϕ was set in 0.5 by volume and the consistency varied with the powder evaluated and SP type used. The results were compared between pastes with and without SP and between reference cement-only pastes and blended pastes with the evaluated supplementary waste-based powders. Two values of Vicat needle penetration depth and corresponding times were chosen to evaluate the reaction speed, they were 35 mm (corresponding approximately to the initial setting time), and 15 mm (to minimize the effects of segregation and contraction).

5.3 Results and discussion

5.3.1 Characterization

SEM images presented in Figure 2 show that BOFS-L particles have a high roughness but with high sphericity. The large IOT-L particles are predominantly quartz with low sphericity and angular edges. Significant amount of small clayey particles adhered onto larger ones were observed in IOT-L images. The quartz particles of the QT-L powder present predominantly low sphericity, with angular and sharp edges. QIT-L particles consist of predominantly particles of tabular shape with sharp edges. The high-efficiency grinding was effective in improving the particle shapes. All fine powders exhibited more equant volumetric shape and smoother edges in comparison to the corresponding coarse powders.

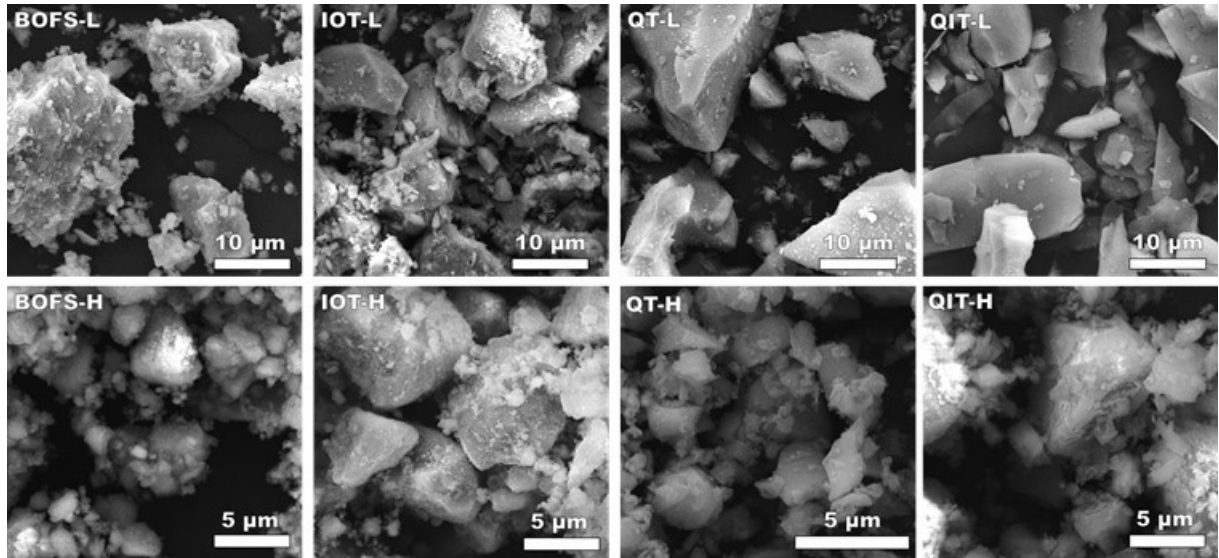


Figure 2. SEM images of the produced powders

Figure 3 shows that the coarser powders BOFS-L, IOT-L, QT-L, and QIT-L achieved very similar PSDs. The PSDs of the finely ground powders IOT-H, QT-H and QIT-H were also very similar. However, the particle size distribution of the equally treated BOFS-H powder is coarser than the other powders. The PSD resembles that of the cement. This coarser distribution, however, cannot be related to the reduced grinding time (15 min), since prior to the preparation of the powders, the stabilization point for BOFS-H was determined to be at 15 min. The presence of discrepant large tabular metallic particles after grinding suggests that the metallic iron content of BOFS increased the ductility of this material. As a result, part of the employed energy was absorbed in deformations, reducing the grinding efficiency, thus causing that the particles remain coarser at the stabilization point.

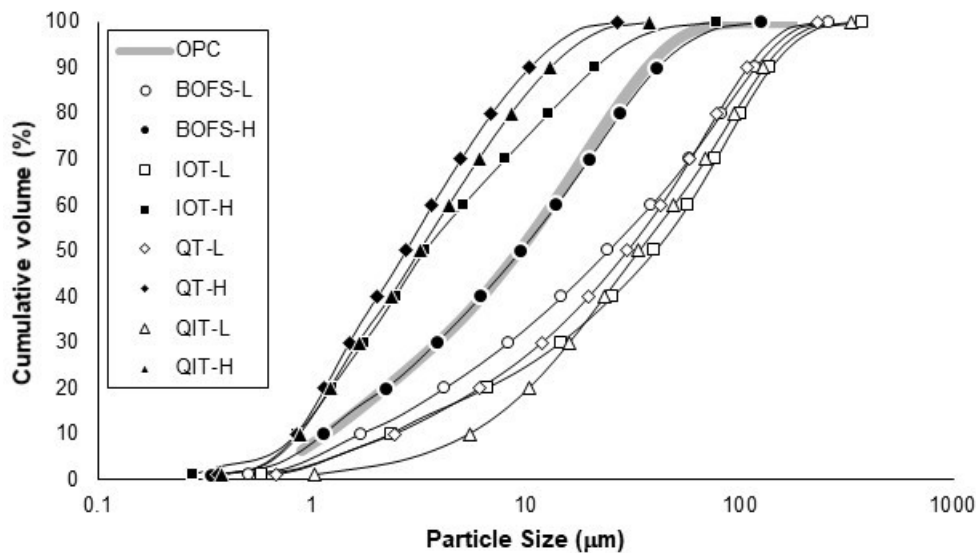


Figure 3. Particle size distribution of the studied powders.

The results of density and BET SSA are listed in Table 5. The higher density values of BOFS and IOT are results of the higher iron content. IOT-L exhibits the highest specific surface area among the coarsely ground particles due to the presence of clay particles ($2.955 \text{ m}^2/\text{g}$). The relatively high SSA of BOFS-L ($2.425 \text{ m}^2/\text{g}$) is related to the higher porosity and roughness of its particles. QT-L and QIT-L have the lowest values ($1.1039 \text{ m}^2/\text{g}$ and $0.3983 \text{ m}^2/\text{g}$, respectively), due to their high content of quartz particles, presenting sharp and fractured edges but with smoothed surfaces. The high-efficiency grinding increased the specific surface area as result of more surface exposure for IOT, QT, and QIT. For BOFS-L, however, this did not occur. On the one hand, the BOFS-L already has a high BET surface area before grinding due to its high roughness, and the high efficiency grinding produced particles considerably less rugged, contributing to a relative reduced SSA. On the other hand, the BOFS-H powder remained comparatively coarse after high-performance grinding.

Table 5. Results of density and specific surface area of the studied powders.

Powder	Density (g/cm ³)	Specific surface area BET (m ² /g)
BOFS-L	3.61	2.4252
BOFS-H	3.61	2.0678
IOT-L	3.54	2.9547
IOT-H	3.54	6.6522
QT-L	2.64	1.1039
QT-H	2.64	4.4123
QIT-L	2.67	0.3983
QIT-H	2.67	5.9054

5.3.2 Evaluation of ζ -potential of the studied powders

Results of pH measurements in deionized water (Figure 4) show that suspensions containing BOFS powders had their pH increased to values above 11.5 due to the dissolution of Ca(OH)₂. The chemical and mineralogical compositions indicate a high presence of Ca as calcium silicates and calcite, but also lime. Little or no changes in pH were observed in the suspensions containing the other fines, which indicates a low presence of dissolved ions in the suspension.

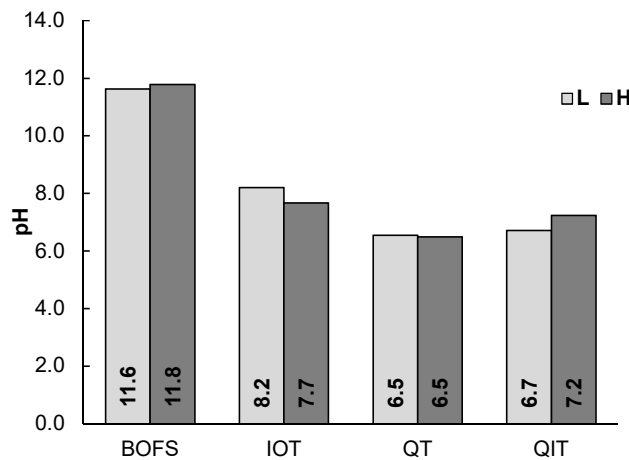


Figure 4. Results of the pH measurements in deionized water for the studied powders.

. The positive effects of the presence of ultrafine silica particle are well known and include improvement in the physical structure of cementitious compounds (refining porosity), and providing of nucleation sites . The more pronounced effect observed for QIT, however, may be related to a more complex ion availability in the solution due to the presence of muscovite minerals. In this sense, studies indicate the activation of clay-based compounds by ultrafine grinding, which suggests potentiated dissolution .

shows the results of ζ -potential measurements for the studied powders in deionized water. The observed behaviors are closely related to the pH values as expected (Malvern Instruments, 2011; Barthel, et al., 2016) As a result of the dissolution of $\text{Ca}(\text{OH})_2$, the ions Ca^+ available were adsorbed in the surface of the BOFS particles changing the ζ -potential to neutral to positive values. On the other hand, IOT, QT and QIT particles presented negative values as expected for quartz particles. Results for QT and QIT are in relatively good agreement with values reported by Vieira and Peres (2007) for quartz. For IOT, no significant differences were observed between values of ζ -potential for coarse and fine powders; however, the particle size largely influenced the ζ -potential values for QT and QIT (the finer powders presented increased negative values compared to coarse powders). The ζ -potential of quartz particles is size dependent (Barisik, et al., 2014), which indicates that the high-efficiency grinding was effective in increasing the content of quartz nanoparticles. The positive effects of the presence of ultrafine silica particle are well known and include improvement in the physical structure of cementitious compounds (refining porosity), and providing of nucleation sites (Qing, et al., 2007; Land & Stephan, 2012). The more pronounced effect observed for QIT, however, may be related to a more complex ion availability in the solution due to the presence of muscovite

minerals. In this sense, studies indicate the activation of clay-based compounds by ultrafine grinding, which suggests potentiated dissolution (Mitrović & Zdujić, 2014).

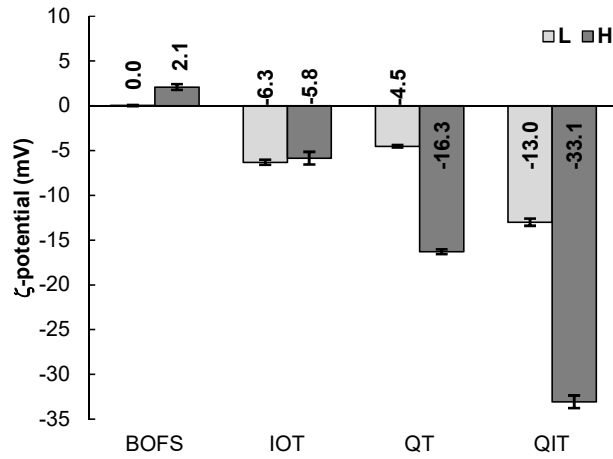


Figure 5. Results of ζ -potential of the studied powders in deionized water.

Figure 6 shows the results of ζ -potential measurements of the powders performed in a saturated solution of $\text{Ca}(\text{OH})_2$. In this medium highly alkaline ($\text{pH} = 12.8$), all the particles presented highly positive values due to adsorption of ions Ca^+ . However, while IOT, QT, and QIT presented values between 19 and 22 mV, BOFS particles reached considerably higher values (26.4 mV), which is very close to the value for a considered stable suspension (+30 mV) (Vieira, 2010; Malvern Instruments, 2011). As a result, enhanced ability in adsorb superplasticizer is expected for BOFS particles (Chen, et al., 2012). One possible cause is the formation of AFm or AFt, increasing the potential of BOFS particles (Plank & Hirsch, 2007; Schmidt, et al., 2014). The brownmillerite ($\text{Ca}_2(\text{Al,Fe})_2\text{O}_5$) is one of the mineralogical phases that make up BOFS, and chemical analysis shows the presence of sulfates.

Based on the results, the slags will most likely have a strong interaction with the anionic PCEs. Good interactions are also expected for the other studied ERMA in a highly alkaline medium, which is the case of cement-based composites. As a consequence, good flow performance is expected in cement-based composites produced with these fines using anionic superplasticizers.

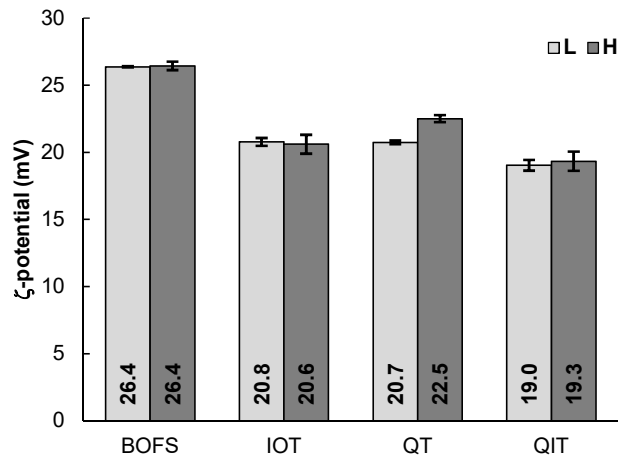


Figure 6. Results of ζ -potential measurements for the studied powders in $\text{Ca}(\text{OH})_2$ solution.

5.3.3 Influence of the powders in the rheological behavior of blended pastes

Figure 7 shows the results of spread measurements for pastes without PCE. The partial cement replacement with all evaluated coarser powders increased the spreading flow of the pastes. The same behavior was also observed for the finer powders BOFS-H and IOT-H. The blends containing QT-H and QIT-H presented almost similar spreading values compared to cement-only REF paste, and the low spreading values are due to their higher SSA (Shanahan, et al., 2016). All pastes produced with the coarser powders presented increased spreading diameters compared to the pastes produced with the corresponding finer one.

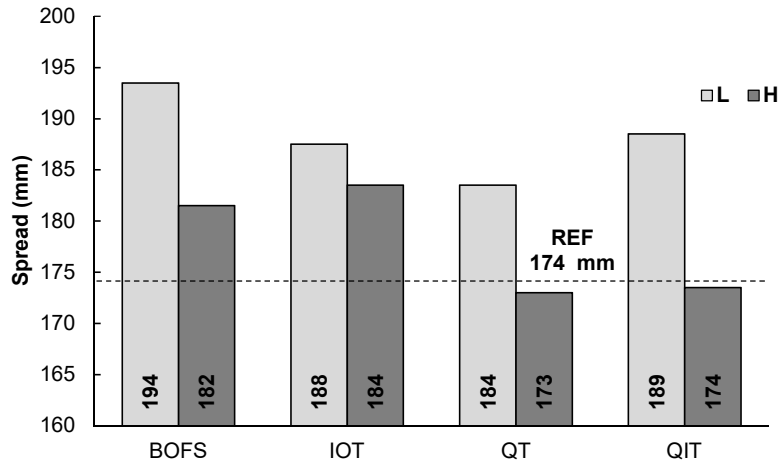


Figure 7. Results of the flow table tests performed in the studied pastes in the absence of superplasticizers.

The curves obtained from the torque measurements using the rheometer for the studied pastes without PCE are presented in Figure 8. All blends show reduced torque values compared to the REF paste, and also the plastic viscosity is lower in the blended systems. QT-L and IOT-L show similar yield stress for both grinding procedures, but the plastic viscosity is higher for the QT-H sample. For each grinding process, the QIT samples show higher and the BOFS samples lower yield stress values. For all samples the viscosity is similar, only for the IOT samples the viscosity is slightly lower regardless of the grinding process.

Slump as well as spread are related to the yield stress (Park, et al., 2005; Flatt, et al., 2006). Good agreement was observed between the results of the spreading measurements and ordinate intercepts for the pastes. Both results point to an increase in flow by a partial replacement of cement by the coarse ERMA, and all blends produced with coarse ERMA presented improved results compared to their fine counterpart.

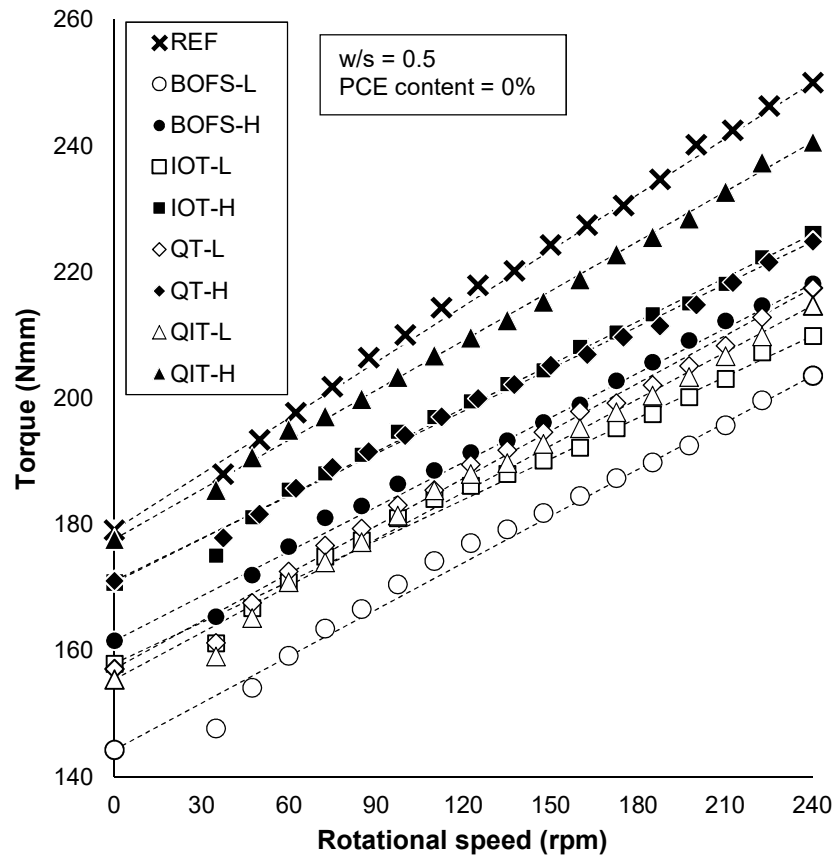


Figure 8. Influence of the studied powders in the flow properties of blended cement pastes.

These promising results indicate that the proposed waste-based mineral admixtures in a replacement rate of 10 % in volume of cement cause no adverse impacts in rheological behavior of cement pastes, on the contrary, they presented plasticizer effect improving the flowability. This way, no additional water consumption is expected, even with the considerable increase in the specific surface area of the blend by adding the fine ERMA. That is a result of good mobility in the medium, which indicates an effective grinding performance on the production of improved shaped particles.

On the other hand, the grain packing is improved by using blends of materials with different particle size distributions, which is also related to reductions in apparent yield stress of the cement blends (Shanahan, et al., 2016). This way, the volume of the gaps

between particles tends to be reduced, and less water is demanded to fill these gaps. As a consequence, more water is available to lubricate the system, improving the workability or compensating the adverse effects of improving the specific surface area (in the case of fine ERMAs). This strategy proved to be useful in obtaining blended pastes with similar-to-meliorated rheological behavior, which also have been reported by other authors using binary and ternary blends (Park, et al., 2005; Shanahan, et al., 2016). Thus, positive implications in mechanical, durability and eco-efficiency performances are expected (Habert, et al., 2010; Hot, et al., 2014), which have been demonstrated by the authors' research group in previous studies (Carvalho, et al., 2019).

5.3.4 Influence of PCE-based superplasticizers on the rheological behavior

Both PCEs were very effective in reducing the yield stress as demonstrated in Figure 9A and Figure 10A. Values of ordinate intercept showed marked reductions, even at low dosages, which is expected for polycarboxylate-based SPs (Puertas, et al., 2005). The values tended to converge to zero for PCE contents close to 0.15 % by cement mass in all cases. The plastic viscosity also showed remarked reductions with the addition of the SPs, as indicated by the evolution of the slopes of the curves rotational speed versus torque (Figure 9B and Figure 10B). This property is associated with stickiness, placeability, and pumpability, but it is also related to segregation in concrete (Park, et al., 2005).

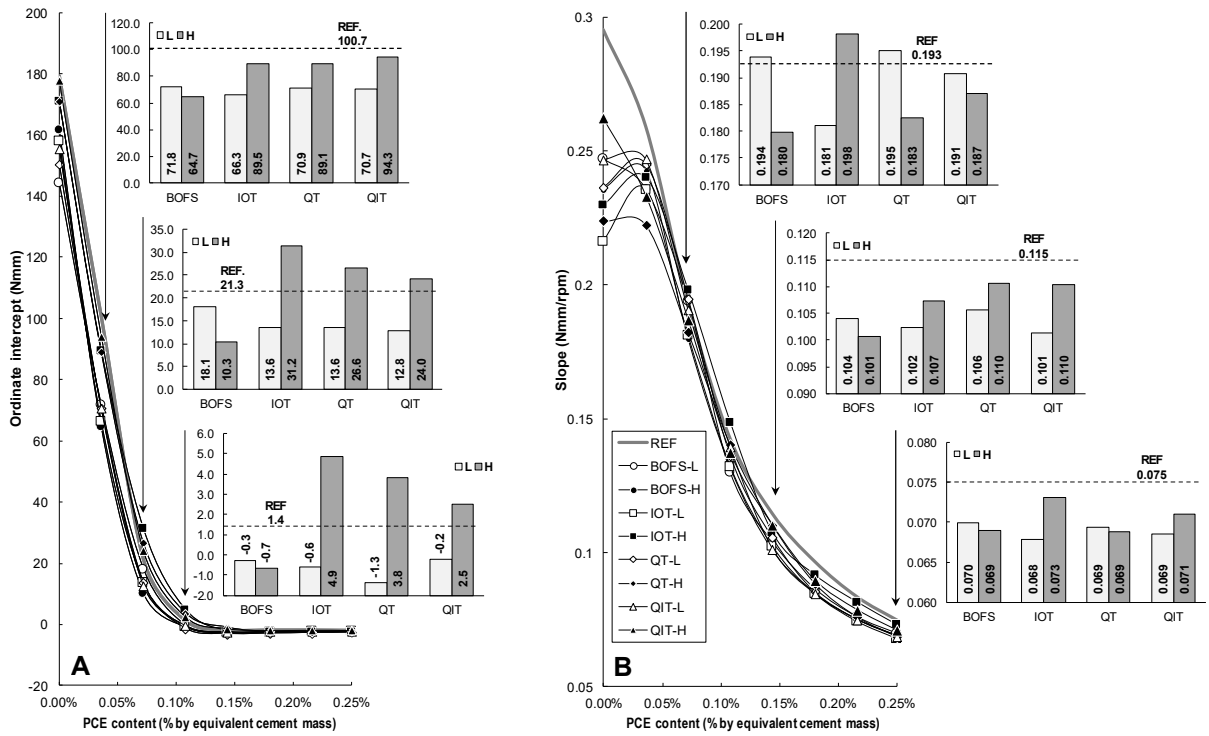


Figure 9. Flow properties of the studied pastes for different PCE-LC contents: A) Evolution of the ordinate intercept of the graphics rotational speed versus torque (related to yield stress); B) Evolution of the slope of the graphics rotational speed versus torque (related to plastic viscosity).

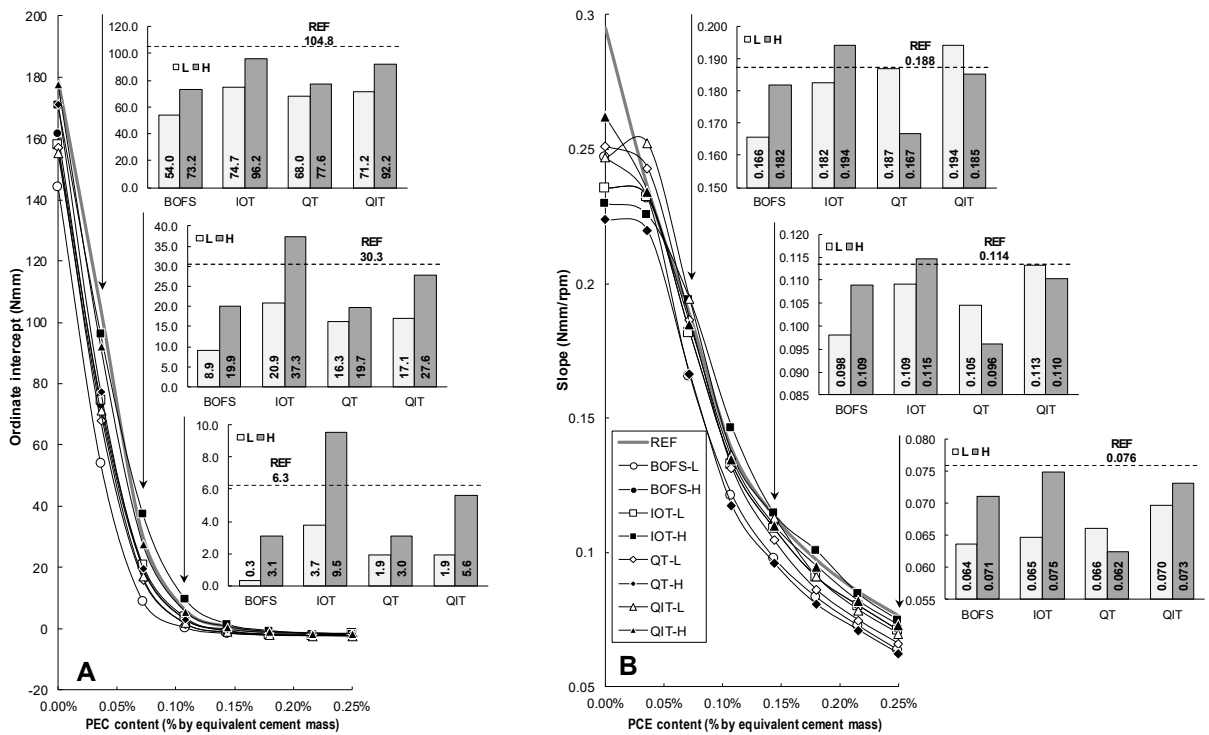


Figure 10. Flow properties of the studied pastes for different PCE-HC contents: A) Evolution of the ordinate intercept of the graphics rotational speed versus torque (related to yield stress); B) Evolution of the slope of the graphics rotational speed versus torque (related to plastic viscosity).

All studied coarse ERMA reduced the yield stress in blended pastes with 10 % cement replacements by volume in association with the PCE-LC (Figure 9A). The most significant reductions were observed in the blends containing BOFS-L. The results observed in the blended pastes containing fine ERMA and LC-PCE show that the reduction in the particle size played an important role in the yield stress. While for the coarse ERMA a clear reduction is observed, the fine ERMA increased the yield stress in comparison to the coarse ERMA, except for very reduced PCE contents. The IOT-H paste presented a clear tendency to achieve higher values for yield stress compared to the other ERMA. The exception was the BOFS-H paste that presented significant reductions in the ordinate intercept for the evaluated PCE contents compared to REF and BOFS-L pastes.

The slopes of the curves rotational speed versus torque of the blended pastes with LC-PCE (Figure 9B) presented close values for all PCE contents, for this reason, no clear trends could be identified on their plastic viscosity behavior. However, the evident reductions on the plastic viscosity of the blended pastes without PCE in comparison with REF paste disappeared by the action of the PCE-LC. With few exceptions and for all PCE contents, the slopes of the blended pastes presented values similar-to-reduced compared to REF paste.

For coarse ERMA, the PCE-HC blended pastes presented higher reductions in the ordinate intercept in comparison to REF paste for all PCE contents comparatively to PCE-LC pastes (Figure 10A), which indicates an improved effect of the PCE-HC with the ERMA compared to PCE-LC. BOFS-L presented the best overall results, showing marked reductions of the yield stresses. Regarding the fine ERMA, QIT-H pastes presented quite similar results of ordinate intercept compared to REF pastes, IOT-H

showed the higher values of ordinate intercept while BOFS-H and QT-H presented the lower for all PCE contents. In comparison with the results observed for the PCE-LC pastes, BOFS-H presented increased yield stresses while QT-H presented reduced yield stresses.

The coarse ERMA s caused reduced influence on the plastic viscosity of the PCE-HC blended pastes compared to REF paste (Figure 10B). For reduced PCE content, QT-L and QIT-L tended to increase the viscosity in comparison to REF paste. However, the results of the PCE-HC blended pastes are similar to those presented by the LC-PCE pastes, except for BOFS-L pastes that presented reduced values compared to PCE-LC BOFS-L pastes for all evaluated PCE contents. The presence of small particles is related to the increase in plastic viscosity (Schmidt et al., 2018; Schmidt, 2016), but this was more clearly observed only in PCE-LC mixtures.

Best overall results presented by the BOFS pastes (highlighting the BOFS-H pastes) may be related to (a) improving particle shape, potentiating the “ball bearing effect” (Park, et al., 2005); (b) relatively large particle sizes compared to the other fine ERMA s (Chen, et al., 2012; Shanahan, et al., 2016); (c) higher absorbance of PCE, as suggested by the evaluation of zeta potential (Chen, et al., 2012); (d) decrease in hydration activity (Park, et al., 2005); and (e) Increased formation of AFt and AFm (Schmidt, et al., 2014). However, the convergence of various favorable characteristics is probably the reason for the best results presented by the BOFS ERMA s, and more dedicated observation is necessary to measure the individual contributions.

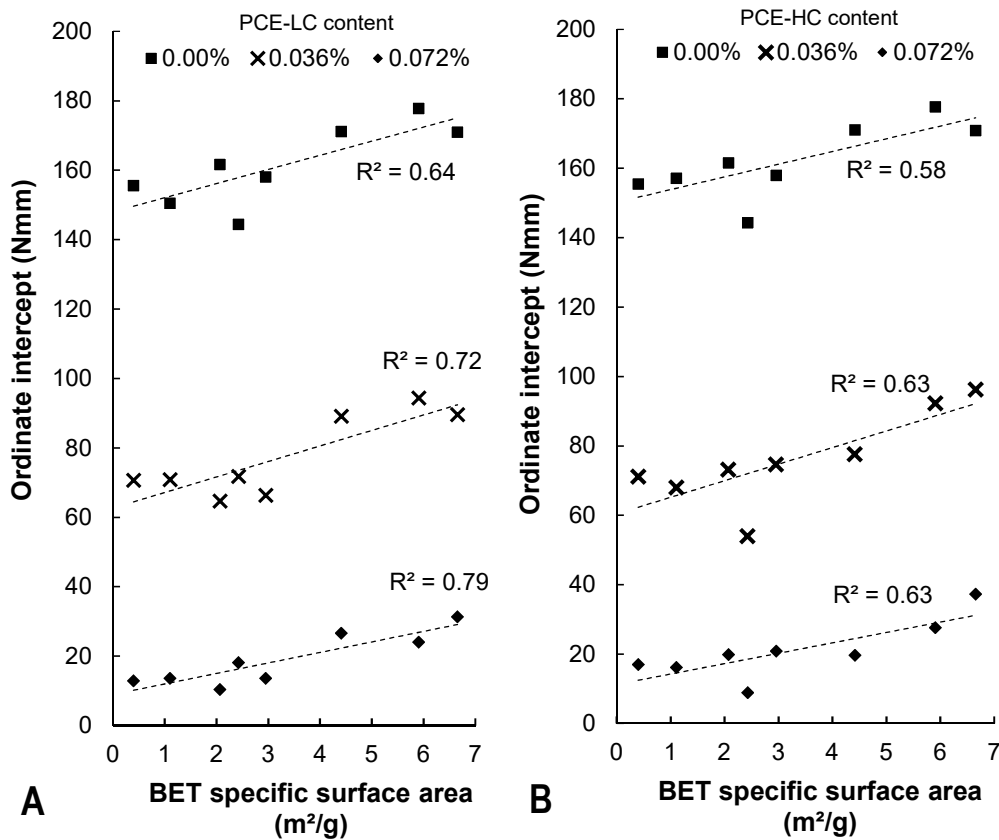


Figure 11. Correlation between BET specific surface area and ordinate intercept: (a) LC-PCE; (b) HC-PCE

Replacement of cement by the ERMAs altered the total specific surface area of the blend, which is reported as a factor with good correlation with the apparent yield stress (Shanahan, et al., 2016). However, Figure 11 shows that the correlations between BET and yield stress were not so strong. This suggests that high BET specific surface areas not necessarily imply in poor rheological performance because this ability could be strongly affected by the overall particle aspect, ζ -potential, pore solution and formation of AFt and AFm (Schmidt, et al., 2018). In this sense, IOT-L, IOT-H and BOFS-L pastes (mainly this last) showed the most significant deviations in the absence of chemical admixtures (better performances than the expected for this criterion). For blends containing PCE-LC, the most significant deviations were observed for BOFS-H, IOT-H, and IOT-L. BOFS-L

pastes present the most significant deviations for pastes containing PCE-HC. Indeed, these ERMAAs present the most significant differences in chemical and mineralogical characteristics compared to QT and QIT ERMAAs. One remarkable characteristic is the high iron content and considerable aluminum content. Their presence may be playing an important role in improving the content of AFt and AFm during early hydration. As a consequence, the PCE adsorption performance is affected. The PCE type also influenced the performance. The BOFS-L particles (high relative BET surface area and high ζ -potential) presented improved interaction with the PCE-HC molecules (higher charge and shorter side chains compared to PCE-LC).

5.3.5 Reaction speed

Figure 12 shows the results of the Vicat needle penetration depths (35 mm and 15 mm) with corresponding times (T35 and T15, respectively). The cement-only REF paste without PCE presented T35 = 207.2 min (3.45 h) and T15 = 236.2 min (3.94 h). The PCE-LC retarded the T35 of the REF paste in 172 min (+83%), and the T15 in 174 min (+74%). For the PCE-HC, the delays observed were 257.0 mm (+124%) and 263.2 mm (+111%) for T35 and T15 respectively.

The retarding effect promoted by the PCE admixture is well known and has been reported for several authors (Hanehara, 1999; Puertas, et al., 2005; Winnefeld, et al., 2007; Shin, et al., 2008; Cheung, et al., 2011; Schmidt, et al., 2014). In this sense, the adsorbed PCE molecules hinder the diffusion of water and calcium ions and affect the hydration kinetics, changing the growth and morphology of the forming hydrates (Mollah, et al., 2000; Winnefeld, et al., 2007). The inadequate control of the aluminate phase hydration by the sulfate in the presence of admixtures, however, is pointed as a cause of problems with

silicate phase hydration in the presence of admixtures once the sulfate availability rate is suppressed (Röbber, et al., 2007; Cheung, et al., 2011). Also, the aluminate phase is more active in higher temperatures (less heat released in the hydration reactions) (Cost, 2006; Cheung, et al., 2011).

The longer delays were observed in pastes containing PCE-HC. Indeed, Winnefeld et al. (2007) observed that the dormant period is prolonged with the increase in charge density. This potentiated retarding effect is related to the increased adsorbed amount and surface coverage of cement particles, which is in turn related to the increase in charge density and the decrease in the length of the side chains (Winnefeld, et al., 2007; Shin, et al., 2008).

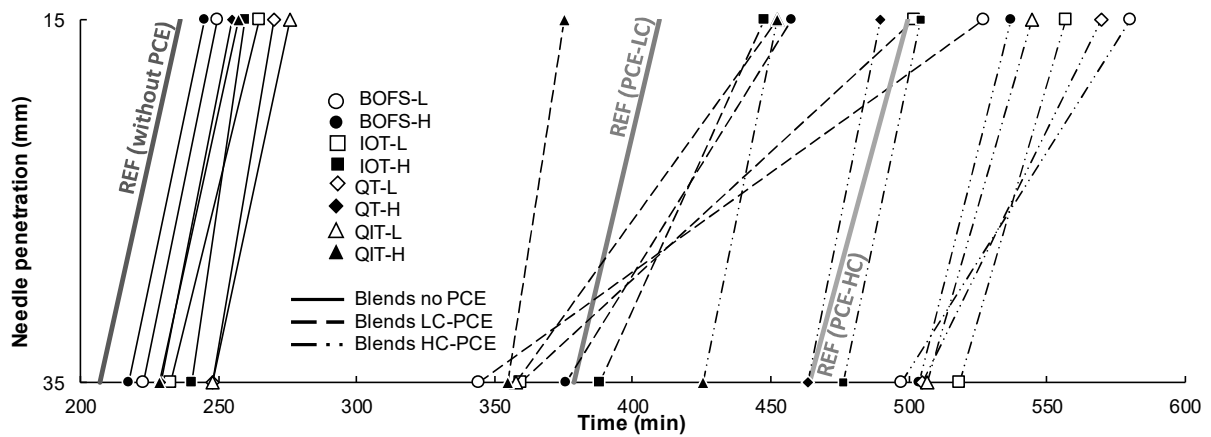


Figure 12. Vicat needle penetration depths and the corresponding times for all tested pastes.

All blended pastes without PCE presented retarding effect compared to cement-only REF paste. Considering the results of T15, the pastes containing fine ERMA s tended to present substantial delays compared to REF paste without superplasticizer. This is clearly observed in IOT-L paste (+39.5 min), QT-L paste (+33.9 min) and IOT-L paste (+28.8 min). The exception was BOFS-L paste with a delay of +13.5 min, smaller than

those observed for IOT-H (+23.1 mm), QIT-H (+21.1 mm) and QT-H (+18.5 mm). The smallest delay was observed for BOFS-H paste (+9.0 mm).

The retarding effects observed for the blended pastes without SP are explained mainly for the dispersion effect, once less cement is used. The blends containing the finer powders are expected to present a relatively accelerating effect compared to coarser powders due to their higher specific surface area (Souri, et al., 2015; Burris & Juenger, 2016). However, the chemical and mineralogical composition of the BOFS powders played an important role in accelerating the hardening of their mixtures, compensating their relatively reduced specific surface area. On the other hand, the relatively large specific surface area of the BOFS-L powder compared to the other coarse ERMA s seemed to be determinant to promote the reduced delays observed.

The behavior of blended pastes containing PCE varied considerably in comparison to REF pastes. One trend observed was the reduction in the slope of the curves of blends containing coarse ERMA s compared to the correspondent fine ones, i.e., a retarding effect between the initial and final setting times compared to the reference. The curves of the fine powders, however, presented none or reduced changes in their slopes compared to reference. Additionally, the PCE type exerted a significant effect on the behavior of the blended pastes. Significant delays were observed between T15 and T35 for coarse ERMA s using PCE-LC. The highest delays were observed in BOFS-L paste (183 min), IOT-L paste (142 min) and QIT-L paste (95 min). The BOFS-H paste also showed a relatively high delay (82 min) and was the exception among the fine ERMA s. Results for QT-L and QT-H pastes with PCE-LC presented non-consistent data, for this, they were not considered in the evaluation. For pastes produced with PCE-HC, all blends with

coarse ERMA presented more significant delays in T15 compared to reference paste. BOFS-H presented the highest delays among the fine powders.

The behaviors, however, were greatly influenced by the segregation phenomenon. With the addition of PCE (0.25% in cement mass), both yield stress and plastic viscosity markedly decreased, and as a result, the tendency to segregation increased (Park, et al., 2005). This way, the blends containing larger particles and denser materials tended to present the most accentuated distortions. In this sense, PCE-HC was more effective in maintaining the stability of the mixtures. Pastes produced with fine ERMA were less susceptible to segregation.

Regarding the Vicat needle test, it proved to be effective in detecting segregation. The more consolidated layer of coarser and denser material formed in the bottom of the mold falsely anticipates the achievement of the initial setting time. Consequently, the consistency is affected as well as the availability of water and other particles in the upper layers, retarding the final setting time. As a result, the slope of the curve is reduced (Figure 12).

The results also show that the use of high charge PCEs with short chains is indicated for blends containing dense and coarse powders in order to prevent segregation. Another route to prevent segregation is the use of fine powders.

The increase in fineness was also effective in reducing or even eliminate delays as a result of the improvement in the reactivity by the ultrafine grinding (Cordeiro, et al., 2016; Mitrović & Zdujić, 2014; Burris & Juenger, 2016; Souri, et al., 2015). The correlation between the final setting time and heat flow curves of cement pastes have been demonstrated by Schmidt (2014). Thus, the results indicated that QT-H and QIT-H were

effective in anticipating the acceleration period, which is consistent with a potentiated nucleation effect by the presence of increased amounts of micro and nanoparticles of quartz (Burriss & Juenger, 2016). The behavior of the QIT-H powder, however, deserves special attention. This material promoted the most significant acceleration effects, which indicates additional cementitious effects. In a study on the pozzolanic activity of natural zeolite in blended cements, Snellings et al. (2010) suggested that increased adsorption of Ca^{2+} in particle surfaces and consequent faster dissolution of C_3S and growth of C-S-H is related to the increase in the rate and quantity of heat released. The same can be suggested for QIT-H, given the ultrafine grinding and similarities in the chemical composition.

5.4 Conclusion

The ζ -potential of the fines was highly influenced by the particle size and chemical/mineralogical composition in deionized water. In a lime saturated solution, the particle size had no influence and all studied ERMAs presented positive ζ -potential values, which indicates good interaction with anionic superplasticizers in an alkaline environment (e.g., pore solution of cement composites). In the absence of superplasticizers, all ERMAs reduced the yield stress and plastic viscosity of blended cement pastes, and the results were greatly influenced by fineness and particle shape. The coarse ERMAs presented higher plasticizer effect compared to fine ERMAs, and BOFS fines presented the best results influenced by their better envelope particle shape. In the presence of superplasticizers, results of yield stress and plastic viscosity of blended pastes were close to results observed for REF pastes, evidencing good compatibility. With few exceptions, all coarse ERMAs presented reduced yield stresses compared with REF and with the correspondent fine ERMAs for the two PCE types. The PCE-HC was more effective in reducing the yield stress of the fine ERMAs in comparison to REF pastes.

With few exceptions, the blended pastes presented reduced plastic viscosity compared with REF for the two PCE types. Strong segregation tendency was observed for the coarser and denser ERMA in presence of the PCE-LC. The PCE-HC was effective to prevent or minimize segregation. The setting was highly affected by the fineness and PCE type. Pastes containing PCE-HC presented the most significant delays. Fineness also significantly affected the setting. With few exceptions, pastes containing the fine ERMA presented faster hardening. QIT-H presented a strong accelerator behavior in the presence of superplasticizers.

5.5 Acknowledgment

The authors acknowledge the Research Group on Solid Waste RECICLOS-CNPq and its supporters (CAPES, FAPEMIG, CNPq, Fundação Gorceix and UFOP), and the Department of Safety of Structures / BAM and its team, for infrastructure use and the valuable contributions.

Funding: This work was financed in part by the Coordenação de Aperfeiçoamento de Pessoal de Nível Superior – Brasil (CAPES) – Finance Code 001.

5.6 References

Ali, M.B. & Hossain, M.S., 2011. A review on emission analysis in cement industries. *Renew. Sust. Energ. Rev.*, (15), pp.2252-61. DOI: 10.1016/j.rser.2011.02.014.

Andrade, H.D., 2018. *Carbonation in steel slag concretes*. Ouro Preto: Federal University of Ouro Preto - UFOP. (Master's thesis) (in Portuguese).

Aprianti, E., 2017. A huge number of artificial waste material can be supplementary cementitious material (SCM) for concrete production – a review part II. *Journal of cleaner production*, 142, pp.4178-94. DOI 10.1016/j.jclepro.2015.12.115.

Barisik, M., Atalay, S., Beskok, A. & Qian, S., 2014. Size Dependent Surface Charge Properties of Silica Nanoparticles. *J Phys Chem C*, 118, pp.1836-42. DOI: 10.1021/jp410536n.

Barthel, M., Schmidt, W., Kühne, H.C. & Rübner, K., 2016. Interaction between waste paper sludge ashes and superplasticizers based on polycarboxylates. In W. Schmidt & S. Msinjili, eds. *Proceedings 2nd International Conference on Advances in Cement and Concrete Technology in Africa*. Dar es Salaam, Tanzania: BAM. pp.181-86.

Bastos, L.A.C., Silva, G.C., Mendes, J.C. & Peixoto, R.A.F., 2016. Using of iron ore tailings from tailing dams as road material. *J. Mater. Civil Eng.*, 28(10), p.04016102. DOI: 10.1061/(ASCE)MT.1943-5533.0001613.

Bingham, E.C., 1922. *Fluidity and plasticity*. 1st ed. New York: McGraw-Hill.

Burris, L.E. & Juenger, M.C., 2016. Milling as a pretreatment method for increasing the reactivity of natural zeolites for use as supplementary cementitious materials. *Cement Concrete Comp*, 65, pp.163-70. DOI: 10.1016/j.cemconcomp.2015.09.008.

Carvalho, J.M.F. et al., 2019. Low environmental impact cement produced entirely from industrial and mining waste. *J Mater Civil Eng*, in Press. DOI: 10.1061/(ASCE)MT.1943-5533.0002617.

Carvalho, J.M.F. et al., 2018. High strength concrete with partial replacement of cement by steel slag fines. In IPEN, ed. *Proceeding of the 23th Brazilian Congress on Materials Engineering and Science*. Foz do Iguaçu: IPEN. p.13p.

Carvalho, J.M.F. et al., 2019. More eco-efficient concrete: an approach on optimization and use of waste-based supplementary cementing materials. *Constr Build Mater*, p.in Review.

Chen, W., Shen, P., Shui, Z. & Fan, J., 2012. Adsorption of Superplasticizers in Fly Ash Blended Cement Pastes and Its Rheological Effects. *Journal of Wuhan University of Technology-Mater*, 27(4), pp.773-78. DOI: 10.1007/s11595-012-0546-8.

Cheung, J., Jeknavorian, A., Roberts, L. & Silva, D., 2011. Impact of admixtures on the hydration kinetics of Portland cement. *Cement Concrete Res*, 41, pp.1289-309. DOI: 10.1016/j.cemconres.2011.03.005.

Cordeiro, G.C., Tavares, L.M. & Toledo Filho, R.D., 2016. Improved pozzolanic activity of sugar cane bagasse ash by selective grinding and classification. *Cement Concrete Res*, 89, pp.269-75. DOI: 10.1016/j.cemconres.2016.08.020.

Cost, V.T., 2006. Incompatibility of common concrete materials—influential factors, effects, and prevention. In N.C.B. Council, ed. *HPC: Build Fast, Build to Last. The 2006 Concrete Bridge Conference*. Reno, NV: National Concrete Bridge Council. p.24p.

Da Silva, M.J. et al., 2016. Feasibility Study of Steel Slag Aggregates in Precast Concrete Pavers. *ACI Mater. J.*, 113(4), pp.439-46. DOI: 10.14359/51688986.

Dias, L.S. et al., 2016. Rejeitos de mineração de quartzito para produção de argamassa colante. In *Anais do 22º Congresso brasileiro de Engenharia e Ciência dos Materiais - Natal - 06 a 10 de novembro de 2016*. Natal. pp.1-12. (in Portuguese).

DIN, 2007. *EN 1015-3: Methods o test for mortar for mansonry - Part 3: Determination of consistence of fresh mortas (by flow table)*. Berlin: Deutsches Institut für Normung - DIN.

DIN, 2011. *EN 197-1: cement - Part !: Composition, specifications and conformity criteria for common cements*. Berlin: Deutsches Institut für Normung - DIN.

DIN, 2016. *EN 196-3: Test method for cement - Part 3: Determination of setting times and room stability*. Berlin: Deutsches Institut für Normung - DIN.

Diniz, D.H., Carvalho, J.M.F., Mendes, J.C. & Peixoto, R.A.F., 2017. Blast Oxygen Furnace Slag as Chemical Soil Stabilizer for Use in Roads. *J. Mater. Civil Eng.*, 29(9), p.04017118. DOI: 10.1061/(ASCE)MT.1943-5533.0001969.

do Carmo, F.F. et al., 2017. Fundão tailings dam failures: the environment tragedy of the largest technological disaster of Brazilian mining in global context. *Perspectives in Ecology and Conservation*, 15(3), pp.145-51.

Dutra, M.B. et al., 2014. Production of standard quartz sand - Recycling of solid waste from mining. In *Proceedings 56th Brazilian Concrete Conference*. Natal: Brayilian Concrete Institute - Ibracon. p.11p. (in Portuguese).

Flatt, R.J., Larosa, D. & Roussel, N., 2006. Linking yield stress measurements: Spread test versus Viskomat. *Cement Concrete Res*, 36, pp.99-109.

Fontes, W.C., Mendes, J.C., Silva, S.N. & Peixoto, R.A.F., 2016. Mortars for laying and coating produced with iron ore tailings from tailing dams. *Constr. Build. Mater.*, 112, pp.988-95. DOI: 10.1016/j.conbuildmat.2016.03.027.

Galvão, J.L.B. et al., 2018. Reuse of iron ore tailings from tailings dams as pigment for sustainable paints. *J. Clean. Prod.* (in press).

García-Gusano, D. et al., 2014. Life cycle assessment of the Spanish cement industry: implementation of environmental-friendly solutions. *Clean. Technol. Envir.*, 17(1), pp.59-73. DOI: 10.1007/s10098-014-0757-0.

Gonçalves, D.R.R. et al., 2016. Evaluation of the economic feasibility of a processing plant for steelmaking slag. *Waste Manage Res*, 34(2), pp.107-12. DOI: 10.1177/0734242X15615955.

Habert, G. et al., 2010. Cement production technology improvement compared to factor 4 objectives. *Cement Concrete Res*, 40(5), pp.820-26. DOI: 10.1016/j.cemconres.2009.09.031.

Hanehara, S..Y.K., 1999. Interaction between cement and chemical admixture from the point of cement hydration, absorption behaviour of admixture, and paste rheology. *Cement Concrete Res*, 29, pp.1159-65.

Hendriks, C.A. et al., 1998. Emission reduction of greenhouse gases from the cement industry. In *Proceedings of the fourth international conference on greenhouse gas control technologies*. pp.939-44.

Hot, J. et al., 2014. Adsorbing polymers and viscosity of cement pastes. *Cement Concrete Res*, 63, pp.12-19. DOI: 10.1016/j.cemconres.2014.04.005.

Huntzinger, D.N. & Eatmon, T.D., 2009. A life-cycle assessment of Portland cement manufacturing: comparing the traditional process with alternative technologies. *J. Clean. Prod.*, 17(7), pp.668-75. DOI: 10.1016/j.jclepro.2008.04.007.

Iacobescu, R.I. et al., 2011. Valorisation of electric arc furnace steel slag as raw material for low energy belite cements. *J. Hazard. Mater.*, pp.287-94. DOI: 10.1016/j.jhazmat.2011.09.024.

Kajaste, R. & Hurme, M., 2016. Cement industry greenhouse gas emissions e management options and abatement cost. *J. Clean. Prod.*, (112), pp.4041-52. DOI: 10.1016/j.jclepro.2015.07.055.

Kanchanason, V. & Plank, J., 2018. Nucleation and Growth of C-S-H - PCE Used as Strength Enhancer in Cement. In J. Liu et al., eds. *Superplasticizers and Other Chemical Admixtures in Concrete - Proceedings Twelfth International Conference*. Beijing: American Concrete Institute - ACI. pp.67-75.

Land, G. & Stephan, D., 2012. The influence of nano-silica on the hydration of ordinary Portland cement. *J. Mater. Sci*, 47, pp.1011-17. DOI: 10.1007/s10853-011-5881-1.

Lei, Y., Zhang, Q., Nielsen, C. & He, K., 2011. An inventory of primary air pollutants and CO₂ emissions from cement production in China. *Atmos. Environ.*, 45(1), pp.147-54. DOI: 10.1016/j.atmosenv.2010.10.066.

Malvern Instruments, 2011. Zeta potential - An introduction in 30 minutes. *Zetasizer Nano Series Tech. Note NRK654*, 1(2), pp.1-6.

Meyers, G.D., McLeod, G. & Anbarci, M.A., 2006. An international waste convention: measures for achieving sustainable development. *Waste Management*, 24, pp.505-13. DOI 10.1177/0734242X06069474.

Mikulčić, H. et al., 2016. Reducing greenhouse gasses emissions by fostering the deployment of alternative raw materials and energy sources in the cleaner cement manufacturing process. *J. Clean. Prod.*, 136, pp.119-32. DOI: 10.1016/j.jclepro.2016.04.145.

Mitrović, A. & Zdujić, M., 2014. Preparation of pozzolanic addition by mechanical treatment of kaolin clay. *Int J Miner Process*, 132, pp.59-66. DOI: 10.1016/j.minpro.2014.09.004.

Mollah, M.Y., Adams, W.J., Schennach, R. & Cocke, D.L., 2000. A review of cement–superplasticizer interactions and their models. *Adv Cem Res*, 12(4), pp.153-61. DOI: 10.1680/adcr.2000.12.4.153.

Ohta, A., Sugiyama, T. & Tanaka, Y., 1997. Fluidizing mechanism and application of polycarboxylate-based superplasticizers. In *Proceedings 5th CANMET/ACI International Conference on Superplasticizers and other chemical Admixtures in Concrete*. Rome: American Concrete Institute. pp.359-78.

Park, C.K., Noh, M.H. & Park, T.H., 2005. Rheological properties of cementitious materials containing mineral admixtures. *Cement Concrete Res*, 35, pp.842-49. DOI: 10.1016/j.cemconres.2004.11.002.

Plank, J. et al., 2006. News on the interaction between cements and polycarboxylate flow agents. In *Proceedings -16th International Conference on Building Materials - ibausil*. Weimar. pp.579-98. (in German).

Plank, J. & Hirsch, C., 2007. Impact of zeta potential of early cement hydration phases on superplasticizer adsorption. *Cement Concrete Res*, 37(4), pp.537-45.

Puertas, F., Santos, H., Palacios, M. & Martínez-Ramírez, S., 2005. Polycarboxylate superplasticiser admixtures: effect on hydration, microstructure and rheological behaviour in cement pastes. *Adv Cem Res*, 17(2), pp.77-89.

Qing, Y., Zenan, Z., Deyu, K. & Rongshen, C., 2007. Influence of nano-SiO₂ addition on properties of hardened cement paste as compared with silica fume. *Constr Build Mater*, 2007(3), pp.539-45. DOI: 10.1016/j.conbuildmat.2005.09.001.

Rößler, C., Möser, B. & Stark, J., 2007. Influence of superplasticizers on C3A hydration and ettringite growth in cement paste. In *Proceedings of the 12th International Congress on the Chemistry of Cement*. Montreal. pp.1-30.

Sakai, E., Yamada, K. & Ohta, A., 2003. Molecular structure and dispersion-adsorption mechanisms of comb-type superplasticizers used in Japan. *J Adv Concr Technol*, 1(1), pp.16-25.

Salas, D.A. et al., 2016. Environmental impacts, life cycle assessment and potential improvement measures for cement production: a literature review. *J. Clean. Prod.*, 113, pp.114-22. DOI: 10.1016/j.jclepro.2015.11.078.

Sant'ana Filho, J.N. et al., 2017. Technical and environmental feasibility of interlocking concrete pavers with iron ore tailings from tailings dams. *J. Mater. Civil Eng.*, 29(9), p.04017104. DOI: 10.1061/(ASCE)MT.1943-5533.0001937.

Schmidt, W., 2014. *Design concepts for the robustness improvement of self-compacting concrete: effects of admixtures and mixture components on the rheology and early hydration at varying temperatures*. Eindhoven: Eindhoven University of Technology. (PhD Thesis - Eindhoven University of Technology), DOI: 10.6100/IR771936.

Schmidt, W., 2016. *Influence of effects on nano and micro scale on the rheological performance of cement paste, mortar and concrete*. Berlin.

Schmidt, W., Brouwers, H.J.H., Kühne, H.C. & Meng, B., 2014. Influences of superplasticizer modification and mixture composition on the performance of self-compacting concrete at varied ambient temperatures. *Cement Concrete Comp*, 49, pp.111-26. DOI: 10.1016/j.cemconcomp.2013.12.00.

Schmidt, W., Leinitz, S., Mota, B. & Crasselt, C., 2018. Influence of the Aqueous Phase of Cement Paste on the Rheology in the Presence of PCE. In J. Liu et al., eds. *Superplasticizers and Other Chemical Admixtures in Concrete - Proceedings Twelfth International Conference*. Beijing: American Concrete Institute - ACI. pp.429-44.

Schober, I. & Flatt, R.J., 2006. Optimizing Polycarboxylate Polymers. *Special Publication*, 239, pp.169-84.

Schober, I. & Mäder, U., 2003. Compatibility of Polycarboxylate Superplasticizers with Cements and Cementitious Blends. *Special Publications - ACI*, 217, pp.453-68.

Shanahan, N., Tran, V., Williams, A. & Zayed, A., 2016. Effect of SCM combinations on paste rheology and its relationship to particle characteristics of the mixture. *Constr Build Mater*, 123, pp.745-53. DOI: 10.1016/j.conbuildmat.2016.07.094.

Shin, J.Y., Hong, J.S., Suh, J.K. & Lee, Y.S., 2008. Effects of polycarboxylate-type superplasticizer on fluidity and hydration behavior of cement paste. *Korean J Chem Eng*, 25(6), pp.1553-61. DOI: 10.1007/s11814-008-0255-3.

Silva, C. et al., 2019. *Tailings dam of Vale collapses and cause destruction in Brumadinho (MG)*. [Online] Available at: <https://www.correiobraziliense.com.br/app/noticia/brasil/2019/01/25/interna-brasil,732919/barragem-de-rejeitos-da-vale-rompe-e-cao-destruicao-em-brumadinho-m.shtml> [Accessed 02 February 2019]. (in Portuguese).

Snellings, R., Mertens, G., Cizer, Ö. & Elsen, J., 2010. Early age hydration and pozzolanic reaction in natural zeolite blended cements: Reaction kinetics and products by in situ synchrotron X-ray powder diffraction. *Cement Concrete Res*, 40(12), pp.1704-13. DOI: 10.1016/j.cemconres.2010.08.012.

Souri, A. et al., 2015. Pozzolanic activity of mechanochemically and thermally activated kaolins in cement. *Cement Concrete Res*, 77(November 2015), pp.47-59. DOI: 10.1016/j.cemconres.2015.04.017.

Vasiliou, E. et al., 2017. Effectiveness of Starch Ethers as Rheology Modifying Admixture for Cement Based Systems. In *2nd International Conference on Bio-based Building Materials & 1st Conference on ECOlogical valorisation of Granular and Fibrous materials*. Clermont-Ferrand, 2017. RILEM.

Vieira, J.P., 2010. *Interaction cement-superplasticizer - evaluation of the stability of behavior*. Lisboa. (Master's thesis - Technical University of Lisbon) (in Portuguese).

Vieira, A.M. & Peres, A.E.C., 2007. The effect of amine type, pH, and size range in the flotation of quartz. *Miner. Eng.*, 20(10), pp.1008-13. DOI: 10.1016/j.mineng.2007.03.013.

WBCSD/IEA, 2009. *Cement Technology Roadmap 2009*. OECD/IEA and World Business Council for Sustainable Development.

Winnefeld, F., Becker, F., Pakusch, J. & Götz, T., 2007. Effects of the molecular architecture of comb-shaped superplasticizers on their performance in cementitious systems. *Cement Concrete Comp*, 29, pp.251-62. DOI: 10.1016/j.cemconcomp.2006.12.006.

Yamada, K., Ogawa, S. & Hanehara, S., 2001. Controlling of the adsorption and dispersing force of polycarboxylate-type superplasticizer by sulfate ion concentration in aqueous phase. *Cement Concrete Res*, 31, pp.375-83.

Zhang, M. et al., 2016. Manifest system for management of non-hazardous industrial solid wastes: results from a Tianjin industrial park. *Journal of Cleaner Production*, 133, pp.252-561. DOI 10.1016/j.jclepro.2016.05.102.

Chapter 6

Pushing the limits of concrete eco-efficiency using engineered recycled mineral admixtures and recycled aggregates

José Maria Franco de Carvalho, Wanna Carvalho Fontes, Carlos Felipe de Azevedo, Guilherme Jorge Brigolini, Wolfram Schmidt, Ricardo André Fiorotti Peixoto

Abstract

Non-conventional densely packed concrete mixtures are proposed and evaluated in this paper using engineered recycled mineral admixtures and recycled aggregates obtained from steel slag, quartz mining tailings, and quartzite mining tailings. High fines content mortars containing coarser- and finer-than-cement recycled powders were designed to obtain blends with broader particle-size ranges and improved packing density. As a consequence, inedited eco-efficiency results were obtained, including sand-concretes presenting compressive strength up to 99 MPa, cement intensity up to 2.33 kg/m³/MPa and consumption of recycled material up to 95vol%. Compressive strengths up to 66 MPa and cement intensity up to 2.34 kg/m³/MPa were also obtained adding coarse aggregates at such mortars, with a consumption of recycled material up to 96.5%. The results launch new insights on the role of the fine fraction on the mixture design of cement-based composites regarding eco-efficiency improvement. Results and discussions on durability and feasibility are also provided.

Keywords: Low-cement concrete, engineered recycled mineral admixture, basic oxygen furnace slag, quartzite mining tailing, quartz mining tailing, packing density.

Journal of Cleaner Production

This manuscript was submitted on February 10th, 2019.

Current status: in review.

6.1 Introduction

Reducing impacts of the construction industry is imperative to meet the demands of a more sustainable world once the sector is responsible for much of the entire world's material and energy consumption, residue generation, and CO₂ emissions (Oikonomou, 2005; John, 2011; Wang, 2014). In this sense, the impacts of concrete production are remarkable; for this reason, the scientific community has invested time and effort in the search for solutions to mitigate these impacts (Hendriks et al., 1998; Huntzinger & Eatmon, 2009; Iacobescu et al., 2011; Ali & Hossain, 2011; Kajaste & Hurme, 2016). Partial replacement of Portland cement by supplementary cementitious materials (SCM) is pointed as the most effective measure for reducing cement consumption and consequently CO₂ emissions (WBCSD/IEA, 2009; Lei et al., 2011; García-Gusano et al., 2014; Kajaste & Hurme, 2016; Salas et al., 2016; Mikulčić et al., 2016). Besides, the use of recycled materials as SCM and aggregates improves eco-efficiency of concretes by providing a suitable destination for waste from other production chains while saving natural resources (Meyers et al., 2006; Zhang et al., 2016; Aprianti, 2017).

Self-compacting concretes (SCC), and high and ultra-high strength concretes has commonly high cement consumption, which is related with environmental degradation (Zuo et al., 2018; Chen et al., 2019). However, the first has a technical requirement for high fines consumption in order to achieve sufficient flowability and stability (Pelisser et al., 2018). Usually, the fines are mainly provided for Portland cement, which explains the high cement consumption (about 500 kg/m³) (Zuo et al., 2018). Nevertheless, the high demand for fines is also an opportunity for the use of increased amounts of supplementary materials (cementitious or not), in binary or ternary blends (Chen et al., 2019; Zuo et al., 2018; Pelisser et al., 2018).

The technical and economic feasibility of using steel slags as aggregates and binders in mortars and concretes has been demonstrated (Da Silva et al., 2016; Gonçalves et al., 2016; Diniz et al., 2017; Marinho et al., 2017; Carvalho et al., 2019), as well as the use of quartz and quartzite mining tailings (Santos, 2015; Dutra, 2015; Dias et al., 2016). In addition, the authors' research group has contributed to the study of optimization methods based on grain packing design and powder engineering using the cited residues to achieved results of high mechanical performance and binder efficiency involving various novel engineered recycled mineral admixtures (ERMAs) (Carvalho et al., 2019). For this, strategies to reduce cement consumption by using concepts of grain packing improvement and cement replacement are applied (Damineli, 2013; Chen et al., 2019).

In this work, however, the authors explore their best overall results using highly effective ERMAs and aggregates to push the limits of binder efficiency and waste consumption in the production of low-cement concretes. The proposed methods and materials have achieved inedited values of cement intensity (CI) in concretes with consumption of recycled materials of up to 96.5% by volume of solids. Consideration regarding durability and feasibility are also discussed.

This work is relevant to sustainability and cleaner production once new insights are launched on the role of engineered recycled mineral admixtures in the obtention of concretes using high amounts of recycled material and low cement consumption. In this regard, the results have proven that the use of coarser-than-cement powders is very effective to improve the concrete eco-efficiency with technological and economic advantages (stability and grinding cost). In addition, other views on mix design and particle-size distributions of fines and aggregates are also suggested.

6.2 Experimental

6.2.1 Materials

6.2.1.1 Raw materials

Three industrial wastes were used in this study: basic oxygen furnace slag (BOFS), quartz mining tailing (QT) and quartzite mining tailing (QIT). The BOFS consisted of a dark grey material with a specific gravity of 3.77 g/cm³. The material was made available by a steelwork located in the city of João Monlevade, Minas Gerais State. It was recovered in granular form and weathered for three years on a storage site. The QT was obtained from a mining operation in the city of Sete Lagoas, Minas Gerais State. The material was also supplied in granular form with a particle-size range compatible with the coarse aggregates used in the concrete production. The material had a beige color and specific gravity of 2.956 g/cm³. Finally, the QIT was supplied by a company in the city of Itabirito, Minas Gerais State, and consisted of white material, with a specific gravity of 2.774 g/cm³. Its particle size covers a range compatible with well-graded sands but has a high content of fines.

The chemical composition of the materials is listed in *Table 1*. The mineral composition of BOFS includes wuestite, larnite, brownmillerite, periclase, calcite, helvine, portlandite and an amorphous phase. QIT consists of quartz (predominantly) and muscovite. QT consists of quartz.

Table 1. Chemical composition of the studied by-products (XRF, oxides).

Oxide	BOFS*	QT	QIT
SiO ₂ %	15.6	95.5	80.0
Al ₂ O ₃ %	4.4	1.5	15.9
Fe ₂ O ₃ %	31.2	1.9	0.4
CaO %	36.8	0.2	-
MgO %	5.0	-	0.1
K ₂ O %	-	-	2.8
Na ₂ O %	-	-	-
SO ₃ %	0.4	-	-
MnO %	3.5	-	-
Cr ₂ O ₃ %	0.8	-	-
V ₂ O ₅ %	0.1	-	-
P ₂ O ₅ %	1.5	-	-
TiO ₂ %	0.5	-	-
Other oxides, %	-	0.8	0.8
LOI, %	1.1	0.3	1.2

* After magnetic separation

6.2.1.2 Binders and chemical admixture

A High early strength Portland cement (PC) (ASTM Type III), specified by the Brazilian standard NBR 5733 as CP-V ARI (ABNT, 1991), was used to produce the concretes. The choice was based on its high fineness and the lack of supplementary cementing materials (95-100% clinker). Table 2 shows some chemical, physical and mechanical properties of the cement used (information provided by the manufacturer). A polycarboxylate-based superplasticizer (SP) was also used in this research.

Table 2. Chemical, physical and mechanical properties of the Portland cement used in the research (data provided by the manufacturer).

Property	Value
MgO content (%)	1.46
SO ₃ content (%)	2.99
CO ₂ content (%)	2.42
Insoluble residue (%)	0.97
Loss on ignition (%)	3.30
Specific surface area (Blaine) (cm ² /g)	4580
Density (g/cm ³)	3.04
Initial setting time (min)	130
Final setting time (min)	183
Compressive strength (1 / 3 / 7 / 28 days), (MPa)	(27.0 / 42.3 / 46.4 / 53.9)

6.2.1.3 *Aggregates*

Conventional aggregates from Belo Horizonte region were obtained and comprises a natural river quartz sand and gneiss gravel. The quartz sand was obtained from a plant located in the city of Ponte Nova, Minas Gerais State, and consisted of fine aggregates with particle-size ranging 0.075 to 6.3 mm. Fractions of fine and coarse gneiss aggregates were provided by a supplier from Belo Horizonte, which included a particle-size range of 0.075 mm to 19 mm.

This study used conventional aggregates (CA) and recycled aggregates obtained from the crushing of BOFS (referred to herein as steel slag aggregates – SSA) and QT (referred to herein as quartz tailing aggregates QTA). All aggregates were separated into two main fractions, considered here as a fine aggregate (particle size range of 0.15 - 2.4 mm) and coarse aggregate (particle size range of 2.4 - 12.5 mm).

The comminution process was carried out for the BOFS and QT recycled aggregates in a Retsch BB 200 laboratory jaw crusher. BOFS aggregates were submitted to a magnetic separation process with the aim of recover part of the metallic iron content (three replications, Inbras HF CC magnetic roll, 950 Gauss intensity).

Aggregates were segregated into particle-size fractions for the following composition, which was adjusted by the modified Andreassen distribution curve (Funk & Dinger, 1994). The fine aggregates were separated by sieving in the ranges 0.15 – 0.30 mm; 0.30 – 0.60 mm; 0.60 – 1.18 mm and 1.18 – 2.36 mm. Similarly, the coarser fraction was separated in the ranges 2.36-4.75 mm; 4.75 – 6.30 mm; 6.30 – 9.50 mm and 9.50 – 12.50 mm.

All procedures were carried out in oven-dried samples (105 ± 5 °C, 24 h). The fine aggregates were stored in plastic containers and maintained indoors. The coarse aggregates were washed in running water and stored in water for complete saturation. Conventional and recycled coarse aggregates were used in the saturated surface dry state for concrete production.

6.2.1.4 Engineered Recycled Mineral Admixtures (ERMAs)

The ERMAs were obtained from BOFS, QT, and QIT using the grinding programs listed in *Table 3*. The fraction that passed through the sieve with a mesh size of 4.75 mm was used. For this purpose, BOFS and QT were crushed in the jaw crusher. BOFS fraction was also subjected to the magnetic separation procedure before grinding. *Table 4* shows the powders obtained and grinding programs used.

Table 3. Grinding programs and setup parameters.

Grinding program	Parameter	Information
Low-efficiency program (L)	Jar and balls (material)	Stainless steel
	Jar volume, cm ³	10,367
	Material produced per cycle, cm ³	1,740 (17%)
	Rotation speed, rpm	200
	Balls (volume, cm ³)	1,658 (16%)
	Balls (Quantity / diameter, mm)	(7/22) (17/28) (34/31) (11/38) (16/41)
High-efficiency program (H)	Jar and balls (material)	YZrO ₂
	Jar volume, cm ³	250
	Material produced per cycle, cm ³	80 (32%)
	Rotation speed, rpm	400
	Balls (volume, cm ³)	64,3 (26%)
	Balls (Quantity / diameter, mm)	(99/10) (191/5)

These fines were selected based on the best results observed by the authors in earlier studies in which a wider range of recycled mineral admixtures was tested in densely

packed sand-concretes (Carvalho et al., 2019). The BOFS-L and QT-L comprise coarser than cement powders, while the BOFS-H, QT-H, and QIT-H are finer than cement. The particle size distribution curves of the ERMA and the Portland cement (OPC) used in concrete production are shown in Figure 1. Table 5 lists the Blaine specific surface areas. Some SEM micrographs of the produced powder and cement used are shown in Figure 2.

Table 4. Fines produced with corresponding grinding programs and times.

Fine	Grinding programs	Grinding times (min.)
BOFS-L	L	180
QT-L	L	120
BOFS-H	(L / H)	(180 / 15)
QT-H	(L / H)	(180 / 45)
QIT-H	(L / H)	(180 / 45)

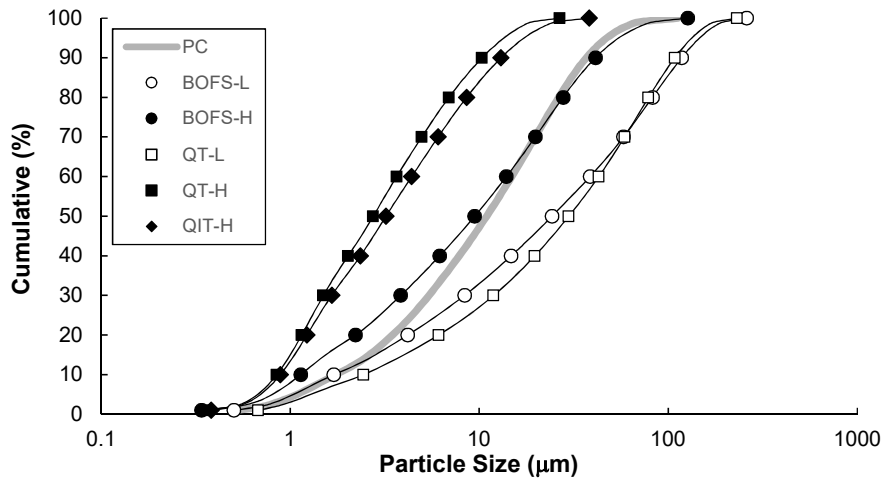


Figure 1. Particle size distributions of the Brazilian Portland cement and the ERMA.

Table 5. Blaine specific surface area of the Brazilian Portland cement and the ERMA.

Portland cement	BOFS-L	BOFS-H	QT-L	QT-H	QIT-H
4572	3028	4620	3100	11818	11519

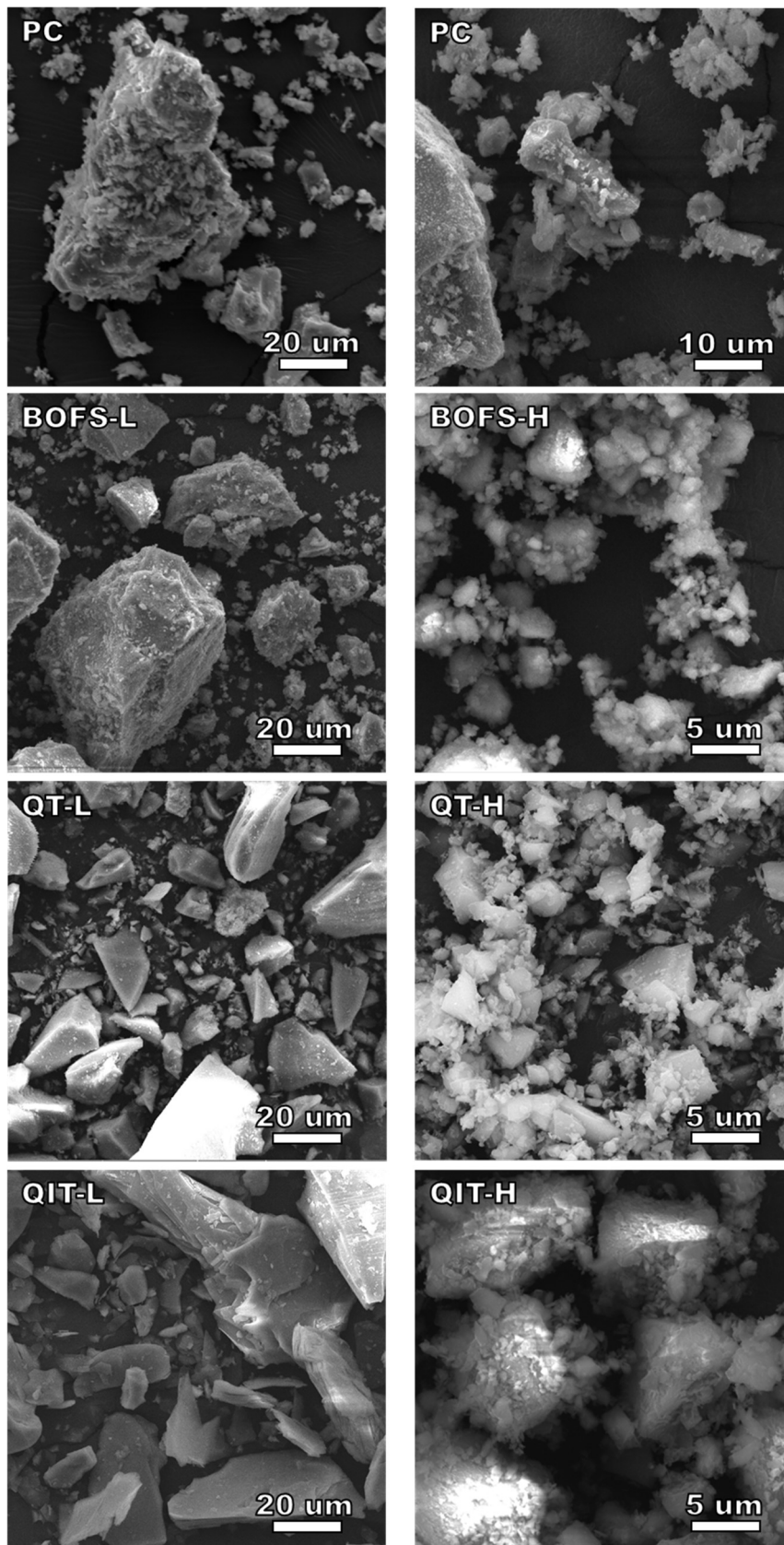


Figure 2. Micrographs of the cement used and ERMAs produced (Carvalho et al., 2019)

6.2.2 Mix design

In this study, two concrete types were proposed: a sand-concrete (without coarse aggregates) and a conventional one. The sand-concrete mixtures were designed using four fractions of fine aggregate, Portland cement, and two ERMAs (one coarser-than-cement and one finer-than-cement). *Table 6* lists the concrete compositions. The dosage of the dry base mixture was designed using the modified Andreassen packing model (Funk & Dinger, 1994). For this purpose, Equation 1 was used to obtain the cumulative volumes (*CPFT*, %) of the particles thinner than D , where D is the particle size; D_L is the largest particle diameter; D_S is the diameter of the smaller particle; and q is the distribution coefficient (q -value). To obtain suitable rheology for a high-powder self-compacting concrete, the q -value was set in 0.2 (Zuo et al., 2018).

Equation 1
$$CPFT(\%) = 100 \left(\frac{D^q - D_S^q}{D_L^q - D_S^q} \right)$$

Table 6. Combinations of constituent materials for the studied concretes

Combination	Fine ERMA	Coarse ERMA	Fine aggregate	Coarse aggregate*
BOFS-CA	BOFS-H	BOFS-L	CA (river sand)	CA (gneiss)
BOFS-SSA	BOFS-H	BOFS-L	SSA	SSA
BOFS-QTA	BOFS-H	BOFS-L	QTA	QTA
BOFS/QIT-CA	QIT-H	BOFS-L	CA (river sand)	CA (gneiss)
BOFS/QIT-SSA	QIT-H	BOFS-L	SSA	SSA
BOFS/QIT-QTA	QIT-H	BOFS-L	QTA	QTA
QT-CA	QT-H	QT-L	CA (river sand)	CA (gneiss)
QT-SSA	QT-H	QT-L	SSA	SSA
QT-QTA	QT-H	QT-L	QTA	QTA

*Not applicable for sand-concretes

6.2.3 *Mixing procedure and determination of the water content*

The superplasticizer dosage was set in 1.0 % of the total mass of fines. This value was adjusted based on previous investigations of the SP saturation point for the same materials. The same dosage was also reported by Pelisser et al. (2018) using binary and ternary blends of cement, metakaolin and fly ash. For sand-concretes, an adapted mini-slump test was proposed, in which a conical mold ($d_1 = 37$ mm, $d_2 = 86$ mm, $h = 77$ mm, spun steel) is filled under a smooth flat surface, and then the mold is lifted. After 30s, the spread diameter was set in 22 ± 1 cm after water content adjustments. For concretes with coarse aggregates, the flow table test for mortars NBR 13276 (ABNT, 2016) was applied, which involves filling of the standard conical mold ($d_1 = 80$ mm, $d_2 = 125$ mm, $h = 65$ mm) in three layers compacted with 15, 10 and 5 punches of the standard hammer for the first, second and third layer, respectively. Then the mold is lifted, and 30 drops are applied (1 cm height, one drop per second). The spread diameter was set in 30 ± 1 cm after water content adjustments.

A three-step hand-mixing procedure was performed using a rigid steel blade paint scraper (11 cm size) and a rigid prismatic plastic container measuring $28 \times 13 \times 12$ cm. The same protocol was used in both concrete and sand-concrete mixtures. In the first step, a dry mixing was performed for 5 minutes. Afterward, 100 mL of water containing the total superplasticizer content was added followed by a homogenization process performed for 5 minutes. Finally, small amounts of water were added carefully using a wash bottle until the achievement of the required consistency after homogenization. The total amount of water was determined by the mass difference of the wash bottle before and after the consistency adjustment. The density in the fresh state was determined using a known volume vessel.

6.2.4 Mechanical performance

Regarding sand-concretes, compressive strength tests were performed in 40 mm × 40 mm × 160 mm prismatic specimens according to the methods NBR 13279 (ABNT, 2005), ASTM C-348 (ASTM, 2014) and ASTM C-349 (ASTM, 2014). For this, a sample composed of four prismatic specimens was obtained for each mixture. The result of the sample was taken as the average value of the four determinations. For concretes with coarse aggregates, cylindrical specimens Ø50 × 100 mm were molded and subjected to compressive strength test. For this purpose, each sample was composed of four specimens, and the result of the sample was taken as the average value of the four determinations.

The cylindrical specimens were molded in multiple layers to favor the escape of trapped air bubbles. Each layer comprised of an approximate volume of 30 mL, and 30 seconds was the approximate time between consecutive launches. After molding, the specimens were placed in a humid chamber (99 % RH; 25 °C), demolded after five days, and kept in the same wet chamber until the test.

6.2.5 Physical properties in the hardened state

Additional concrete mixtures were designed for similar compressive strengths, and cylindrical samples measuring Ø50 × 100 mm were prepared and subjected to physical characterization in the hardening state comprising water absorption, void index, and specific gravity. For this purpose, the specimens were oven dried (105±5°C) until constancy of mass and their masses were measured. Ultrasonic pulse velocities in the dry samples were measured using a tester Tico (Proceq). After that, the specimens were kept in water for a complete saturation (7 days). The saturated surface dry condition was

achieved using a damp cloth, and the mass in this state was measured for each specimen. Finally, the mass immersed in water was measured by hydrostatic weighing.

6.2.6 *Expansibility in autoclave*

Soundness tests were performed in some blended cement pastes in the Laboratory of Construction Materials / UFOP using an autoclave Matest E070. The tests were conducted according to the method ASTM C151 (ASTM, 2018) using prismatic specimens measuring 25 mm × 25 mm × 285 mm. The pastes were prepared with a relative solid volume $\phi = 0.47$. The Brazilian Portland cement CPV-ARI was used in this test.

6.2.7 *Isothermal calorimetry*

Calorimetric investigations were carried out in the Division of Technology of Construction Materials / BAM / Germany. The tests were performed in a cement only REF paste and blended pastes with the investigated ERMA. A European Portland cement CEM I 42.5R was used, and the relative solids volume ϕ was set in 0.5 for all pastes. An 8-channel isothermal heat flow calorimeter (TAM Air) was used.

6.3 Results and discussion

6.3.1 *Proportioning*

For the sand-concrete BOFS/QIT-SSA, the base dry mixture consisted of 5 % of fine ERMA, 5 % of Portland cement, 47 % of coarse ERMA, 8 % of sand fraction 0.15 - 0.30 mm, 12 % of sand fraction 0.30 - 0.60 mm, 13 % of sand fraction 0.60 - 1.18 mm, and 15 % of sand fraction 1.18 - 2.36 mm [*Figure 3(a)*]. All fractions by

volume in relation to the total volume of solids. This composition reached a close fit with the Modified Andreassen curve (Funk & Dinger, 1994); for this, it was chosen as a reference for all studied dry-mixtures. The component that presented the most significant distortion was the fine ERMA, once the particle-size parameters of BOFS-H diverged compared to QT-H and QIT-H. The coarse ERMA BOFS-L and QT-L showed no significant differences in their particle size distributions and the aggregate fraction compositions were the same for all different materials. Two other dry-mixtures were derived from the reference one varying only the Portland cement and the coarse powder contents. The same relative proportions were used for the concretes with the addition of coarse aggregates (*Figure 3b*). *Table 7* shows the studied mixtures with their adopted identification code and proportioning.

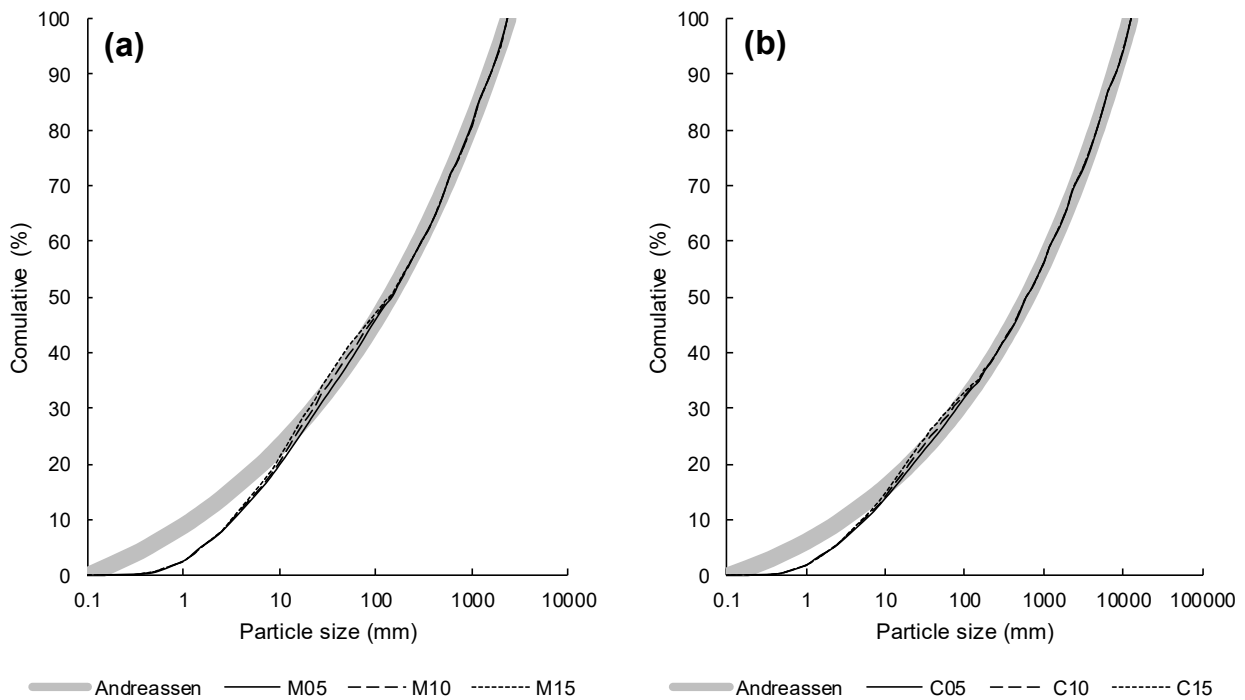


Figure 3. Modified Andreassen curve and dry-mixture curves obtained from the adjustment procedure for the (a) sand-concretes BOFS/QIT-SSA, and (b) concretes with coarse aggregates BOFS/QIT-SSA.

Table 7. Designed mixtures and proportioning

Component	Designed mixture and Proportioning (% by volume)					
	M05	M10	M15	C05	C10	C15
Finer-than-cement powder	5.00	5.00	5.00	3.47	3.47	3.47
Portland cement	5.00	10.00	15.00	3.47	6.94	10.42
Coarser-than-cement powder	42.00	37.00	32.00	29.17	25.69	22.22
Fine aggregate (0.15 - 0.30 mm)	8.00	8.00	8.00	5.56	5.56	5.56
Fine aggregate (0.30 - 0.60 mm)	12.00	12.00	12.00	8.33	8.33	8.33
Fine aggregate (0.60 - 1.18 mm)	13.00	13.00	13.00	9.03	9.03	9.03
Fine aggregate (1.18 - 2.36 mm)	15.00	15.00	15.00	10.42	10.42	10.42
Coarse aggregate (2.36 – 4.75 mm)	-	-	-	11.11	11.11	11.11
Coarse aggregate (4.75 – 6.30 mm)	-	-	-	6.25	6.25	6.25
Coarse aggregate (6.30 – 9.50 mm)	-	-	-	6.25	6.25	6.25
Coarse aggregate (9.50 – 12.50 mm)	-	-	-	6.94	6.94	6.94

In this study, the solid fraction consists mainly of coarse ERMA, with reduced or none binder properties. This material plays an intermediate role between a powder and a fine aggregate. For this reason, the fines:aggregate ratio (F/A) is used instead of the binder:aggregate ratio (B/A) in the evaluation and discussion.

The obtained proportion was confirmed by the experimental evaluation using SP and the water content adjusted for the required consistency. The F/A reached was 1.08 for the sand-concretes, which is considered high compared to the well-accepted reference of 0.75 (Chen et al., 2019). This ratio, however, ensures a sufficient volume of paste required to fill the voids between aggregates and to form films involving the particles to lubricate the system (Damineli et al., 2010; Ling & Kwan, 2016; Ling & Kwan, 2018). For the concretes, the F/A ratio obtained was 0.56, which is also considered suitable for Chen et al. (2019).

6.3.2 Grain packing, water consumption, and rheological behavior

Figure 4 shows the results of the packing density for all tested sand-concretes. In most cases, the M15 sand-concretes had a reduced packing density compared to M10 and M05,

which is mainly due to the better particle shape of the ERMAs compared to cement particles (*Figure 2*), and the better fit with the modified Andreassen curve. The most significant exception was the BOFS/QIT-QTA sand-concretes. In this case, the interaction between BOFS-L and QTA seems to play an important role, once the reduction in the BOFS-L consumption improved the flowability. A similar trend was also observed for BOFS-QTA sand-concretes. All sand-concretes containing BOFS-L and QIT-H showed water:solids ratios above the average (including the better overall result). It is likely due to the use of a good-shaped coarse ERMA (BOFS-L), Portland cement, and an effectively thinner powder (QIT-H). In this sense, the mixtures containing QT ERMAs (similar particle sizes) did not exhibit the same performance due to their worst flow performance in comparison to BOFS-L (supposedly influenced by particle shape and interaction with the SP). Finally, the aggregates exerted minor influence, but sand-concretes produced with SSA showed better performances in combination with BOFS-L and worst performances in combination with QT ERMAs.

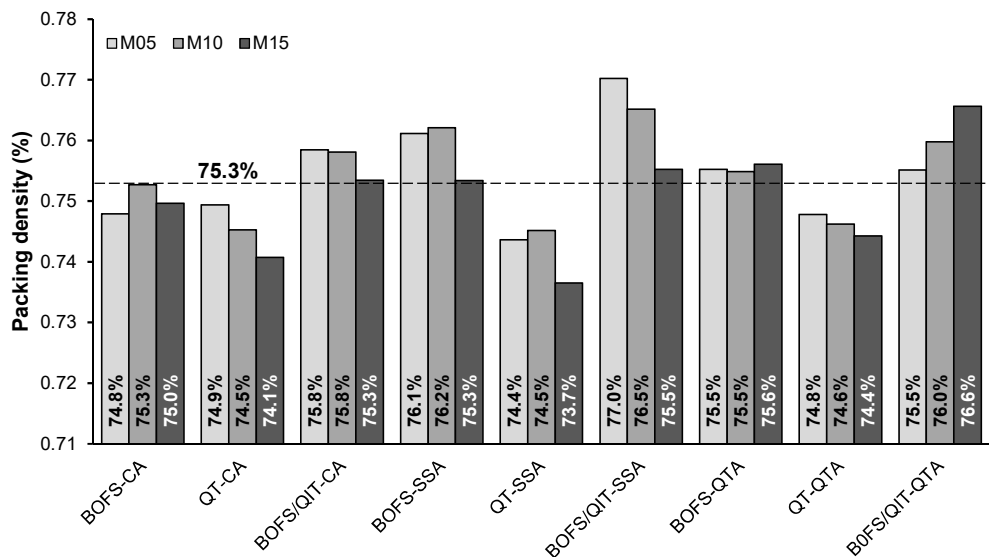


Figure 4. Results of the packing density of the sand-concretes produced in this research.

The incorporation of coarse aggregates reduced the water:solids ratio as expected (Figure 5), but the results were more diffuse compared to sand-concretes. In this sense, the relative total amount of water for the specified flow was reduced, and the use of a relatively large interval for the spread diameter on the flow table implied in relatively large variations in water consumption. However, the volumetric and smoothed quartz aggregates contributed to satisfactory results of the QTA concretes. The worst particle shape of gneiss aggregates resulted in a relative worst performance of the CA concretes.

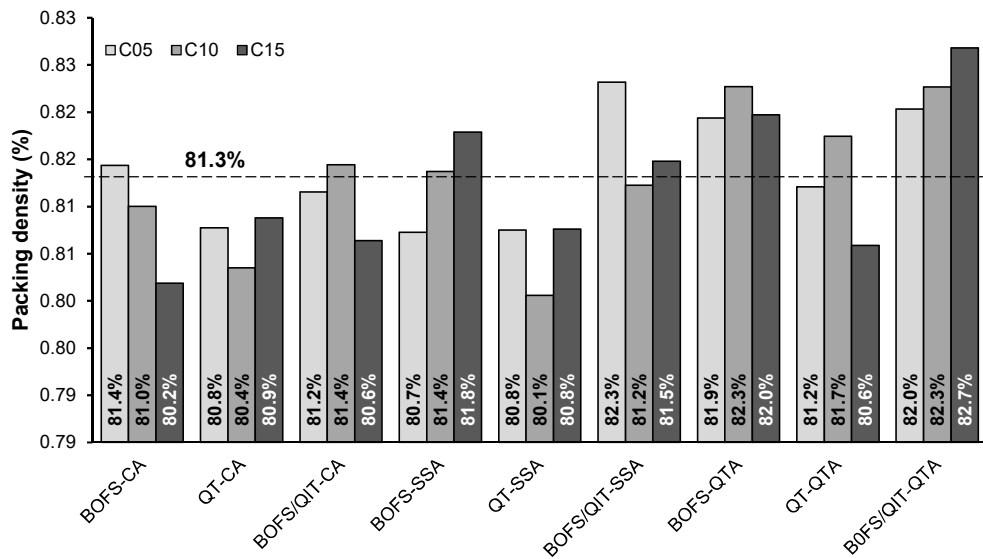


Figure 5. Relative solid fractions ϕ for the tested concrete.

Despite lower water consumption, the sand-concretes had good ability to flow through obstacles and fill corners of formworks without the need for mechanical compaction. However, the mixture showed difficult mixing and no pumpability. With the addition of coarse aggregates, the flow became more difficult, and mechanical compaction is required. In this way, the use as ready-mixed concrete for applications in-loco will require adjustments, but it has been observed that a small additional amount of water is sufficient to achieve flow performance compatible with SCCs. The use of the concrete proposed in precast elements, however, is reasonable. Finally, the sand-concretes showed a significant

ability to expel air bubbles and reduced exudation. In this regard, the QT concretes showed the worst performance, but no adjustments were made, and the designed proportions were maintained. Aspects of the concretes in the flow test are shown in *Figure 6*.

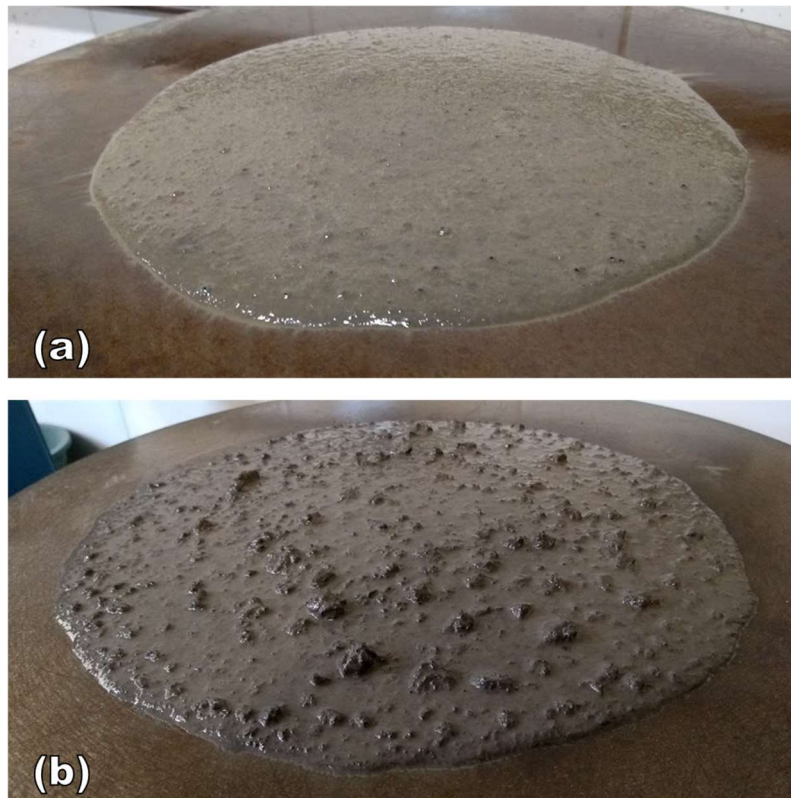


Figure 6. Aspects in the flow test: (a) sand-concrete; (b) concrete.

Figure 7 shows the densities of the sand-concretes in the fresh state. In general, the results were governed by the densities of raw material and packing performance. Sand-concretes with the highest BOFS consumption showed the highest densities, but in some cases, composites containing the blends BOFS-L/QIT-H reached higher values for the same proportions, including the maximum overall value (3216 kg/m^3 - BOFS/QIT-SSA M05).

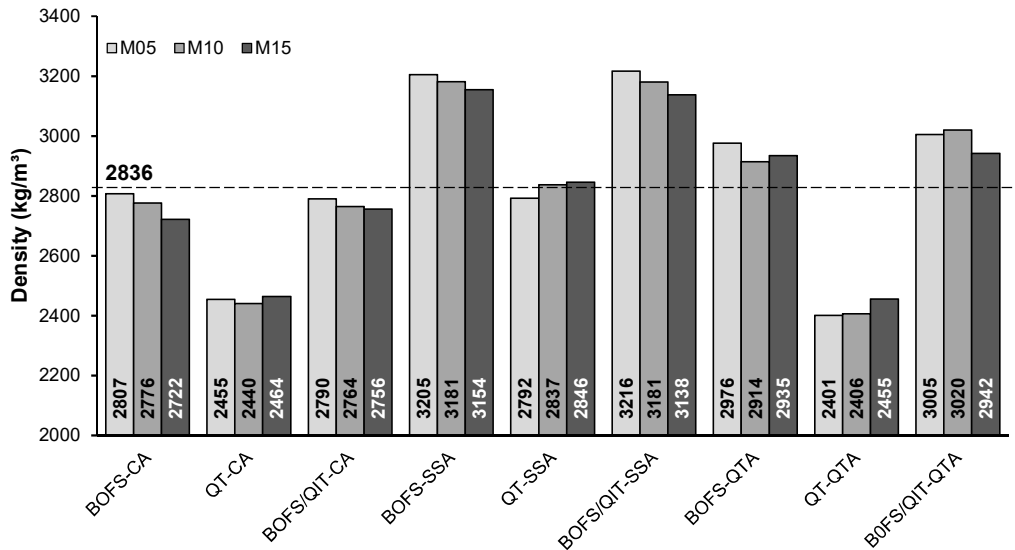


Figure 7. Sand-concretes: Densities in the fresh state

Figure 8 shows the densities of the concretes in the fresh state. Some of them had slightly reduced density values compared to the corresponding sand-concretes. One reason is the higher density of the ERMA compared to the aggregates, and the relatively low content of ERMA in the concretes compared to sand-concretes. Another cause is the higher content of air in the concretes compared to sand-concretes due to the worst flowability and presence of coarse aggregates, which made the escape of air bubbles more difficult. This trend was more evident in BOFS-CA concretes (average variation of -0.6%), BOFS-SSA concretes (-2.8%), BOFS/QIT-SSA concretes (-3.2%), and BOFS/QIT-QTA concretes (-0.8%).

On the other hand, the QT concretes had higher densities than their corresponding sand-concretes. These results suggest that the air bubbles from the QT concretes escaped more easily compared to the other concretes. In this sense, the same property also favored the higher exudation observed in such concretes, which is explained by the QT particles' characteristics. While the sharp edges and the elongated aspect do not favor the grain packing, their smooth surfaces are believed to favor the flow of fluids.

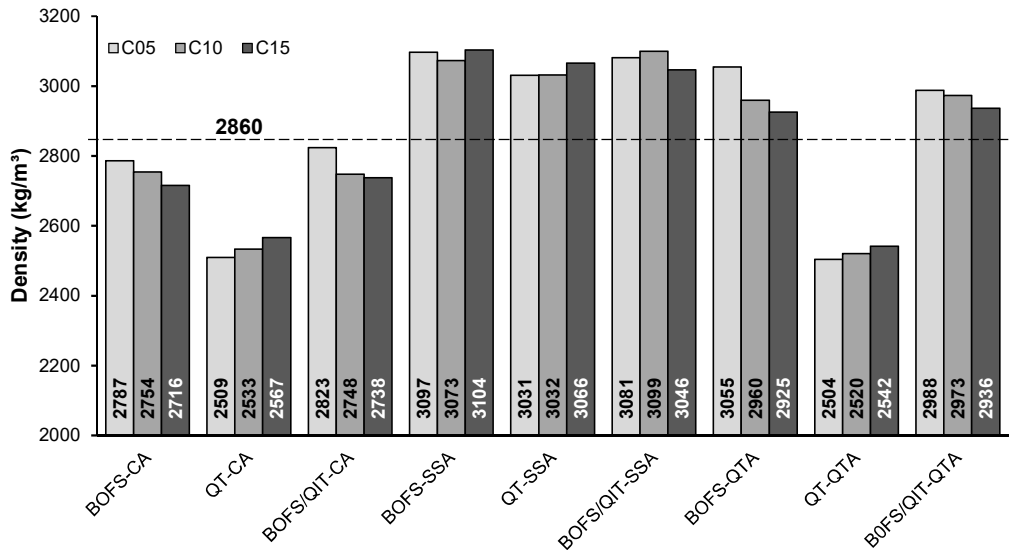


Figure 8. Concretes: Densities in the fresh state.

6.3.3 Mechanical performance and eco-efficiency evaluation

The chart of *Figure 9* shows curves of the tested composites containing results of mechanical performance given by compressive strength and eco-efficiency indicated by cement intensity (CI). The curves were interpolated from three points obtained from the three different cement contents. For simplicity, linear trendlines were used to highlight the trends. These charts can also be used as dosage curves.

Sand-concretes produced with BOFS-L achieved remarkably better results compared to sand concretes produced with QT RMAs. Sand-concretes produced with steel slag fine aggregates had higher compressive strength values for all cement contents and blends. The highest compressive strength value was observed for the mixture BOFS/QIT-SSA M15 (98.9 MPa) with a cement consumption of 344.4 kg/m³. With these results, the cement intensity CI was 3.48 kg/m³/MPa. However, the best overall eco-efficiency performance was achieved by the mixture BOFS/QIT SSA M05. This sand-concrete reached 50.25 MPa with a cement consumption of 117.1 kg/m³ (CI = 2.33 kg/m³/MPa).

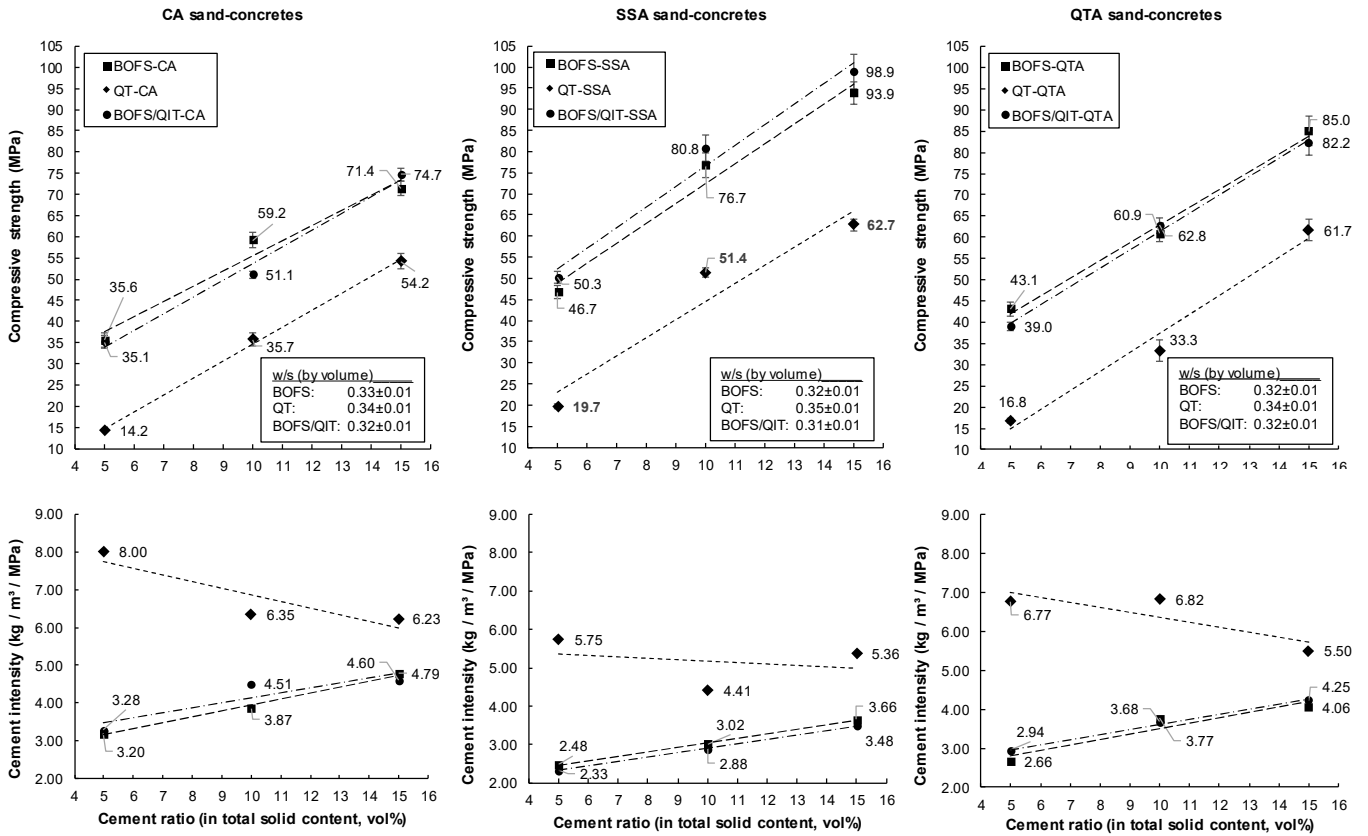


Figure 9. Chart of mechanical and eco-efficiency curves for sand-concretes: (a) CA sand-concretes; (b) SSA sand-concretes; (c) QTA sand-concretes.

Error! Reference source not found. presents a chart containing the results of compressive strength and cement intensity for the concretes with coarse aggregates. Very similar trends were observed in comparison to sand-concretes, but the blends BOFS-L/BOFS-H and BOFS-L/QIT-H showed results consistently different for all studied aggregates. The mixture containing BOFS-L and QIT-H showed better results in combination with the SSA and QTA aggregates while the blend BOFS-L/BOFS-H showed better results in combination with CA. Concretes containing coarse aggregates showed reduced compressive strengths compared to sand-concretes, which is explained by the lower relative cement consumption. Concretes made with SSA aggregates showed the best performances for QT blends and BOFS blends C10 and C15. QTA aggregates in association with BOFS blends reached better results for reduced cement consumptions.

The best overall mechanical performance was observed for the concrete BOFS/QIT SSA C15 (66.3 MPa) for a cement consumption of 254.4 kg/m³ (CI = 3.92 kg/m³/MPa). The best overall eco-efficiency was achieved by the concrete BOFS/QIT QTA C05 (compressive strength of 37.0 MPa; cement consumption of 86.6 kg/m³; CI = 2.34 kg/m³/MPa).

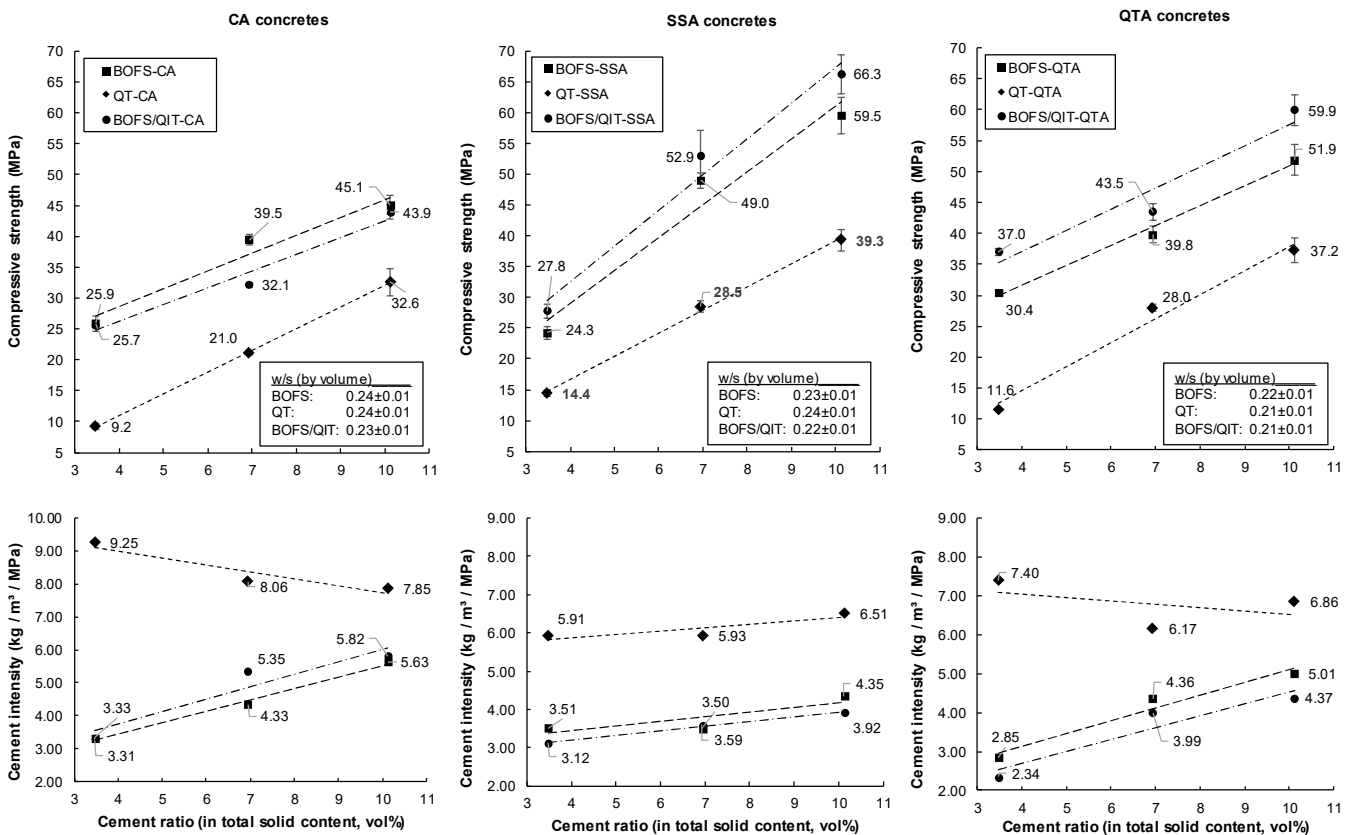


Figure 10. Chart of mechanical and eco-efficiency curves for concretes: (a) CA concretes; (b) SSA concretes; (c) QTA concretes.

There are few reports of similar levels of binder efficiency in literature, and no reports of CI below 3 kg/m³/MPa have been found. Recently, Pelisser et al. (2018) achieved a CI = 7.0 kg/m³/MPa in an SCC with cement consumption of 472 kg/m³ and compressive strength of 67.3 MPa. In the same study, the authors also reported a CI = 8.4 kg/m³/MPa

in a low-cement SCC (cement consumption of 240 kg/m³, 28.6 MPa). Vahren et al. (2016) reported attainment of cement intensities between 6.2 and 8.5 kg/m³/MPa in sand-concretes with cement consumptions between 109 and 445 kg/m³/MPa. According to the calculations of Pelisser et al. (2018), the lowest overall result reported in the literature was achieved by Yazici (2008), using fly ash and silica fume as supplementary cementitious materials in a SCC with cement consumption of 180 kg/m³ and compressive strength of 54 MPa (CI = 3.3 kg/m³/MPa).

Increases in eco-efficiency indicator CI were observed with the reduction in the cement consumption for the concretes and sand-concretes produced with the ERMA BOFS-L. This trend was observed for all mixtures and represents an interesting finding of this research. The increase in CI indicator is commonly related to increases in the compressive strength, i.e., good binder efficiency is generally reported associated with high and ultra-high strength concretes. However, the increase in compressive strength is not necessarily required in most applications (Pelisser et al., 2018). Also, these concretes always have high cement consumption. The methodology proposed in this study was successful in the reverse direction, and included concretes with reduced cement consumptions and low compressive strengths in the set of highly eco-efficient concretes.

Consumption of recycled material is another remarkable feature of this research. The reduced cement consumption and the use of recycled mineral admixtures and aggregates led to maximum consumptions of recycled material corresponding to 95 % in total solid volume for sand-concretes. For concretes, this percentage was 96.5 %.

6.3.4 *Physical characterization in the hardened state*

Results of physical characterization of hardened concrete specimens produced in this study using BOFS-L, BOFS-H, and QIT-H are listed in Table 8. These concretes were designed using the charts shown in Figure 10 for a compressive strength equal to or greater than 30 MPa. These samples reached the specified compressive strength with low cement consumption (111 and 123 kg/m³) and presented low porosity (water absorption of 4.8% and 5.0%) as a result of the high packing density of the mixtures (82.4% and 81.0%).

Table 8. Characterization results in tests performed on hardened concrete samples.

Composition	BOFS/QIT-SSA	BOFS-SSA
Cement consumption (kg/m ³)	111.1	122.7
Cement proportion c (% of solids in vol.)	3.76	4.19
Compressive strength (MPa)	33.9	32.6
Packing density (%)	82.4	81.0
CI (kg/m ³ /MPa)	3.28	3.77
Specific density in hardened state (kg/m ³)	3,415	3,453
Water absorption (%)	4.81	5.02
Void index (%)	14.1	14.8
Ultrasonic pulse velocity (m/μs)	4301	4122

6.3.5 *Considerations on applicability and feasibility*

6.3.5.1 *Implications on hydration kinetics*

Figure 11 shows some heat flow curves obtained by isothermal calorimetry test. These are: a reference cement only REF paste (European CEM I 42.5R); Blended pastes containing the used ERMA in cement replacement rates of 25 % by volume; and some ternary cement blends correspond to the paste fraction of concretes C05 and C15. The

pastes were produced with a solids ratio $\phi = 0.5$ by volume, and no chemical admixtures were used.

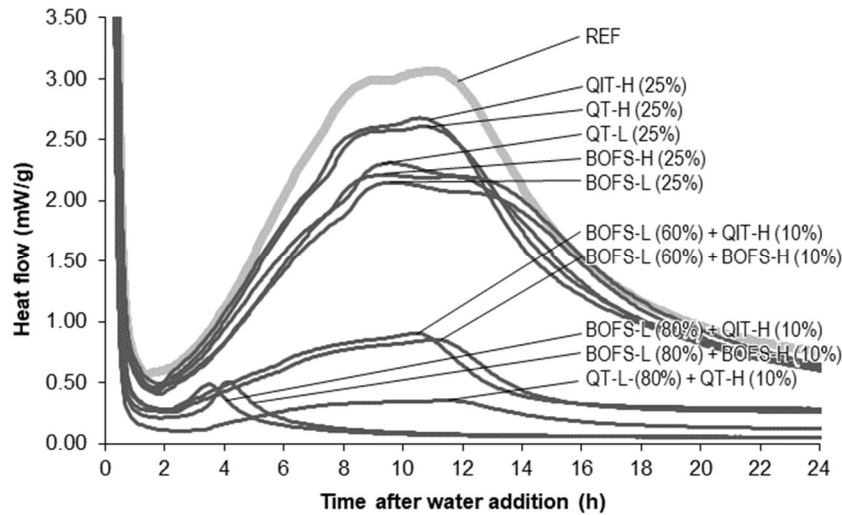


Figure 11. Heat flow curves of a CEM I 42.5R cement-only REF paste and some blended pastes containing the studied ERMA.

The partial replacement reduces heat-flow due to the dilution effect and slow reactivity of supplementary materials. The curves of binary blends with a replacement rate of 25 % by volume show that the fineness and chemical/mineralogical composition exerted a significant influence. The quartz-based ERMA had higher maximum heat flow values during the acceleration period in comparison with BOFS fines. QT-H and QIT-H blends presented the highest maxima and accelerated effect compared to the other fines. This performance is related to the presence of an increased amount of reactive ultrafine quartz particles (Palaniandy et al., 2007; Mitrović & Zdujić, 2014; Souri et al., 2015). Additionally, the chemical/mineralogical composition of QIT is probably responsible for its best performance (Burriss & Juenger, 2016).

As expected, ternary blends containing 30 % and 10 % by volume of cement presented an accentuated reduction in the heat flow maxima in the acceleration period. The blends

containing QIT-H showed faster peaks in the acceleration period compared to the corresponding blend containing BOFS-H. Reducing cement content from 30 % to 10 % by volume resulted in a remarkable difference in the behaviors of the ternary blends containing BOFS. While the blends containing 30 % cement by volume showed behavior compatible with the blends containing 75 % cement by volume, the blends containing BOFS and 10 % cement by volume presented a quick and reduced peak. This behavior may be related to an imbalance of sulfate content in these blends. As a result, the C₃A peak was separated from the C₃S peak and anticipated (Cheung et al., 2011). In this regard, high amounts of BOFS containing brownmillerite may be the main responsible for the imbalance. The blends containing QT ERMA and 10 % cement by volume showed normal behavior and the lowest peak.

In addition, polycarboxylate-based superplasticizers affect hydration kinetics (Hanehara, 1999; Yamada et al., 2001; Puertas et al., 2005; Schmidt et al., 2014). Due to the retarding effect, more time was needed to perform the demolding. For prevention, the authors demolded the specimens on the fifth day of age.

6.3.5.2 Implications on durability

Quartz fines and aggregates are materials with recognized high quality for use in cement composites as inert material due to its high chemical stability and mechanical performance (Dutra et al., 2014). Untreated steel slags, however, contain considerable amounts of calcium and magnesium oxides and metallic iron. For this reason, the direct application of this product in cement composites is not indicated once expansive reactions involving these compounds can damage the cement matrix, leading to a loss in performance (Jiang et al., 2018). Nevertheless, the recovery of the metal fraction by

magnetic separation and stabilization of expansive oxides by weathering has proven to be effective in obtaining stable aggregates and fines (Diniz et al., 2017; Da Silva et al., 2016; Jiang et al., 2018). The production of fines from steel slag also requires special attention regarding the grinding process, that exposes unstable compounds encapsulated into the particles. Additionally, the increase in fineness also increases reactivity. In this work, however, no additional specific treatments were performed in the BOFS fines to stabilize the product after grinding.

The results of the autoclave soundness test (*Figure 12*) showed that pastes containing QT and QIT in a cement replacement rate of 25 % by volume had no expansion. Moderate expansions were observed in pastes containing BOFS-L and BOFS-H, respectively, due to the expansive oxides exposed during the grinding process, but both results were within the normative limit of 0.80% [ASTM C150 (ASTM, 2018)]. Samples with a cement replacement rate of 60 % of cement by volume by BOFS fines (20 % BOFS-H and 40 % BOFS-L) showed an average expansion of 1.01 %, which was above the normative limit. However, the samples remained intact and showed no visible damages.

Pastes with 10 % cement, 10 % BOFS-H and 80 % BOFS-H failed in the soundness test (*Figure 13a*). Similarly, pastes containing 10 % cement, 10 % QIT-H and 80 % BOFS-L also failed but exhibited less expansion (*Figure 13b*). The results are not a surprise but show the role of the primary binder (cement) in stabilizing the matrix. With a cement replacement of 60 % by volume, the matrix remained intact; on the contrary, the ability of the matrix in restraining the expansion was significantly reduced with the radical reduction of cement content.

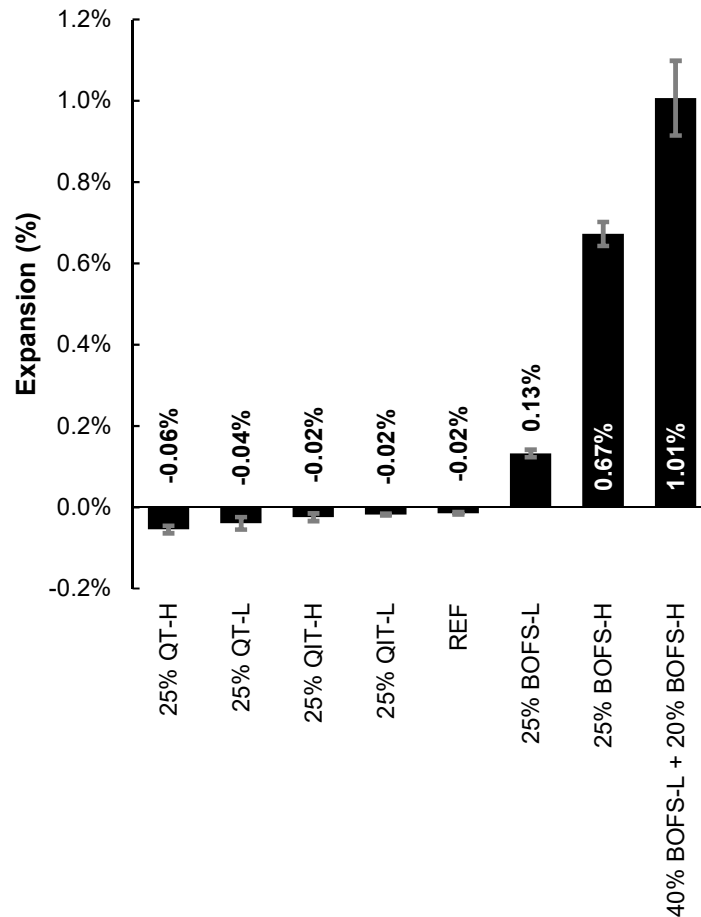


Figure 12. Results of the soundness test (autoclave expansion)

The drastic reduction in cement content and the increase in ERMA dispersed cement particles. As a result, the early hydration is very efficient, but the short-term strength is poor. Finally, the effective stabilization process dedicated to BOFS fines is recommended and is likely to mitigate undesirable behaviors. In this respect, previous studies indicate that it is feasible and even profitable (Gonçalves et al., 2016). Besides, the stabilization and use of steel slag products can be boosted by the development of the carbonation industry (conversion of CO₂ into valuable products) (Euractiv, 2017).



Figure 13. Samples with 90 % cement replacement by volume before and after the soundness test: (a) 80% BOFS-L + 10% BOFS-H; (b) 80% BOFS-L + 10% QIT-H.

In a recent study, Andrade (2018) showed that concretes produced with total replacement of conventional aggregates by steel slag aggregates presented better performances compared to conventional concretes in accelerated carbonation tests. It is well known that resistance to chloride ion penetration or carbonation is closely related to porosity. The amount of hydration products is expected to be reducing the cement content considerably. For this reason, a densely packed mix design is mandatory in order to ensure the durability by reaching low porosity in low-cement concretes.

6.3.5.3 *Perspectives and recommendations*

The performance results show that the proposed ERMAs, RAs and mix designs were effective in obtaining concretes with consistent low cement consumptions, although its application is limited considering the exploratory aspect of the research. Therefore, the authors consider the techniques are promising and contribute to the development of more eco-efficient concretes comprising reduced consumption of natural resources and increased consumption of industrial and mining by-products as recycled building materials, and launch new insights on the subjects.

The cementitious properties of BOFS-based ERMAs were determinant for their best results and should be taken into account in the feasibility assessment. In this regard, a comprehensive approach, including the treatment and production of aggregates and fines should be made. Production of fines involves extra costs with grinding and more effective stabilization compared to the production of aggregates. In this sense, the high mechanical performance of the material is also related to its low grindability, which lead to an increased cost in obtaining fines. Fortunately, the study showed that the less expensive coarse ERMA obtained with BOFS is very effective in improving cement efficiency, and it was consumed in high amounts. Thus, a material with great potential was obtained with a reduced impact on production costs. The study also showed that BOFS-H can be successfully replaced by another cheaper superfine powder, and achieve improvements in performance (mechanical and durability).

Concretes with very low cement intensities, low paste content and low to moderate compressive strength require additional care in comparison to sand-concretes. The latter presented both better mechanical, rheological and efficiency results.

Finally, recovering the metallic fraction is indicated as a relevant element in the economic viability of steel slag processing (Gonçalves et al., 2016). In this sense, the authors observed that (i) the weathered slag presented reduced efficiency in the recovery of metallic fraction since the oxidized material on the particles' surfaces has its magnetic properties reduced, and (ii) magnetic separation is not efficient when applied in powders. Therefore, it is recommended to use non-weathered material in magnetic recovery. Furthermore, different dedicated processes are required for aggregates and powders in order to increase the amounts of recovered metallic material and to obtain a lighter and safer mineral admixture. Effective stabilization of expansive oxides should be carried out considering the carbonation industry concept (Euractiv, 2017). For this, some techniques can be found in the literature (Jiang et al., 2018).

6.4 Conclusions

The mix design and proposed ERMAs were very effective at producing low-cement concretes with high consumption of recycled material. The best performances were observed for the blends containing the steel slag coarse ERMA and the quartzite fine ERMA. The concretes made with recycled aggregates achieved similar to meliorated performances compared to conventional aggregates. The extremely low cement consumptions resulted in a slow strength gain, and the expansions observed in pastes containing steel slag ERMAs in the autoclave test indicate that an effective stabilization treatment is required. All cement efficiency results obtained in this study are among the lowest reported in the literature (below 9.5 kg/m³/MPa). However, some results reached inedited very low values (below 3.0 kg/m³/MPa). The minimum cement intensity was 2.33 kg/m³/MPa, observed in the sand-concrete produced with steel slag fine aggregates (48 % by volume of solids), steel slag coarse ERMA (42 %), cement (5 %) and quartzite

fine ERMA (5 %). The consumption of recycled material was up to 95 % by volume of solids in sand-concretes, and up to 96.5 % by volume of solids in concretes.

6.5 Acknowledgments

The authors acknowledge the financial support provided by Coordenação de Aperfeiçoamento de Pessoal de Nível Superior – Brasil (CAPES), Fundação de Amparo à Pesquisa do Estado de Minas Gerais – Brasil (FAPEMIG), and Conselho Nacional de Desenvolvimento Científico e Tecnológico – Brasil (CNPq). The authors also acknowledge the Research Group on Solid Waste RECICLOS-CNPq for infrastructure use and collaboration.

Funding: This work was financed in part by the Coordenação de Aperfeiçoamento de Pessoal de Nível Superior – Brasil (CAPES) – Finance Code 001.

6.6 References

ABNT, 1991. *NBR 5733: High early strength Portland cement - Specification*. Rio de Janeiro: Brazilian Association of Technical Standards - ABNT.

ABNT, 2005. *NBR 13279: Mortars applied in walls and ceilings - Determination of the flexural and the compressive strength in the hardened stage*. Rio de Janeiro: Associação Brasileira de Normas Técnicas. (in Portuguese).

ABNT, 2016. *NBR 13276: Mortars applied on walls and ceilings - Determination of the consistence index*. Rio de Janeiro: Associação Brasileira de Normas Técnicas - ABNT.

Ali, M.B. & Hossain, M.S., 2011. A review on emission analysis in cement industries. *Renew. Sust. Energ. Rev.*, (15), pp.2252-61. DOI: 10.1016/j.rser.2011.02.014.

Andrade, H.D., 2018. *Carbonation in steel slag concretes*. Ouro Preto: Federal University of Ouro Preto - UFOP. (Master's thesis) (in Portuguese).

Aprianti, E., 2017. A huge number of artificial waste material can be supplementary cementitious material (SCM) for concrete production – a review part II. *Journal of cleaner production*, 142, pp.4178-94. DOI 10.1016/j.jclepro.2015.12.115.

ASTM, 2014. *C348-14: Standard Test Method for Flexural Strength of Hydraulic-Cement Mortars*. West Conshohocken: American Society of Testing and Materials.

ASTM, 2014. *C349-14: Standard Test Method for Compressive Strength of Hydraulic-Cement Mortars (Using Portions of Prisms Broken in Flexure)*. West Conshohocken: American Society of Testing and Materials.

ASTM, 2018. *C150/C150-M: Standard Specification for Portland Cement*. West Conshohocken: ASTM International.

ASTM, 2018. *C151: Standard Test Method for Autoclave Expansion of Hydraulic Cement*. West Conshohocken: American Society of Testing and Materials.

Burris, L.E. & Juenger, M.C., 2016. Milling as a pretreatment method for increasing the reactivity of natural zeolites for use as supplementary cementitious materials. *Cement Concrete Comp*, 65, pp.163-70. DOI: 10.1016/j.cemconcomp.2015.09.008.

Carvalho, J.M.F. et al., 2019. Low environmental impact cement produced entirely from industrial and mining waste. *J Mater Civil Eng*, in Press. DOI: 10.1061/(ASCE)MT.1943-5533.0002617.

Carvalho, J.M.F. et al., 2019. More eco-efficient concrete: an approach on optimization in the production and use of waste-based supplementary cementing materials. *Constr Build Mater*, 206, pp.397-409. doi.org/10.1016/j.conbuildmat.2019.02.054.

Chen, J.J., Ng, P.L., Kwan, A.K.H. & Li, L.G., 2019. Lowering cement content in mortar by adding superfine zeolite as cement replacement and optimizing mixture proportions. *J. Clean Prod*, 210, pp.66-76. DOI: 10.1016/j.jclepro.2018.11.007.

Cheung, J., Jeknavorian, A., Roberts, L. & Silva, D., 2011. Impact of admixtures on the hydration kinetics of Portland cement. *Cement Concrete Res*, 41, pp.1289-309. DOI: 10.1016/j.cemconres.2011.03.005.

Da Silva, M.J. et al., 2016. Feasibility Study of Steel Slag Aggregates in Precast Concrete Pavers. *ACI Mater. J.*, 113(4), pp.439-46. DOI: 10.14359/51688986.

Da Silva, M.J. et al., 2016. Feasibility Study of Steel Slag Aggregates in Precast Concrete Pavers. *ACI Mater J*, 113(4), pp.439-46. DOI: 10.14359/51688986.

Damineli, B.L., 2013. *Concepts for the formulation of concretes with low binder consumption: Rheologic control, packing and particle dispersion*. São Paulo: USP. Doctoral Thesis, University of São Paulo (In Portuguese).

Damineli, B.L., Kemeid, F.M., Aguiar, P.S. & John, V.M., 2010. Measuring the eco-efficiency of cement use. *Cement Concrete Comp*, 32, pp.555-62. DOI: 10.1016/j.cemconcomp.2010.07.009.

Dias, L.S. et al., 2016. Quartzite mining tailings for production of adhesive mortar. In Alves Jr., C., ed. *Proceedings of 22th Brazilian Congress on Material Science and Engineering - CBECIMAT*. Natal, 2016. (in Portuguese).

Diniz, D.H., Carvalho, J.M.F., Mendes, J.C. & Peixoto, R.A.F., 2017. Blast Oxygen Furnace Slag as Chemical Soil Stabilizer for Use in Roads. *J Mater Civil Eng*, 29(9), p.04017118. DOI: 10.1061/(ASCE)MT.1943-5533.0001969.

Dutra, M.B., 2015. *Concrete production with optimum particle size sand obtained from quartz mining tailings*. Ouro Preto: UFOP. Master's thesis - Universidade Federal de Ouro Preto (in Portuguese).

Dutra, M.B. et al., 2014. Production of silicon standard sand - recycling of solid waste from mining. In *Proceedings of the 56th Brazilian Concrete Conference*. Natal: Ibracon. p.13p. (in Portuguese).

Euractiv, 2017. *CO2 Value Europe: A New Association Dedicated to the Utilisation of CO2*. [Online] Available at: <http://pr.euractiv.com/pr/co2-value-europe-new-association-dedicated-utilisation-co2-161247> [Accessed 1 December 2018].

Funk, J.E. & Dinger, D.A., 1994. Particle size control for high-solids castable refractories. *American Ceramic Society Bulletin*, 73(10), pp.66-69.

García-Gusano, D. et al., 2014. Life cycle assessment of the Spanish cement industry: implementation of environmental-friendly solutions. *Clean. Technol. Envir.*, 17(1), pp.59-73. DOI: 10.1007/s10098-014-0757-0.

Gonçalves, D.R.R. et al., 2016. Evaluation of the economic feasibility of a processing plant for steelmaking slag. *Waste Management & Research*, 34(2), pp.107-12.

Gonçalves, D.R.R. et al., 2016. Evaluation of the economic feasibility of a processing plant for steelmaking slag. *Waste Manage Res*, 34(2), pp.107-12. DOI: 10.1177/0734242X15615955.

Hanehara, S..Y.K., 1999. Interaction between cement and chemical admixture from the point of cement hydration, absorption behaviour of admixture, and paste rheology. *Cement Concrete Res*, 29, pp.1159-65.

Hendriks, C.A. et al., 1998. Emission reduction of greenhouse gases from the cement industry. In *Proceedings of the fourth international conference on greenhouse gas control technologies*. pp.939-44.

Huntzinger, D.N. & Eatmon, T.D., 2009. A life-cycle assessment of Portland cement manufacturing: comparing the traditional process with alternative technologies. *J. Clean. Prod.*, 17(7), pp.668-75. DOI: 10.1016/j.jclepro.2008.04.007.

Iacobescu, R.I. et al., 2011. Valorisation of electric arc furnace steel slag as raw material for low energy belite cements. *J. Hazard. Mater.*, pp.287-94. DOI: 10.1016/j.jhazmat.2011.09.024.

Jiang, Y., Ling, T.C., Shi, C. & Pan, S.Y., 2018. Characteristics of steel slags and their use in cement and concrete—A review. *Resour Conserv Recy*, 136, pp.187-97. DOI: 10.1016/j.resconrec.2018.04.023.

John, V.M., 2011. Concreto sustentável. In G.C. Isaia, ed. *Concreto Ciência e Tecnologia*. São Paulo: IBRACON. pp.1843-70.

Kajaste, R. & Hurme, M., 2016. Cement industry greenhouse gas emissions e management options and abatement cost. *J. Clean. Prod.*, (112), pp.4041-52. DOI: 10.1016/j.jclepro.2015.07.055.

Lei, Y., Zhang, Q., Nielsen, C. & He, K., 2011. An inventory of primary air pollutants and CO₂ emissions from cement production in China. *Atmos. Environ.*, 45(1), pp.147-54. DOI: 10.1617/s11527-007-9281-6.

Ling, .S.K. & Kwan, A.K.H., 2016. Adding limestone fines as cementitious paste replacement to lower carbon footprint of SCC. *Constr build mater*, 111, pp.326-36. DOI: 10.1016/j.conbuildmat.2016.02.072.

Ling, S.K. & Kwan, A.K.H., 2018. Filler technology for low-carbon high-dimensional stability concrete. *Constr Build Mat*, 163, pp.87-96. DOI: 10.1016/j.conbuildmat.2017.12.083.

Marinho, A.L.B. et al., 2017. Ladle Furnace Slag as Binder for Cement-Based Composites. *J. Mater. Civil Eng.*, 29(11), p.04017207. DOI: 10.1061/(ASCE)MT.1943-5533.0002061.

Meyers, G.D., McLeod, G. & Anbarci, M.A., 2006. An international waste convention: measures for achieving sustainable development. *Waste Management*, 24, pp.505-13. DOI 10.1177/0734242X06069474.

Mikulčić, H. et al., 2016. Reducing greenhouse gasses emissions by fostering the deployment of alternative raw materials and energy sources in the cleaner cement manufacturing process. *J. Clean. Prod.*, 136, pp.119-32. DOI: 10.1016/j.jclepro.2016.04.145.

Mitrović, A. & Zdujić, M., 2014. Preparation of pozzolanic addition by mechanical treatment of kaolin clay. *Int J Miner Process*, 132, pp.59-66. DOI: 10.1016/j.minpro.2014.09.004.

Oikonomou, N.D., 2005. Recycled concrete aggregates. *Cement and concrete composites*, 27(2), pp.315-18.

Palaniandy, S., Azizli, K.A., Hussin, H. & Hashim, S.F., 2007. Study on mechanochemical effect of silica for short grinding period. *Int J Miner Process*, 82(4), pp.195-202. DOI: 10.1016/j.minpro.2006.10.008.

Pelisser, F., Vieira, A. & Bernardin, A.M., 2018. Efficient self-compacting concrete with low cement consumption. *J Clean Prod*, 175, pp.324-32. DOI: 10.1016/j.jclepro.2017.12.084.

Puertas, F., Santos, H., Palacios, M. & Martínez-Ramírez, S., 2005. Polycarboxylate superplasticiser admixtures: effect on hydration, microstructure and rheological behaviour in cement pastes. *Adv Cem Res*, 17(2), pp.77-89.

Salas, D.A. et al., 2016. Environmental impacts, life cycle assessment and potential improvement measures for cement production: a literature review. *J. Clean. Prod.*, 113, pp.114-22. DOI: 10.1016/j.jclepro.2015.11.078.

Santos, D.H., 2015. *Ecomassa - Blended mortar produced with quartzite mining tailings*. Ouro Preto: UFOP. Master's thesis - Postgraduate Program in Civil Engineering - Universidade federal de Ouro Preto.

Schmidt, W., Brouwers, H.J.H., Kühne, H.C. & Meng, B., 2014. Influences of superplasticizer modification and mixture composition on the performance of self-compacting concrete at varied ambient temperatures. *Cement Concrete Comp*, 49, pp.111-26. DOI: 10.1016/j.cemconcomp.2013.12.00.

Souri, A. et al., 2015. Pozzolanic activity of mechanochemically and thermally activated kaolins in cement. *Cement Concrete Res*, 77(November 2015), pp.47-59. DOI: 10.1016/j.cemconres.2015.04.017.

Varhen, C. et al., 2016. Effect of the substitution of cement by limestone filler on the rheological behaviour and shrinkage of microconcretes. *Constr Build Mater*, 125, pp.375-86. DOI: 10.1016/j.conbuildmat.2016.08.062.

Wang, N., 2014. The role of the construction industry in China's sustainable urban development. *Habitat International*, 44, pp.442-50. DOI: 10.1016/j.habitatint.2014.09.008.

WBCSD/IEA, 2009. *Cement Technology Roadmap 2009*. OECD/IEA and World Business Council for Sustainable Development.

Yamada, K., Ogawa, S. & Hanehara, S., 2001. Controlling of the adsorption and dispersing force of polycarboxylate-type superplasticizer by sulfate ion concentration in aqueous phase. *Cement Concrete Res*, 31, pp.375-83.

Yazici, H., 2008. The effect of silica fume and high-volume Class C fly ash on mechanical properties, chloride penetration and freeze–thaw resistance of self-compacting concrete. *Construction and Building Materials*, 22(4), pp.456-62. DOI: 10.1016/j.conbuildmat.2007.01.002.

Zhang, M. et al., 2016. Manifest system for management of non-hazardous industrial solid wastes: results from a Tianjin industrial park. *Journal of Cleaner Production*, 133, pp.252-561. DOI 10.1016/j.jclepro.2016.05.102.

Zuo, W. et al., 2018. Optimum design of low-binder Self-Compacting Concrete based on particle packing theories. *Construction and Building Materials*, 163, pp.938-48. DOI: 10.1016/j.conbuildmat.2017.12.167.

Chapter 7

Final considerations

Abstract

This research was devoted to the obtention of low-impact cement-based composites focused on using industrial and mining wastes as recycled aggregates, supplementary materials and raw material in the production of binders. The techniques investigated and experiments proposed were very successful in showing great potential and opportunities. Despite the limited range of waste employed, the author believes the results broaden the range of by-products able for use in the construction industry. Additionally, several considerations regarding the characterization and production of the studied materials represent useful information for expand and upgrade the current practice regarding production and use of a binder, supplementary cementing materials, and eco-efficient concretes.

7.1 Low-impact binders

The belitic cement reported in Chapter 2 presented characteristics compatible to which expected from a belitic cement, even obtained entirely with industrial and mining wastes. Adjustments in proportioning regarding chemical composition could be addressed in further investigations, as well as, mitigation routes to avoid expansion. The production, however, proved to be feasible, and partial replacement for ordinary Portland cement showed best results in improving the mechanical performance at early ages.

This research limited the approaches involving thermal treatment to this experiment, once the subject fits well to the objective in improving the eco-efficiency, acting directly in the production of a binder closely related to Portland cement. Additionally, it permitted the supply of a personal interest of the author in a deeper understanding of the processes involving cement production. In this sense, all the aspects involving the proposal and experimental program were very successful.

7.2 The role of grinding in producing highly effective engineered recycled mineral admixtures

Thermal treatments are controversial due to the energy demanded and emissions involved. However, grinding is also a controversial theme, mainly regarding the production of micro- and nanoparticles. In fact, it involves high energy consumption in a currently low-efficient process. On the other hand, it seems to be a promising route with good expectations for the near future, considering improvements in grinding technology and use of green energy.

The in-depth investigation on grinding performance of the different residues using a laboratory cylindrical ball mill and a high-efficiency planetary ball mill showed the importance of dedicated grinding. Considerable differences regarding the grinding efficiency depending on the mill set up and mineralogical/geological characteristics were observed. Such observations are valuable to design dedicated processes to improve efficiency and reducing cost. Additionally, the influence of grinding on particle morphology has particular interest regarding impacts in rheology and hydration kinetics.

In the search for improvement in the packing density, it became clear the opportunity in obtaining powders with an intermediate particle size between fine sand and cement. Using this strategy, it was possible the incorporation of high amounts of recycled material in densely packed concrete mixtures designed using the Modified Andreassen model. As a result, improvements in eco-efficiency given by the cement intensity indicator was observed. The coarse powders represent a reduced grinding cost, and their physical properties are the main features regarding performance in cement-based composites.

On the other hand, high-efficiency grinding produced finer-than-cement powders able to replace 25% by volume of cement without loss in compressive strength, and it was observed for all tested residues. Reducing the particle size to a range below 10 μ m, chemical/mineralogical composition and other interactions in the cement paste took place, impacting the hydration kinetics positively. Increase nucleation sites and pozzolanic properties were developed.

7.3 Highly eco-efficient concretes

The exploratory studies presented in chapter 4 revealed the potential of the proposed fines in obtaining high-strength concretes (fine ERMA), and high-eco-efficient concretes

(ternary blends of fine ERMAs, cement, and coarse ERMAs), in densely packed mixtures. Encouraging results were observed in this first study regarding the application of these new concepts in cement-based composites, reaching values of cement intensity among the lowest reported in the literature.

Considering this, the audacious project reported in chapter 6 went beyond, adopting a more refined dosage based on the Modified Andreassen curve. Thus, a proportioning containing high amounts of coarse ERMAs, low cement content and a reduced amount of fine ERMAs was proposed. Additionally, recycled aggregates were also considered in this research. As a result, concretes with normal strength containing ca. 95% of recycled material were obtained for inedited values of cement intensity.

7.4 By-products used in this research

Among the studied by-products, the quartz tailings presented the expected good performance given the high quartz content. The aggregates obtained with this residue presented the expected good performance (chapter 6), as well as their ERMAs. In this regard, the fine ERMA impacted positively in the hydration kinetics providing nucleation sites, contributing to the increase in the hydration degree of the cement in pastes. The same was observed for fine ERMAs produced with quartzite tailings, but the presence of muscovite made this product even more effective in early hydration of blended cement pastes. Their coarse ERMAs presented an intermediary performance, with low influence in the hydration kinetics. Better results, however, were observed for quartz ERMAs considering the better morphology of its particles.

Quartzite was also successfully used in cement production due to its high silica content. It was also the main font of aluminum. Grits were used only in the production of the belitic cement as the substitute of limestone.

The high content of clayey material reduced the performance of iron ore tailings as supplementary material. Concretes produced with this material presented higher porosity, indicating a higher tendency in incorporating air. On the other hand, it does not mean low strength, but lower compared to the other studied residues. Additionally, the ability to incorporating air also has technological advantages.

The weathered basic oxygen furnace slag used was very effective as aggregate and played an important role as a raw material in the production of the belitic cement. However, a more effective reduction in its iron content is very desirable in improving the grindability, reducing expansibility, and reducing weight. In this sense, efficient magnetic segregation before weathering is supposed to be more effective and profitable. The cementitious properties of their ERMAs were verified, and they presented the best average rheological performance and interaction with polycarboxylate-based superplasticizers. As a result, the best eco-efficiency results were observed in concretes containing basic oxygen furnace slags as ERMAs and/or aggregates.

7.5 Proposals for future works

The concepts explored in this work are expansible to a broader range of industrial and mining by-products. Additionally, many opportunities for more in-depth investigations were identified. Follows some proposals for future works:

- Obtaining alitic cements produced entirely with industrial and mining wastes.

- Obtaining ERMA_s potentialized with thermal treatments.
- Expanding the grinding programs exploring different mills and setups in order to reduce cost and improve efficiency.
- Studying the production of ERMA_s in industrial scale using current grinding technologies.
- Investigating the perspectives on grinding technology regarding the production of superfine ERMA_s
- Expanding the high packing density dosages using other theories and experimental approaches.
- Expanding the durability studies regarding carbonation and chloride diffusion, among other aspects.
- Exploring techniques to reduce the iron content in steel slags and evaluating the impacts in the proposed steel slag-based ERMA_s.

7.6 General conclusion

Cement-based composites with improved eco-efficiency were obtained in this study by reducing CO₂ emissions related to consumption of conventional Portland cement, and by enhancing the consumption of industrial and mining waste as recycled raw material. In this sense, a belitic cement produced entirely with industrial and mining waste was proposed and obtained. For this Grits from the pulp and paper industry, basic oxygen furnace slag and quartzite mining tailings were used. This binder showed mechanical performance similar to the reference belitic cement produced with conventional raw materials in the same experimental conditions. Engineered Recycled Mineral Admixtures (ERMA) were also designed and produced using basic oxygen furnace slag, iron ore tailings, quartz mining tailings, and quartzite mining tailings. Coarser-than-cement and

finer-than-cement powders were designed and obtained by grinding. The ultrafine grinding was effective in improving the morphology and cementitious properties of the studied residues. Performance evaluations showed that the proposed ERMAs caused no adverse impacts on the rheology of cement pastes and interacted well with PCE-based superplasticizers. The coarse ERMAs presented none or reduced binder activity, while the fine ERMAs presented significant cementitious properties. In densely packed concretes, the utilization of the proposed ERMAs improved the packing density. The coarse ERMAs were very effective in improving the eco-efficiency by reducing the cement intensity while the fine ERMAs contributed to enhancing the compressive strength. The coarse and fine ERMAs obtained from the steel slag and quartz tailings, and the fine ERMA obtained from quartzite mining tailings showed the best performances. Thus, very eco-efficient cement-based composites were obtained using these materials in association with recycled aggregates, in mixtures designed to enhance the grain packing. As a result, consumptions of recycled material up to 96.5% by volume of solids, and cement intensities up to 2.33 kg/m³/MPa, were obtained. The results of this research are very promising and launch new insights on the production, optimization, and use of supplementary cementitious materials from industrial waste in the obtention of eco-efficient cement-based composites.